ENERGY CONSERVATION

ORNL/Sub-80/24706/1

Phase II Brayton/Rankine 10-Ton Gas-Fired Space Conditioning System

First Annual Technical Report

AiResearch Manufacturing Company
of California
A Division of Garrett Corporation

Report Prepared by
AiResearch Manufacturing Company of California
2525 West 190th Street
Torrance, California 90509

under

Subcontract No. 86X-24706C

for

Oak Ridge National Laboratory
Oak Ridge, Tennessee 37830
operated by
UNION CARBIDE CORPORATION
for the
U.S. Department of Energy
Contract No. W-7405-eng-26
and
Gas Research Institute
Chicago, Illinois 60616
under
Letter Contract No. 5014-341-0114

Printed in the United States of America. Available from
National Technical Information Service
U.S. Department of Commerce
5285 Port Royal Road, Springfield, Virginia 22161
NTIS price codes—Printed Copy: A06 Microfiche A01

This report was prepared as an account of work sponsored by an agency of the United States Government. Neither the United States Government nor any agency thereof, nor any of their employees, makes any warranty, express or implied, or assumes any legal liability or responsibility for the accuracy, completeness, or usefulness of any information, apparatus, product, or process disclosed, or represents that its use would not infringe privately owned rights. Reference herein to any specific commercial product, process, or service by trade name, trademark, manufacturer, or otherwise, does not necessarily constitute or imply its endorsement, recommendation, or favoring by the United States Government or any agency thereof. The views and opinions of authors expressed herein do not necessarily state or reflect those of the United States Government or any agency thereof.

ORNL/Sub-80/24706/1
AiResearch 81-17784
Dist. Category UC-95d

PHASE II BRAYTON/RANKINE 10-TON GAS-FIRED SPACE CONDITIONING SYSTEM

FIRST ANNUAL TECHNICAL REPORT

AIRESEARCH MANUFACTURING COMPANY
OF CALIFORNIA

A DIVISION OF GARRETT CORPORATION

Date Published - July 1982

Report Prepared by

AiResearch Manufacturing Company of California
2525 West 190th Street
Torrance, California 90509

under

Subcontract No. 86X-24706C

for

Oak Ridge National Laboratory
Oak Ridge, Tennessee 37830
operated by
UNION CARBIDE CORPORATION
for the
U. S. Department of Energy
Contract No. W-7405-eng-26

and

Gas Research Institute
Chicago, Illinois 60616
under
Letter Contract No. 5014-341-0114

CONTENTS

Section		Page
	ABSTRACT	v.
1	INTRODUCTION AND SUMMARY	1-1
	Introduction	1-1
	Summary	1-1
2	SYSTEM DISCUSSION	2-1
	System Description	2-1
	System Operation	2-3
	System Development Status	2-6
3	DESIGN AND DEVELOPMENT ACTIVITIES	3-1
	Mark III Rotating Assembly	3-1
	Recuperator	3-8
	Combustor	3-11
	Controls	3-23
	Sink Heat Exchanger	3-33
	System Packaging	3-37
	System Breadboard Testing	3-57
4	SYSTEM ANALYSIS	4-1
	Analytical Tasks	4-1
	Performance Prediction/Optimization	4-1
	Engine Thermodynamic and Stress Analysis	4-15
	Laboratory Test Support	4-15
	Miscellaneous Analysis	4-18
	Fuel Consumption and Cost Analysis	4-18

AIRESEARCH AND GRI DISCLAIMER

LEGAL NOTICE. This report was prepared by the AiResearch Manufacturing Company as an account of work sponsored by the Gas Research Institute (GRI). Neither AiResearch, GRI, members of GRI, nor any person acting on their behalf:

a. Makes any warranty or representation, express or implied, with respect to the accuracy, completeness, or usefulness of the information contained in this report, or that the use of any information, apparatus, method, or process disclosed in this report may not infringe privately owned rights; or

b. Assumes any liability with respect to the use of, or for damages resulting from the use of, any information, apparatus, method, or process disclosed in this report.

ABSTRACT

This report summarizes the technical accomplishments to date in the design, development, and demonstration program undertaken by the AiResearch Manufacturing Company, leading to commercialization of a 10-ton heat-actuated space conditioning system for light-commercial building applications. The system consists of a natural-gas-powered Brayton-cycle engine and a Rankine-cycle heat pump, combined in a single roof-top package.

The heat-actuated space conditioning system provides more efficient use of natural gas and is intended as an all-gas alternative to the electric heat pump. The system employs a subatmospheric natural-gas-fired heat pump. A centrifugal R-12 refrigerant compressor is driven directly from the Brayton engine rotating group through a hermetically sealed coupling. Unique features that offer high life-cycle performance include a permanent magnet coupling, foil bearings, an atmospheric in-line combustor, and a high-temperature recuperator. Predicted overall engine efficiency is 27 percent and predicted overall unit coefficient of performance at the energy source is 1.0 in cooling and 1.2 to 1.4 in heating at 95°F and 47°F ambient temperature respectively.

During the past year, major emphasis in the development program was placed on: (1) development of major components of the engine assembly, (2) packaging design, and (3) control system evaluation. Major component development has proceeded well, with completion of development tests on the combustor and sink heat exchanger. Since completion of fabrication, the Mark III rotating assembly and recuperator are well into their development test programs. In addition, an engine package assembly has been designed and fabricated and is being used as a test bed for recuperator development.

SECTION 1

INTRODUCTION AND SUMMARY

SECTION 1

INTRODUCTION AND SUMMARY

INTRODUCTION

This report summarizes the technical accomplishments to date in the design, development, and demonstration program undertaken by the AiResearch Manufacturing Company leading to commercialization of a 10-ton heat-actuated space conditioning system for light-commercial building applications. The system consists of a natural-gas-powered Brayton-cycle engine and a Rankine-cycle heat pump, combined in a single roof-top package. The design and development effort reported herein was performed from March 1, 1979 through December 31, 1980, under Gas Research Institute (GRI) Letter Contract No. 5014-341-0114, dated February 28, 1979; a letter revision thereto from F. Reid Hayden, dated June 13, 1980; and Union Carbide Corporation, Nuclear Division (UCC-ND), Subcontract No. 86X-24706C.

SUMMARY

The heat-actuated space conditioning system provides more efficient use of natural gas and is intended as an all-gas alternative to the electric heat pump. The system employs a subatmospheric natural-gas-fired heat pump. A centrifugal R-12 refrigerant compressor is driven directly from the Brayton engine rotating group through a hermetically sealed coupling. Unique features that offer high life-cycle performance include a permanent magnet coupling, foil bearings, an atmospheric in-line combustor, and a high-temperature recuperator. Predicted overall engine efficiency is 27 percent and predicted overall coefficient of performance (COP) at the energy source is 1.0 in cooling and 1.2 to 1.4 in heating.

During the past year, major emphasis in the development program was placed on: (1) development of major components of the engine assembly, (2) packaging design, and (3) control system evaluation. Major component development has proceeded well, with completion of development tests on the combustor and sink heat exchanger. Since completion of fabrication, the Mark III rotating assembly and recuperator are well into their development test programs. In addition, an engine package assembly has been designed and fabricated and is being used as a test bed for recuperator development. These achievements are discussed more fully in subsequent sections of this report.

The marketing effort was expanded with the initiation of a market survey and analysis activity by both Dunham-Bush and Lennox Industries, Inc. The Dunham-Bush heat pump package design was nearing completion at year's end. It is anticipated that go-ahead will be given on the Lennox development program in the near future.

During 1981, the remaining engine component development tests will be completed; the engine assembly will be tested as a package and fully developed. Four prototype engine assemblies are being fabricated. One will be installed in a heat pump assembly at Dunham-Bush for performance and demonstration tests.

Similarly, one will be delivered to Lennox for incorporation into the Lennox-designed heat pump and subsequent testing. The third engine assembly will undergo performance testing at AiResearch, and the fourth engine assembly will undergo life-cycle tests at AiResearch. The engine assembly and heat pump test programs will be initiated in 1981 and will be completed in 1982.

Marketing and commercialization plans will be updated and ongoing cost-reduction efforts will continue in 1981. It is expected that initiation of a field test program will result in units being installed at selected sites by mid-1982. The marketing analysis and commercialization effort on the program are covered in AiResearch Report 81-17800, a separate data submittal under the contract.

Section 2 of this report describes system operation and briefly summarizes the system development status. Section 3 discusses development progress on the individual components and subsystems of the engine assembly and heat pump. Section 4 describes the system analytical design activities, system performance predictions, and operation performance advantages of the Brayton/Rankine space conditioning system.

SECTION 2

SYSTEM DISCUSSION

SECTION 2

SYSTEM DISCUSSION

SYSTEM DESCRIPTION

The 10-ton Brayton/Rankine space conditioning system, which is currently undergoing Phase II development testing, is shown schematically in Figure 2-1. The system consists of two separate thermodynamic loops. The first loop is a conventional Rankine-cycle vapor compressor heat pump system that uses a high-speed centrifugal compressor instead of a positive displacement type. The second loop consists of a Brayton-cycle engine, which provides the energy for the centrifugal vapor compressor and waste heat energy to the building during the heating mode of operation. A compact, efficient, gas-fired mechanical system is provided by utilizing the natural speed match of the Brayton rotating group and the centrifugal R-12 refrigerant compressor. To maintain the desirable hermetic sealing of the vapor compression system, the refrigerant compressor is coupled to the Brayton unit through a high-speed magnetic coupling.

The semi-open, subatmospheric-pressure Brayton cycle engine consists of a centrifugal compressor, a radial inflow turbine, a recuperator, a sink heat exchanger, and an in-line atmospheric combustor. Ambient air is drawn through the recuperator, where it is preheated before being introduced into the atmospheric-pressure, natural-gas-fired combustor in a mixture that is slightly above stoichiometric. Compressor discharge gas is also cycled through the recuperator and used as a diluent to provide added flow and the desired turbine inlet temperature. Expansion takes place through the turbine component, from which sufficient power is extracted to drive both the Brayton and refrigerant compressors. The turbine discharge gas, which is at subatmospheric pressure, is processed through the recuperator, where it preheats combustor inlet air. The temperature of the low-pressure gas is reduced further by using the sink heat exchanger to reduce compressor power consumption. The compressor pumps the gas back to atmospheric pressure and a small portion is exhausted; the remainder is recycled as diluent. The sink heat exchanger cooling air, which now has a temperature greater than 100°F, is combined with building recirculation air in the heating mode, supplementing the vapor cycle unit heating capacity.

The R-12 refrigerant circuit (Rankine cycle) is similar to a conventional 10-ton heat pump, consisting of the typical air conditioning components such as compressor, refrigerant coils, fans, various control valves, accumulator, and controls. The refrigerant circuit is unlike the conventional heat pump, however, with respect to the configuration of the refrigerant compressor and its directly related surge controls. The centrifugal-type compressor is directly driven at the Brayton-side turbine speed (55,000 to 80,000 rpm) through a non-slip magnetic coupling. The magnetic coupling also provides a means of statically isolating, and therefore hermetically sealing, the refrigerant circuit.

To ensure that the refrigerant compressor does not operate in surge, a bypass valve recirculates vapor from the compressor discharge back to the suction side. Flow is sensed as a function of the velocity head at the compressor

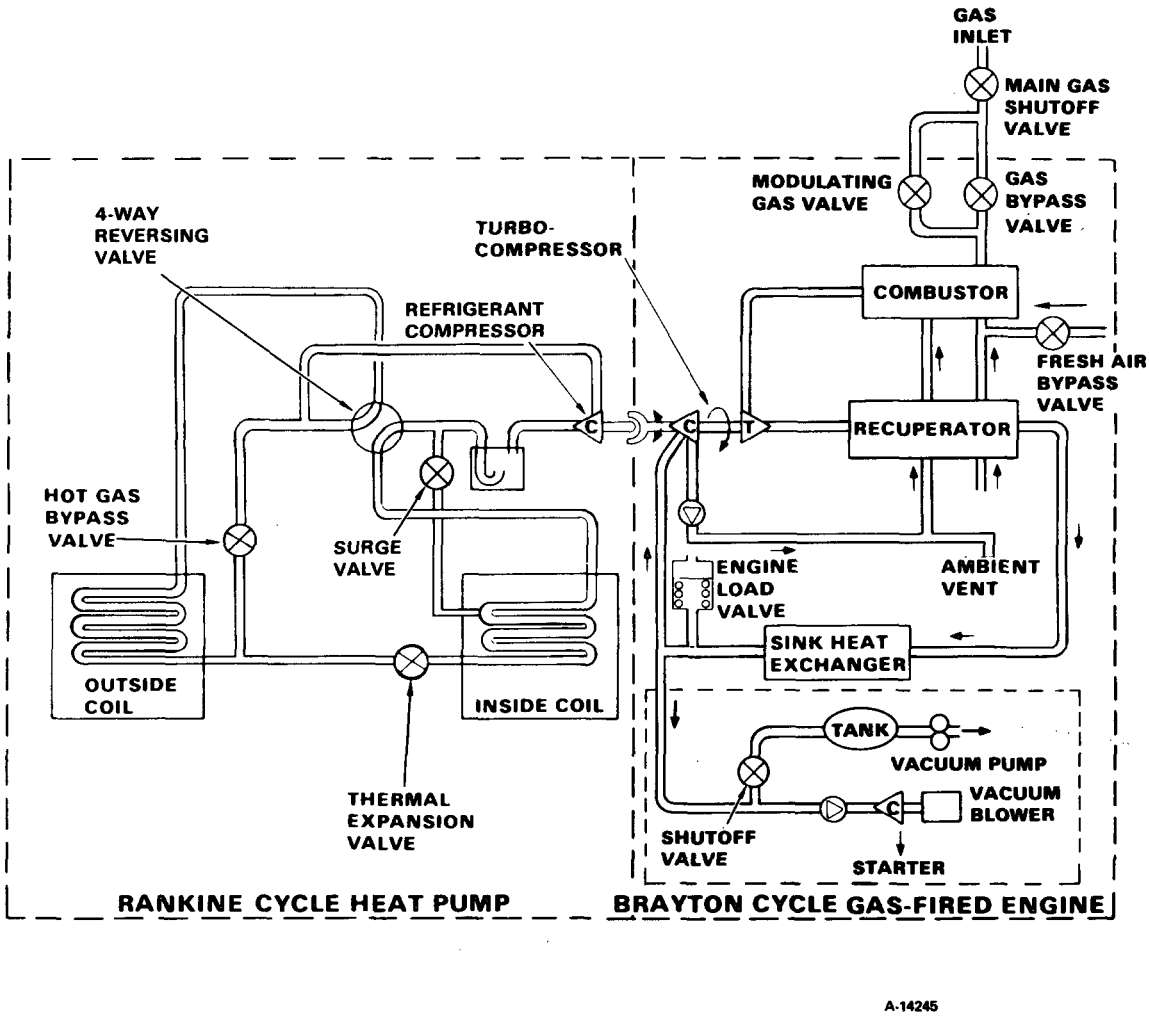

Figure 2-1. Brayton/Rankine Gas-Fired Space Conditioning System Schematic

discharge, and the surge valve flow area is varied as required to maintain the minimum compressor flow. The valve is closed with system equilibrium flows above the minimum value.

Figure 2-2 shows the configuration of the Brayton-cycle engine assembly with each of the major components identified. The subatmospheric nature of the cycle is beneficial not only because it uses natural gas at line pressure and fresh air at ambient pressure, but also because it allows simplified, low-pressure-drop component and package designs. In the design of the recuperator, interface manifolds and ducts are not needed on the high-pressure side. A plenum-type enclosure separates the recuperator into primary and service core sections and directs the flow through each section.

Because of the low internal differential pressure (ambient ± 2 in. H_2O), the box-design enclosure walls are sheet metal and of simple construction. The enclosure is also easily insulated and is provided with strategically located access panels for maintenance accessibility to all components. The basic engine configuration and construction will be identical for the Dunham-Bush and the Lennox heat pumps; however, details such as fuel- and exhaust-line locations and heat pump wall interfaces may vary.

Figure 2-3 shows a conceptual heat pump configuration utilizing the Brayton-cycle engine. The actual configuration of the two heat pump designs to be tested in Phase III will be determined separately by Dunham-Bush and Lennox during Phase II. Dunham-Bush is presently involved with the detail design task, while Lennox will commence this task in the near future.

SYSTEM OPERATION

The Brayton-Rankine heat pump must operate under the same conditions and provide the same overall environmental control as the conventional heat pump. Its total spectrum of operation also includes the same four basic modes: (1) refrigeration cooling, (2) economizer cooling, (3) heat pump heating, and (4) auxiliary heating. The difference between the Brayton/Rankine unit and the conventional heat pump is the way in which some of the operational requirements are satisfied. For example, in the heating mode, the Brayton/Rankine heat pump capacity is augmented by the waste heat from the sink heat exchanger (up to about 70 percent of total capacity), thereby reducing the steady-state capacity requirements of the R-12 circuit. For ambient temperatures below approximately 5°F, the system is switched to the low-temperature-ambient (LTA) mode, which increases the sink heat exchanger waste heat to about 90 percent by raising the hot-side inlet temperature to the sink heat exchanger. This is accomplished by increasing the amount of fresh air and natural gas supplied to the combustor. As a result, auxiliary electric heaters are not required. The refrigeration and enconomizer cooling modes of the Brayton/Rankine system are essentially identical to those of the conventional heat pump.

In all modes of operation, control of the integrated Brayton/Rankine system is a function of the sensed error between the thermostat setting and the actual room temperature. System activation, maximum system output, and deactivation occur within a range of ± 3°F from the nominal thermostat setting. Fuel input to the engine, after system activiation, is modulated between preset limits

ORNL-PHOTO 4597-81

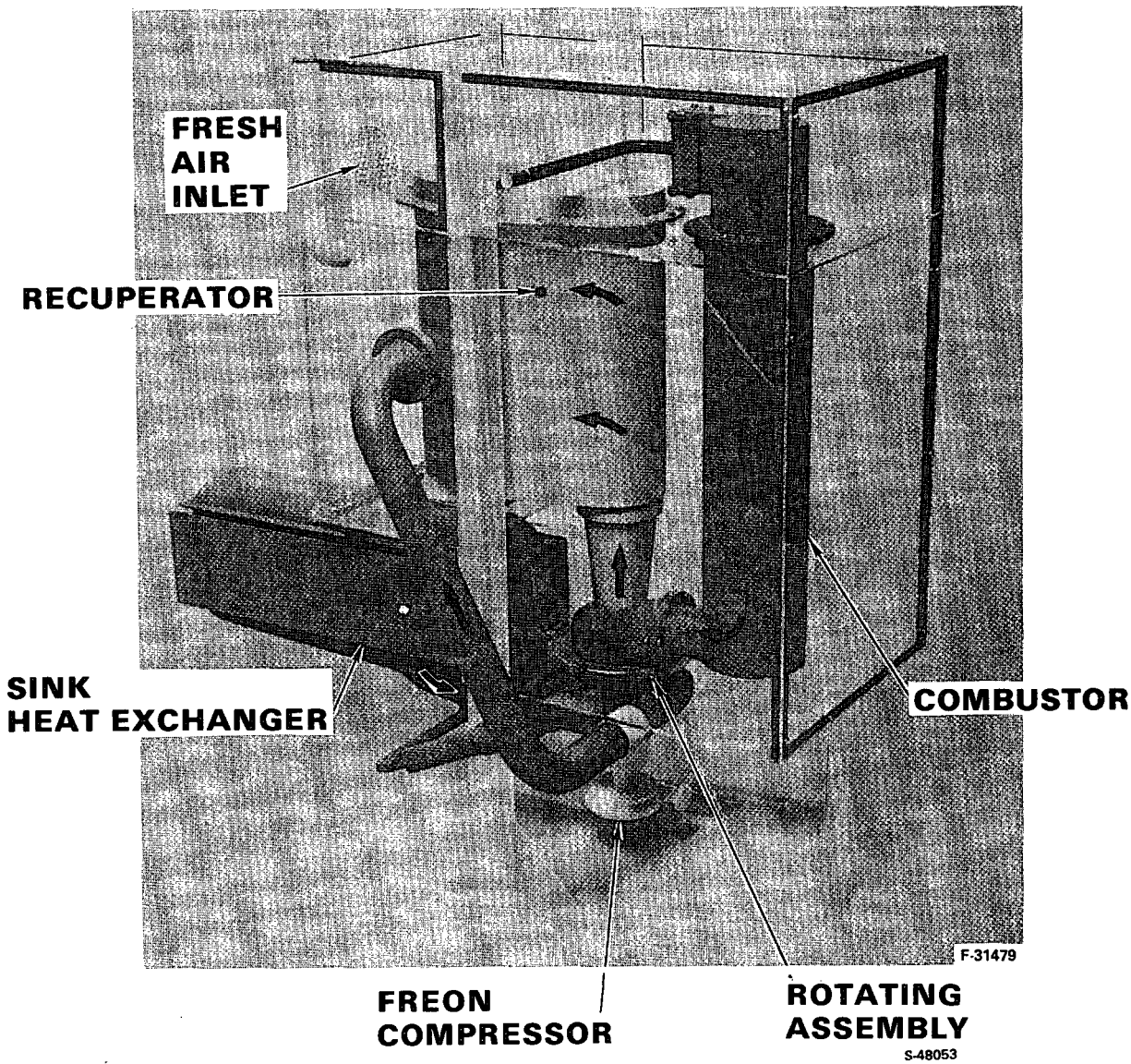

Figure 2-2. Brayton Cycle Engine Assembly Configuration

ORNL-PHOTO 4598-81

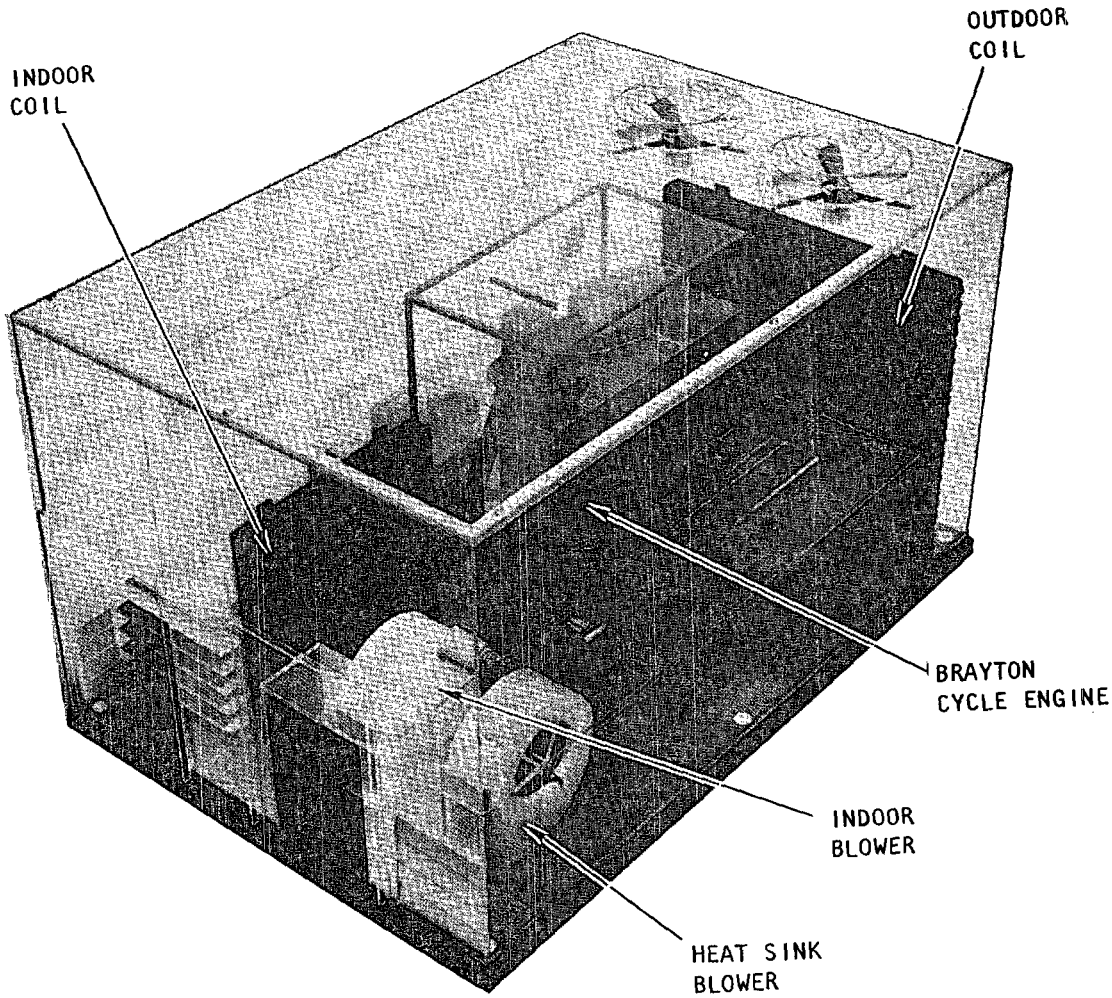

F-33823

Figure 2-3. Conceptual Brayton/Rankine Gas-Fired Space Conditioning System Configuration

as required to satisfy the prevailing building load. For building loads below the minimum capacity, system operation is cyclic. The modulation gas flow range was optimized analytically by considering COP variations with speed and ambient temperature, cyclic performance degradation factors, and average operating time in each 5°F ambient temperature BIN. A significant percentage of total unit operation, regardless of installation site, will be within the modulation range where efficiency is highest. Modulation within the defined gas flow limits results in rotating assembly speeds of between 55,000 and 80,000 rpm and a turbine inlet temperature range of 1100°F to 1600°F. The speed at the cooling design point (95°F ambient) is 75,000 rpm and the resultant turbine inlet temperature is 1570°F.

SYSTEM DEVELOPMENT STATUS

Major system components have been designed and commercial parts selected. Design of the Mark III Brayton engine is essentially complete. The heat pump package is in the detail design phase at Dunham-Bush and is nearing completion. System design/cost analysis is an ongoing effort.

Breadboard system testing is essentially complete; the test data basically confirm the performance prediction analysis. Testing of the Freon side of the development system is continuing. Integration of the development engine assembly with the development Freon system is scheduled for mid-1981.

Engine Development

Complete performance evaluations and hardware optimizations of the engine were performed using the computer model. Steady-state thermal analyses and a stress analysis have also been performed on the package layout. Breadboard testing has been completed, and extrapolated breadboard engine data basically confirm the analytical predictions. With fabrication of the development box enclosure completed, development testing of a fully configured engine assembly will soon commence.

Rotating Assembly Development

With completion of design and fabrication of the Mark III rotating assembly, testing of the Mark II development unit has been terminated. The first Mark III rotating group has been assembled and is completing shakedown tests. The Brayton rotating section and Freon compressor section are being developed as individual components initially, and will be mated and tested as an assembly later. Fabrication of the four prototype Mark III units, with containment provisions added, has been initiated with assembly and test expected in the second quarter of 1981.

Recuperator Development

The recuperator design and structural analysis have been completed. Tooling for the prototype units has been fabricated and two trial cores have been brazed. The first full-size unit has been fabricated and installed in the engine enclosure in preparation for performance evaluation. Detail part assembly of an 18-percent reduced-size unit is in progress.

Combustor Development

Fabrication and testing of the new combustor design were conducted at Eclipse. Results demonstrated that design parameters were met. Development testing was conducted on the prototype configuration at AiResearch as part of the system breadboard test program. Compatibility with the other engine components was confirmed. Design changes were incorporated by Eclipse to reduce thermal losses. A combustor assembly of the latest configuration has been received at AiResearch and placed in the system breadboard test setup.

Controls Development

Breadboard controls testing has been conducted, and all controls have been integrated into the system breadboard test setup. Bench calibration of the modulating gas valve has been concluded; it indicated that satisfactory operation can be attained over the full system range. Initial testing of the overspeed valve has been conducted. Further testing for the final configuration will be done in conjunction with development system testing. Initial control safety device testing was accomplished on the breadboard setup. Final testing will be done on the development engine package. Initial testing of the surge valve, using the Mark II Freon compressor, showed good results. Vacuum start testing on the breadboard test setup has been completed. Testing will continue in conjunction with the development system tests.

Sink Heat Exchanger Development

A life cycle analysis of the design indicated that the life of the unit was compatible with system requirements. Development testing of the unit has been completed. Test results showed that pressure losses were less than predicted on both the hot-gas and cooling-gas sides. Effectiveness, although slightly below the predicted value, was still suitable for the system. Analysis showed that the prototype core could be approximately 10 percent shorter in the no-flow dimension than the development unit. This change will reduce the unit cost without significant impact on system performance.

SECTION 3

DESIGN AND DEVELOPMENT ACTIVITIES

SECTION 3

DESIGN AND DEVELOPMENT ACTIVITIES

This section describes the design and development activities related to the 10-ton Brayton/Rankine space conditioning system during this reporting period. Progress in both engine component and engine/heat pump packaging is discussed in detail. System breadboard testing, which was initiated in the latter part of 1980, is also discussed.

MARK III ROTATING ASSEMBLY

Design and Functional Improvements

Several design and functional improvements were implemented on the Mark III Brayton/Rankine rotating assembly, with major emphasis placed on production implementation and cost reduction.

1. Brayton Turbocompressor

Design improvements incorporated into the new assembly, designated as the Mark III (shown pictorially in Figure 3-1 and in cross section in Figure 3-2), were as follows:

Turbine

(a) The pilot diameter of the nozzle OD was changed to improve producibility.

(b) Other design modifications were made to the nozzle to permit casting.

(c) The turbine and seal on the exit diffuser were simplified.

Compressor

(a) The housing material was changed from ductile iron to aluminum alloy.

(b) The upper bearing housing was redesigned for integration with the compressor housing.

(c) The shaft end was changed from two-piece to one-piece construction. This change also affected the impeller design.

(d) The diffuser pilot and O-ring groove were eliminated to permit the casting of the diffuser.

(e) Mechanical containment of the turbine wheel in case of a trihub failure was incorporated into the diffuser design.

ORNL-PHOTO 4599-81

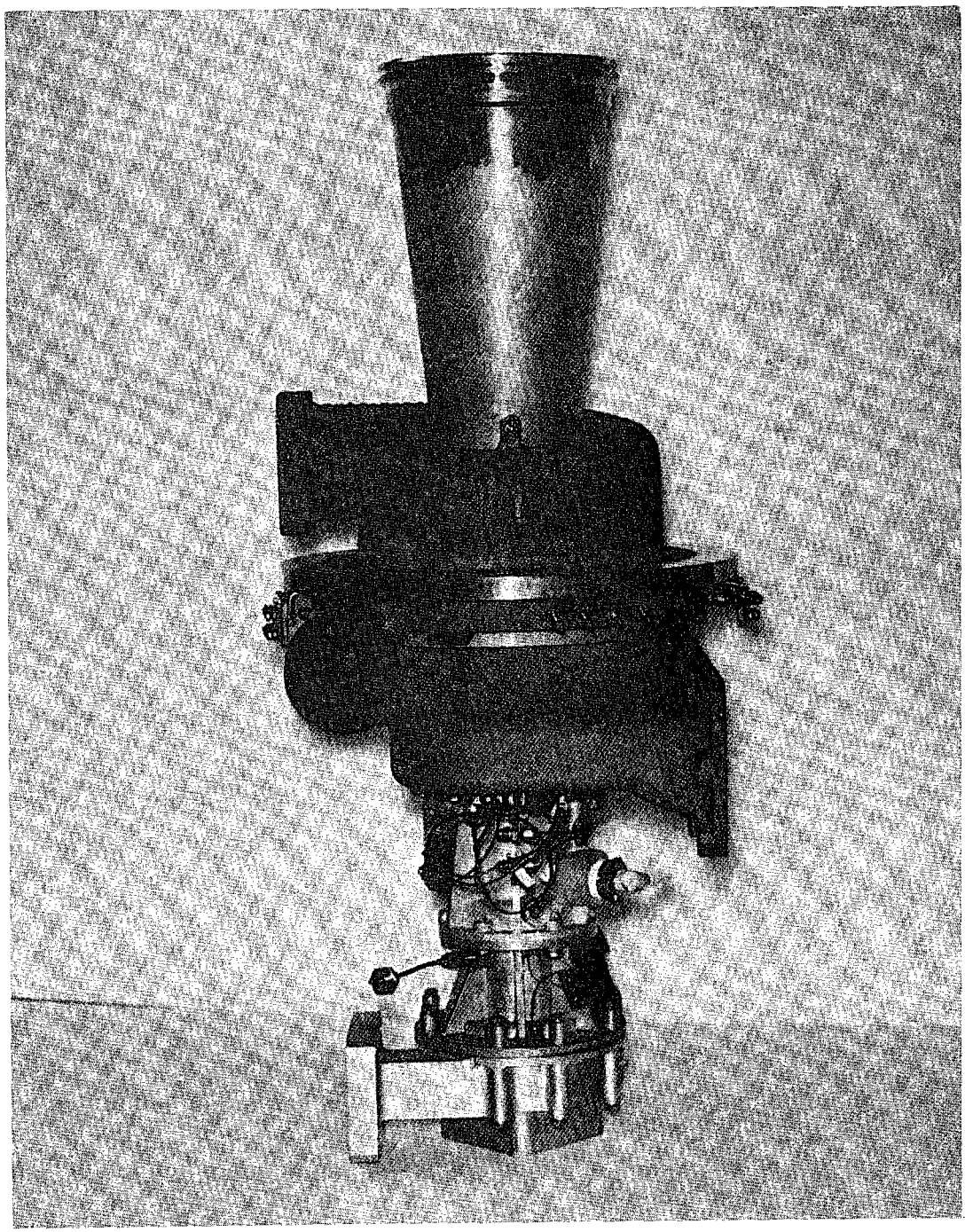

83876-4

Figure 3-1. Mark III Brayton/Rankine Rotating Assembly

ORNL-DWG 81-15021

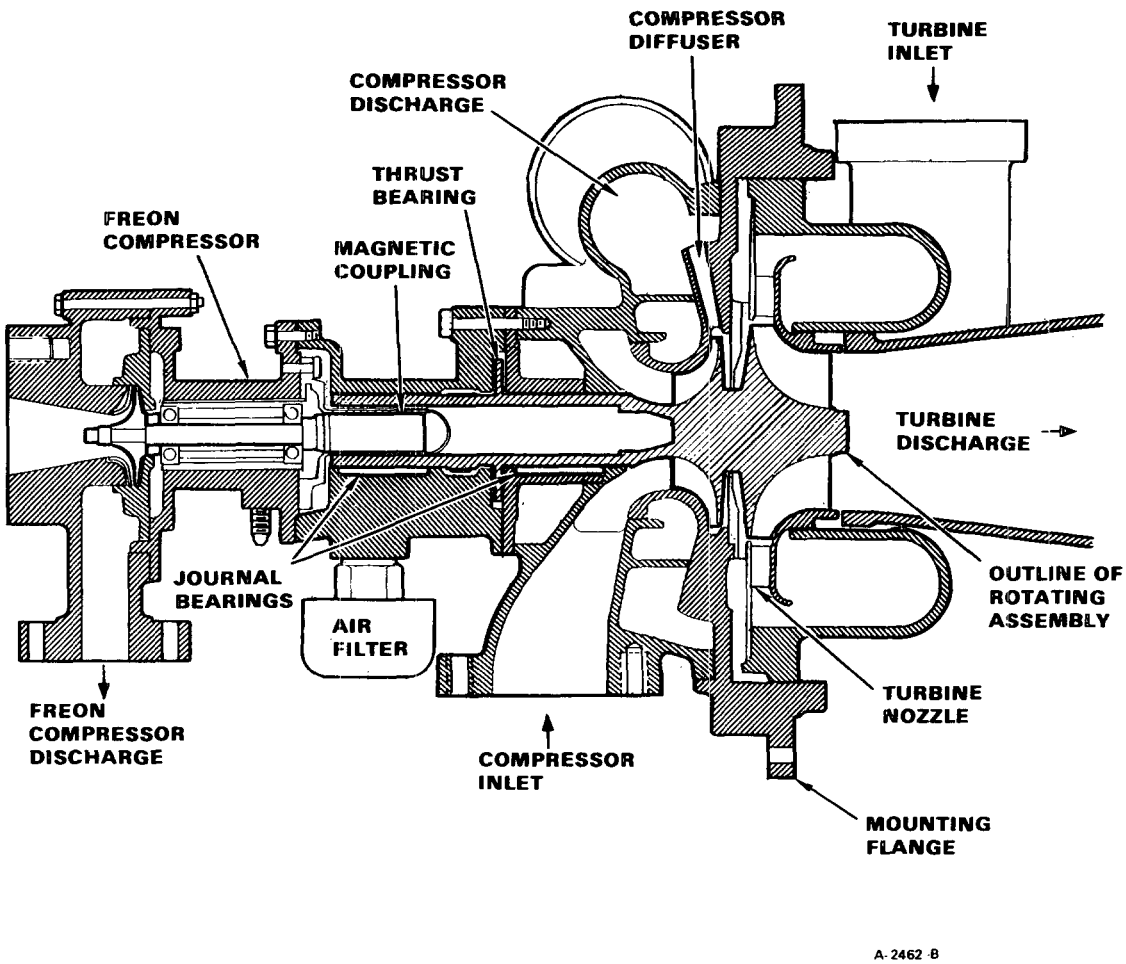

Figure 3-2. Mark III Brayton/Rankine Rotating Assembly Cross Section

(f) The engine mounting flange, which previously was part of the housing, was combined with the diffuser assembly.

(g) The discharge section was enlarged to a 3-in. ID, and rotated 30 deg.

(h) The diffuser exit area was increased.

(i) The inlet region was altered to interface with the sink heat exchanger.

Bearing Housing Assembly

(a) A steel retainer ring at the thrust bearing disc OD was eliminated.

(b) The housing was modified to simplify air plumbing and allow some air to enter the labyrinth compressor inlet seal and maintain pressure in the journal bearing cavity.

(c) An external air filter for bearing cooling was added.

(d) The alignment pin design was modified to reduce cost.

2. Freon Compressor

Design changes to the Freon compressor, shown disassembled in Figure 3-3, were as follows:

Compressor

(a) The impeller diameter was enlarged to a 2-in. OD to meet the requirements of a 75,000-rpm design point.

(b) To improve performance, the vane diffuser was changed to a pipe type and enlarged to accommodate the 2-in. impeller.

(c) The housing, torus, and diffuser materials were all changed to aluminum alloy.

Bearing Housing

(a) The main housing was combined with the bearing carrier to eliminate eight parts and simplify the design.

(b) The bearing lubricant jets were relocated, and the distribution passages altered, to ensure a lubricant mist through both bearings.

(c) To help ensure proper lubricant flow, a slinger was added to the shaft assembly behind the impeller.

(d) A commercial oil, Dupont Zephron 150 SUS, was selected as a replacement for the less readily available MIL-L-6085 oil currently in use for aerospace applications. Final evaluation of the oil will come after completion of development testing

ORNL-PHOTO 4600-81

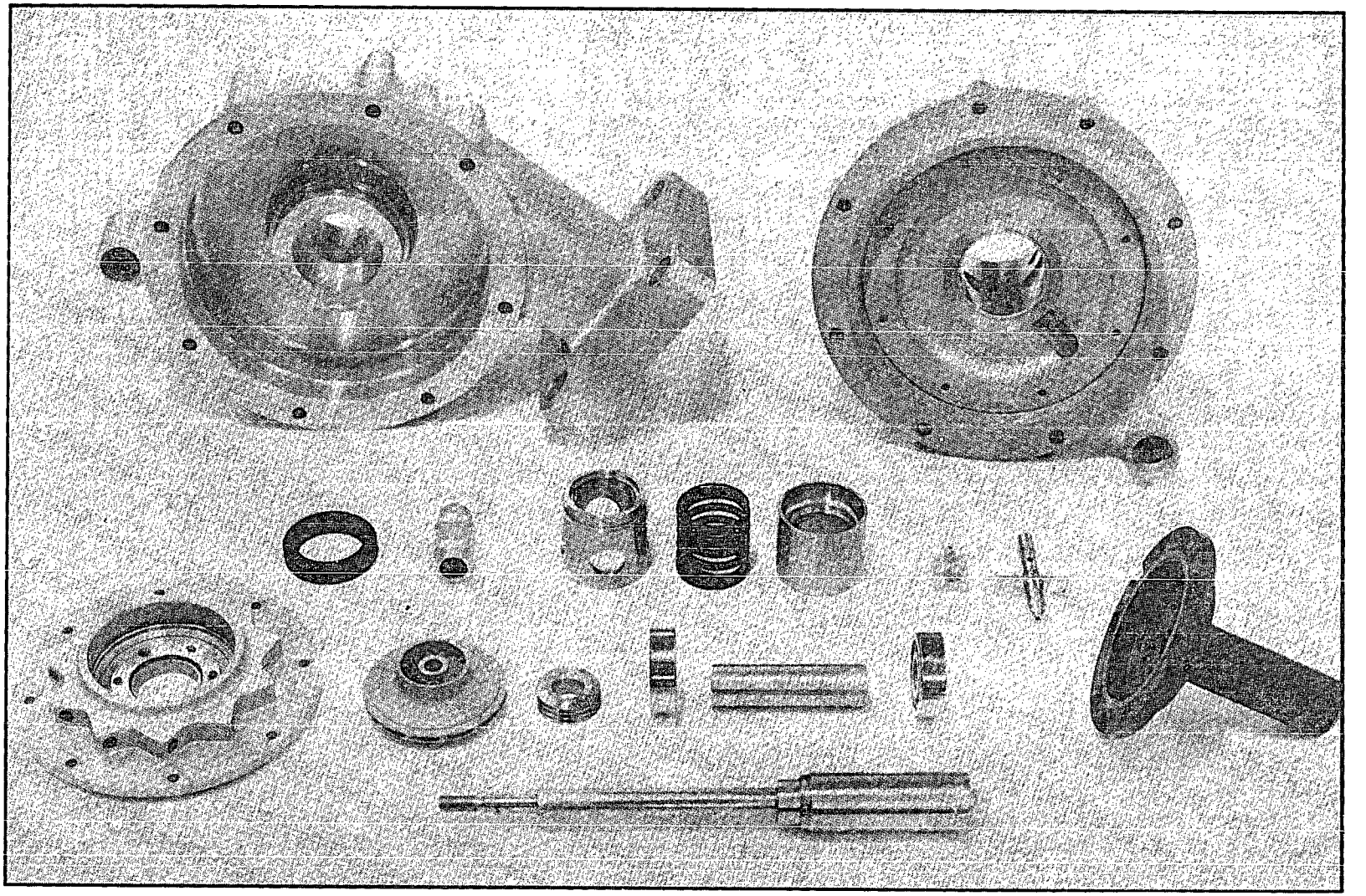

F-33157

Figure 3-3. Disassembled Mark III Freon Compressor

Development Testing

1. Brayton Turbocompressor

Testing of the Mark III Brayton turbocompressor was conducted in breadboard test facility No. 1. A problem in starting the turbine, using the vacuum start procedure, was encountered during initial testing. The cause of the problem was determined to be excessive air leakage between the turbine torus and nozzle, resulting in air bypassing the nozzle. A piston ring, which had been omitted as a potential cost saving, was installed in the housing. This sealed the turbine nozzle and eliminated the turbine starting problem. Further investigation will be conducted to decrease the cost required to maintain this seal around the nozzles.

Further testing revealed two problems: compressor wheel interference resulting in a wheel rub, and shaft excursion at speeds over 70,000 rpm. Damage to parts due to interference was minimal, and the light scuff marks in the shroud were removed by polishing. The interference appeared to be caused by thermal expansion of the compressor inlet housing greater than expected from material change from steel to aluminum alloy. Bearing spring rate tests were rerun on the journal and thrust bearings to evaluate the shaft excursion problem, and results indicated that an increase in journal bearing sway space would improve shaft stability, provided the dynamic balance was within tolerance. Balance tests were then conducted on the shaft assembly and indicated that an axial misalignment could occur during shaft final assembly, resulting in excessive unbalance. Work is underway to conduct a trim balance on the shaft assembly after installation into the final turbocompressor assembly; this action will ensure a correct final shaft balance.

A special dynamometer was constructed for component calibration of the turbocompressor. The dynamometer (shown in Figure 3-4) consists of an 8-kw permanent magnet generator suspended in a hydrostatic bearing housing. A torque arm is connected to the armature, and a load cell is connected to the outer stationary housing. Calibration of the dynamometer was completed using the special Rankine air-drive turbine. Results indicated lower-than-predicted performance, but enough load was generated to calibrate the turbocompressor satisfactorily.

Further testing of the Brayton turbocompressor will be conducted to verify mechanical integrity and performance.

2. Freon Compressor

A special air-drive turbine was constructed using an A7E aircraft cooling turbine with the same female magnetic coupling drive used in the Brayton unit. This drive turbine and the Mark III Freon compressor were installed in the newly constructed test facility No. 2. During initial testing of the compressor, a failure occurred involving the stationary diaphragm covering the male compressor magnets. Evaluation of the failure indicated possible expansion of the diaphragm and a rub with the female magnets. The diaphragm wall thickness was increased and testing continued. Subsequent testing showed excessive rotor excursion and high vibration. The compressor was removed and a resilient

ORNL-PHOTO 4601-81

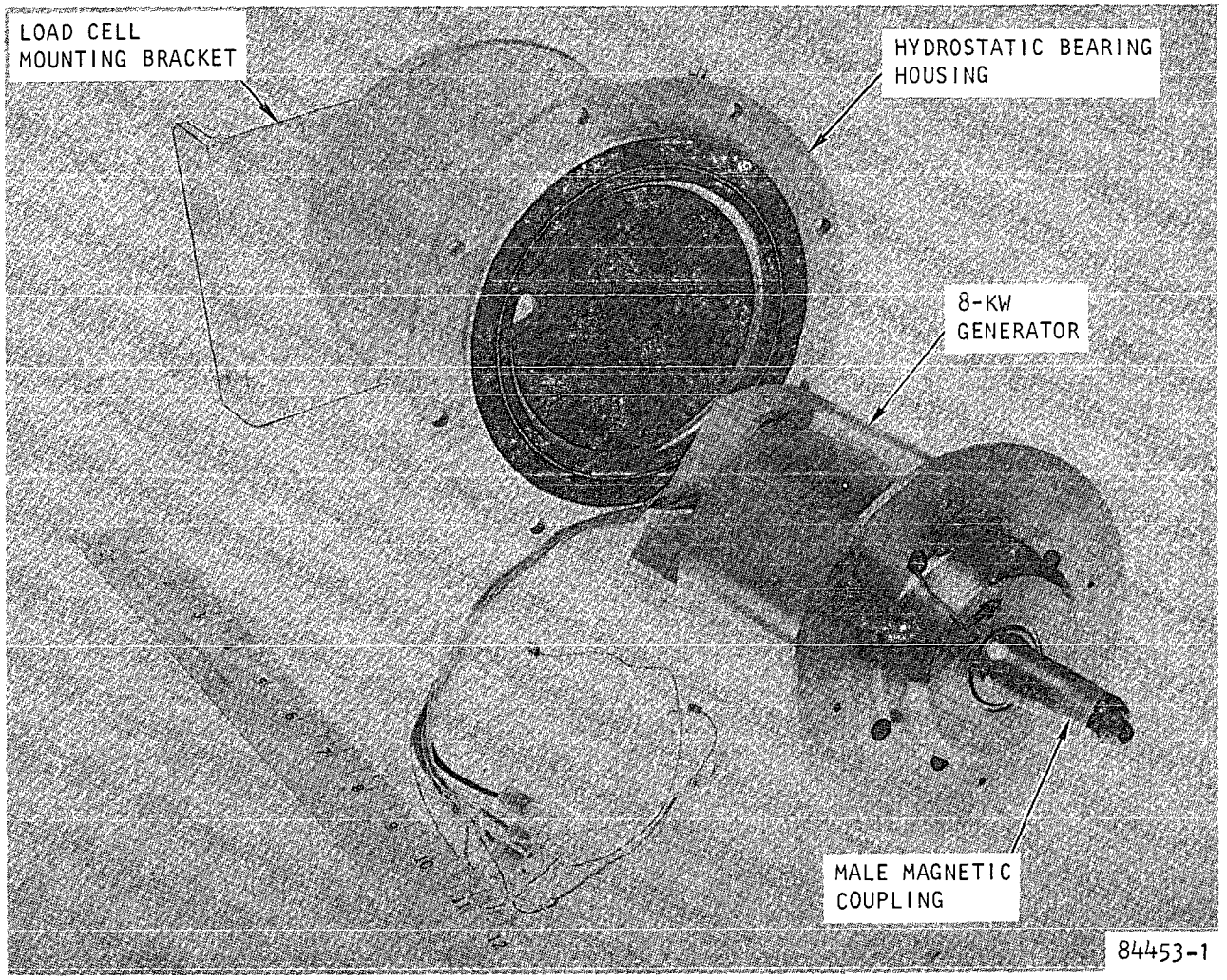

F-33956

Figure 3-4. Special Dynamometer Used to Calibrate Mark III Brayton Turbocompressor

bearing mount, which had been used on the earlier Mark II unit, was installed, changing the natural frequency of the rotor suspension system. Testing indicated that the new mount improved shaft dynamics with reduced, but still excessive, vibration. Component calibration testing continued until another diaphragm failure occurred. A detailed design analysis has been initiated, concentrating on the diaphragm design and the possible influence of bearing lubricant entering the diaphragm cavity and causing viscous forces, which generated extreme pressure and temperature. Efforts are also underway to increase the clearance between the female magnets and the diaphragm.

Conclusions

As expected with any new state-of-the-art machine, several development problems have been encountered in the Brayton/Rankine rotating unit; these problems are being resolved. Performance for both the Brayton and Rankine components appears to be very near the predicted values, and mechanical integrity, although still not satisfactorily demonstrated, will be achieved during the next few months. Fabrication of parts for four new prototype Mark III Brayton/Rankine units has been initiated. Refurbishment of the development unit is planned in the future for use as a demonstration unit.

RECUPERATOR

Analytical Design Effort

The recuperator effort began with the investigation of five analytical design approaches, two of which were eliminated because of excessive weight and/or excessive number of detail parts. Cost tradeoffs of the remaining three resulted in the selection of the plate-fin formed, tube-plate design shown in Figure 3-5.

Thermal and Structural Analysis Results

Concurrent with the analytical design effort, an investigation of potential recuperator materials, thermal and structural studies of the plate-fin design, and a review of alternate, all-prime-surface heat exchangers were conducted.

Major criteria in material selection for the plate-fin recuperator design were the stress levels in starting and operating conditions and the corrosion characteristics at operating temperatures. For the subatmospheric cycle in which the recuperator operates, the low operating pressure would induce minimal structural stresses, with the predominant stresses being thermally induced. For the initial study, the steady-state design point temperature gradient was utilized as input to a two-dimensional structural analysis computer model. The results of this analysis were as follows:

(a) Maximum equivalent steady-state stress was 15,800 psi. This occurs in a cold region (approximately 500°F) and is at an acceptable level.

(b) The steady-state stress at the manifold-to-core transitions (corners) is relatively low (approximately 5000 psi at the hot end) and is at an acceptable level.

Recirculating-Fluid Cooling Systems

AiResearch has designed, developed, and qualified numerous recirculating-fluid cooling systems for various types of equipment ranging from delicate electronic parts to high-flow lubricating oil and hydraulic oil systems. These systems have either liquid or gas closed loops to cool the equipment. Depending on the requirements of each application, the system may include pumps, fans, heat exchangers, valves, accumulators, reservoirs, switches, and controls.

The typical system shown below cools the U.S. Army Hawk Missile mobile ground radar equipment. This air-to-liquid electronic equipment cooling unit is used for environmental conditioning of electronic equipment mounted in radar vans. The cooling unit is extremely compact and requires only half the space originally allotted. Controls include a low-temperature fan switch and low-flow, high-temperature, and high-pressure safety interlock switches. The fluid circuit is a dual system that cools the radar transmitter tubes directly and provides cooling fluid for the internal fan heat exchanger unit used to cool the closed high-voltage power supply compartment. The heat sink is ambient air. The cooling system weighs 130 lb, has dimensions of 24 by 24 by 20 in., and provides 10 kw of cooling capacity. The cooling fluid is Coolanol 45 maintained at a supply temperature of 130°F on a 125°F hot day at sea level using ambient air as the heat sink.

ORNL–PHOTO 1438–82

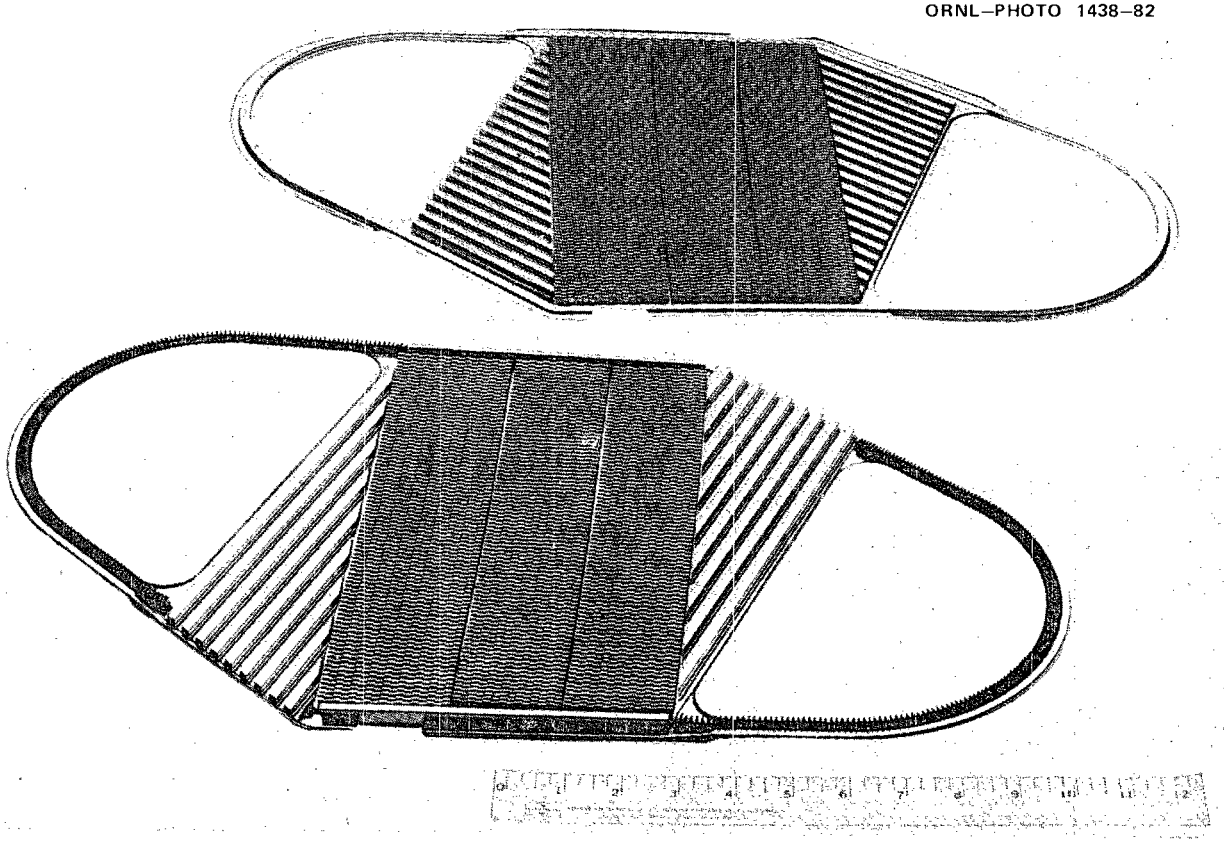

Figure 3-5. Recuperator Details

F-33254

(c) The hot-inlet face had an equivalent steady-state stress of 12,000 psi. This stress occurs in a region exposed to 1200°F and exceeds the strength capability of the low-cost material contemplated, which is type 409 ferritic stainless steel.

To alleviate the problem of excessive stresses at the hot-inlet face, further consideration was given to reducing the stress at the leading edge by (1) thermal expansion coefficient mismatch (prestressed structure), (2) use of bimetallic tube plates, and (3) various means of decoupling the hot end of the recuperator from the cold end. A more cost-effective approach, however, was considered to be geometric variations. Unfortunately, acceptable stress levels could not be achieved with the latter approach.

Structural Evaluation Results

Structural evaluations of design approaches intended to achieve reduced stresses at the hot-inlet face were then made, utilizing a representative finite element model. Similarity to existing high-temperature recuperator configurations was assumed, thus assuring a reasonable representation of stress distribution. This initial analysis considered the steady-state temperature condition only. Results showed that control of thermal stress at the tube-plate leading edge on the hot-inlet face of the core was of critical importance in providing a long cyclic life. The stress in the critical location can be reduced by proper selection and placement of materials with different coefficients of thermal expansion. The critical stress in a type 409 stainless steel tube plate can be reduced from 10.4 to 6.9 ksi, when a high coefficient of expansion material is brazed on the leading edge. An additional reduction to about 4.0 ksi is obtained with a bimetallic tube plate, when a properly located diagonal weld is made between type 347 stainless steel on the cold end and type 409 stainless steel on the hot end.

Computer Model Program

A layout drawing of the tube plate was then made, configured on the basis of the analytical results described above and yielding acceptable pressure losses and flow distributions. From dimensional data and performance requirements, detailed computer thermal and structural models of the tube plate were prepared. Using a three-dimensional, finite element program, both steady-state and transient conditions were examined. With improved modeling, physical configuration changes, and more precise programming, the stress levels at the hot-inlet face were lowered sufficiently to permit the use of type 409 stainless steel. The transient analysis, using the desired system startup transient, indicated lower stress levels than those occurring at steady-state conditions.

The review of alternate, all-prime-surface matrices produced potential advantages too small to justify the necessary development effort at this phase of the program.

Size Reduction Study

After establishing a satisfactory recuperator design, a system study of the engine was initiated to reduce recuperator size. A heat exchanger performance computer program was utilized to predict pressure loss and effectiveness

for a recuperator of reduced stack height. This information was entered into the system performance computer program, which then was used to determine a new system design point. Preliminary results indicated that the pressure drop would increase somewhat at the new design point as a result of using the smaller unit, but that heat transfer performance in terms of effectiveness was only slightly reduced. This apparent anomaly is attributed to several factors:

(a) The system performance computer program was balanced at a somewhat reduced flow rate, which tended to raise the effectiveness. This trend, of course, was offset by the reduced size.

(b) The airflow per heat exchanger passage was increased, which tended to increase the heat transfer coefficient, and thus offset the decrease in heat transfer area.

(c) With a higher flow rate per passage, the effect of axial conduction is reduced, so that heat is transported from the hot end to the cold end of the recuperator by conduction through the tube plates. With higher flows, the heat flux returning to the cold end is diminished, thus reducing the performance penalty.

From this effort, a recuperator with a stack height reduced by 16 percent resulted, with attendant weight and production cost reductions.

Prototype Fabrication

Fabrication of the -1 recuperator, shown in Figure 3-6, has been completed and the unit has been installed in the engine package enclosure in preparation for performance evaluation testing. Detail part assembly of the -2 recuperator, which incorporates the reduced stack height, has begun.

COMBUSTOR

Design Approach

Initially Eclipse Manufacturing Co. constructed a test burner from mild steel and conducted preliminary tests at full load and low load. The burner, shown in Figure 3-7, was a cylindrical tube type, 4 in. in diameter by 18 in. long. Initial results were encouraging. With the burner operating at 175,000 Btu/hr input heat, the flame length was approximately 18 in. and burner efficiency was in excess of 95 percent, as indicated by measured gas/airflow and exhaust products. The burner also operated well at various fuel/air ratios down to 50,000 Btu/hr input. Testing was conducted using ambient air for the fresh air to the burner. The test setup is shown in Figure 3-8.

The combustor was then redesigned and retested by Eclipse under several conditions simulating the full operating range of the blower and burner. Diluent gas, fresh air, and burner gas flows and temperatures were varied individually and data were taken at each condition. Overall average efficiency was 97.8 percent compared with the 97 percent design minimum. Efficiency was calculated from a total heat balance across the combustor. Maximum pressure drop across the burner was 1.5 in. H_2O, as compared to the design pressure

ORNL-PHOTO 4603-81

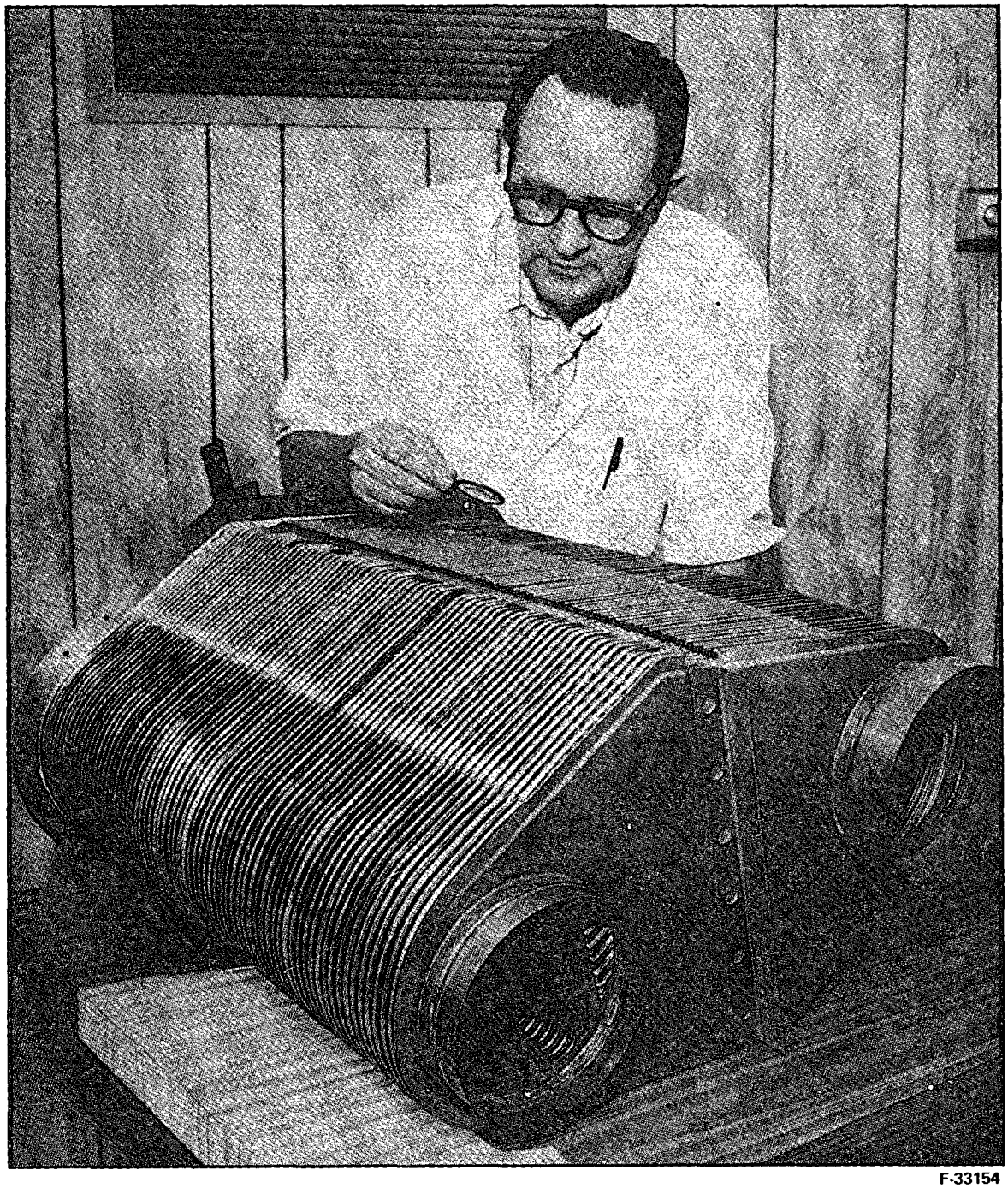

F-33154

Figure 3-6. Development Recuperator, 194440-1 Configuration

ORNL-PHOTO 4604-81

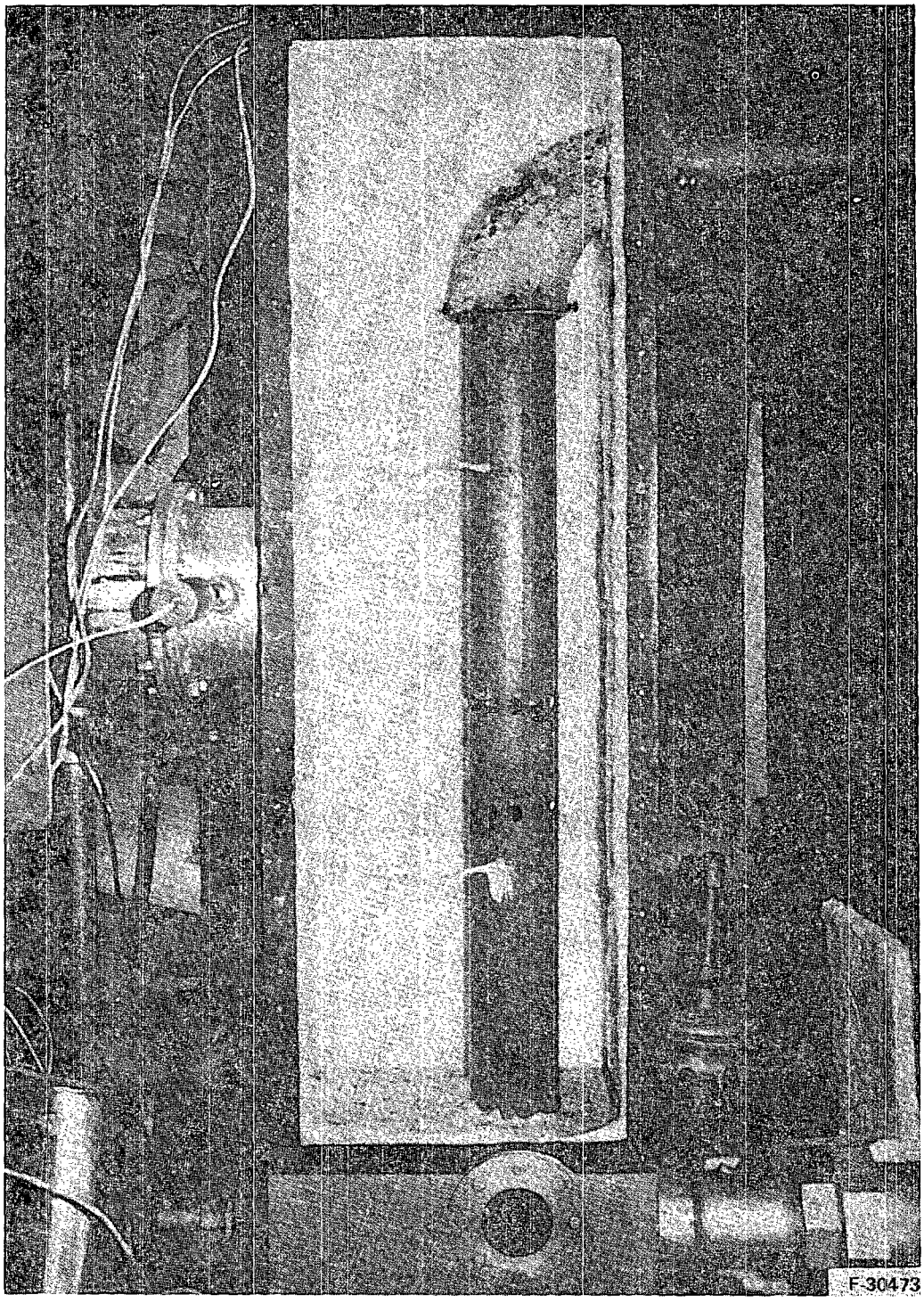

Figure 3-7. Initial Combustor in Test Setup

ORNL-PHOTO 4605-81

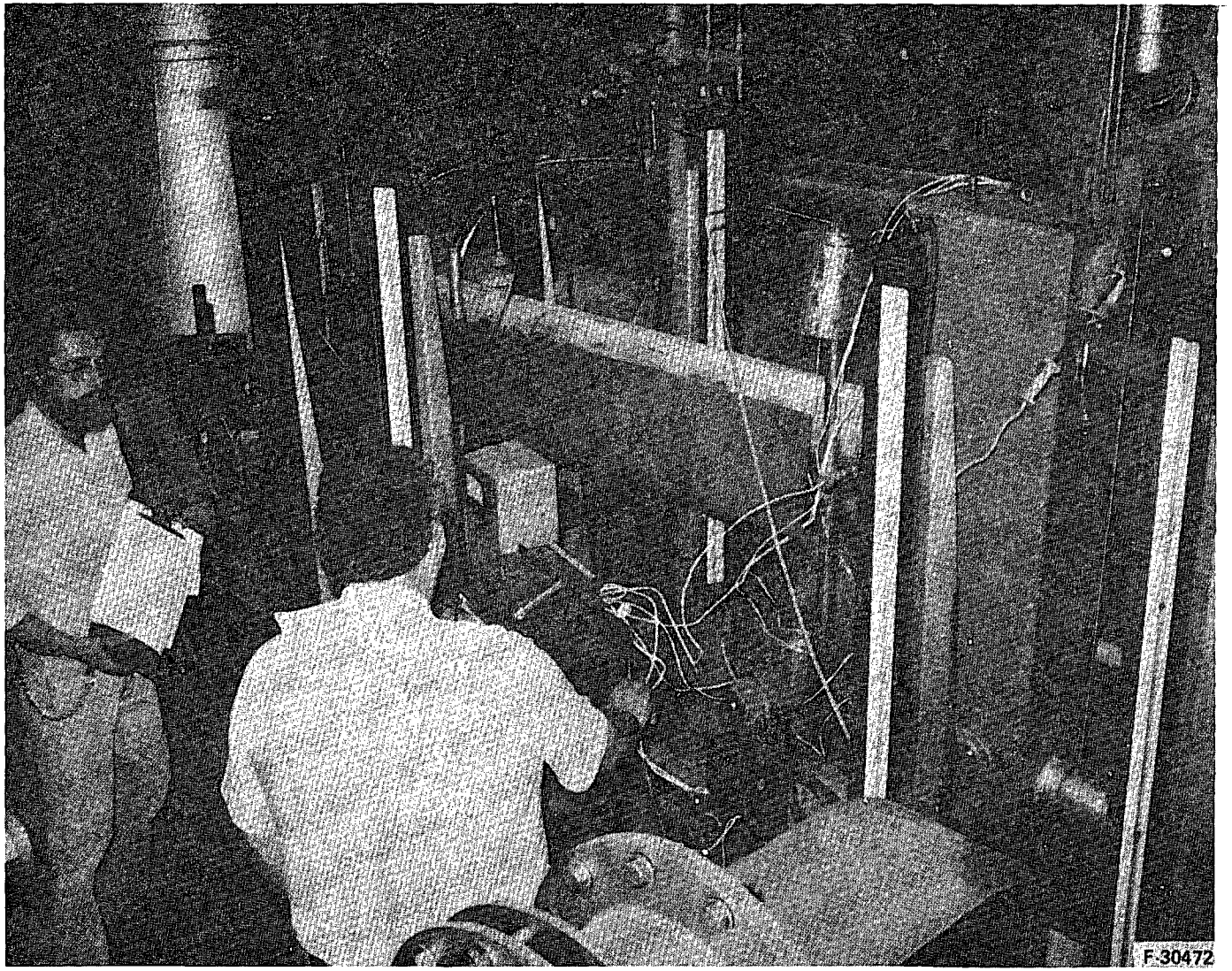

Figure 3-8. Combustor Test Setup

drop of 2.0 in. H_2O maximum. The axial flame length was 26 in., which exceeded the design requirement of 18 in. maximum, and metal scaling occurred on the burner inner nozzle. Eclipse modified the burner in an attempt to reduce the excessive flame length, and the nozzle scaling problem was eliminated by changing the nozzle material from type 316 to type 330 stainless steel. Reduction of flame length was unsuccessful on this configuration.

A new combustor was then designed and a mild steel test sample constructed. The new design used a tangential burner, which imparted a continuous swirl to the combustion products. The tangential design allowed a longer total flame length, while retaining the desired axial flame length. Testing indicated an acceptable axial flame length with minimal pressure drop.

Prototype Testing

Testing of the new combustor design in the prototype configuration first was conducted at Eclipse. Figure 3-9 shows the combustor arrangement inside the test box. Figure 3-10 shows the test box and sensors from the burner end. The prototype combustor utilized a multinozzle cast burner mounted tangentially relative to the combustion chamber (see Figure 3-11). Three types of tests were conducted:

(a) System simulation tests to evaluate axial flame length at various gas flows and air/fuel ratios.

(b) Pressure drop versus flow for both the fresh air and diluent gas circuits, measured individually and in combination.

(c) Burner efficiency tests to determine the minimum air/fuel ratio yielding complete combustion.

Results demonstrated that the flame length was within acceptable limits throughout the full operating range, provided the air/fuel ratio is maintained above the stoichiometric ratio. Pressure loss characteristics, shown in Figure 3-12, were very close to design values.

Efficiency test results were not totally conclusive quantitatively because of facility and instrumentation limitations. Tests were conducted using an oxygen and combustibles analyzer, which indicated that the minimum excess air (above stoichiometric) required for complete combustion was between 0 and 10 percent. Thermal data were also taken, and after correction for losses, indications were that system requirements could be met.

A new combustor test box was constructed and installed in the AiResearch breadboard test setup shown in Figure 3-13. A commercial flame safety and ignition system was also added to the setup. Figure 3-14 shows the flow connections from the combustor test box. Figure 3-15 shows the upper burner section of the combustor showing how the flame is tangentially fired into the combustor. Figure 3-16 shows the lower diluent section of the combustor, where diluent air is drawn into the combustor and mixed with the combusted gas from the burner section.

ORNL-PHOTO 4606-81

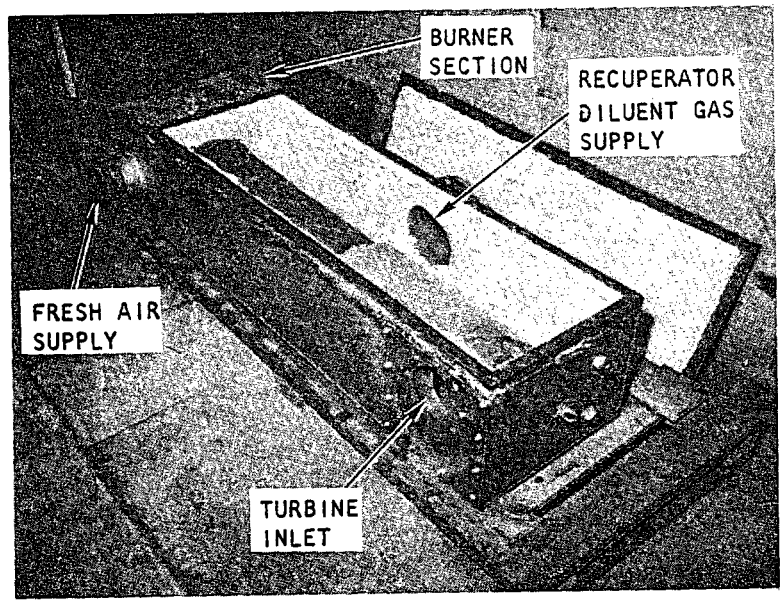

Figure 3-9. Test Enclosure With Cover Removed

ORNL-PHOTO 4626-81

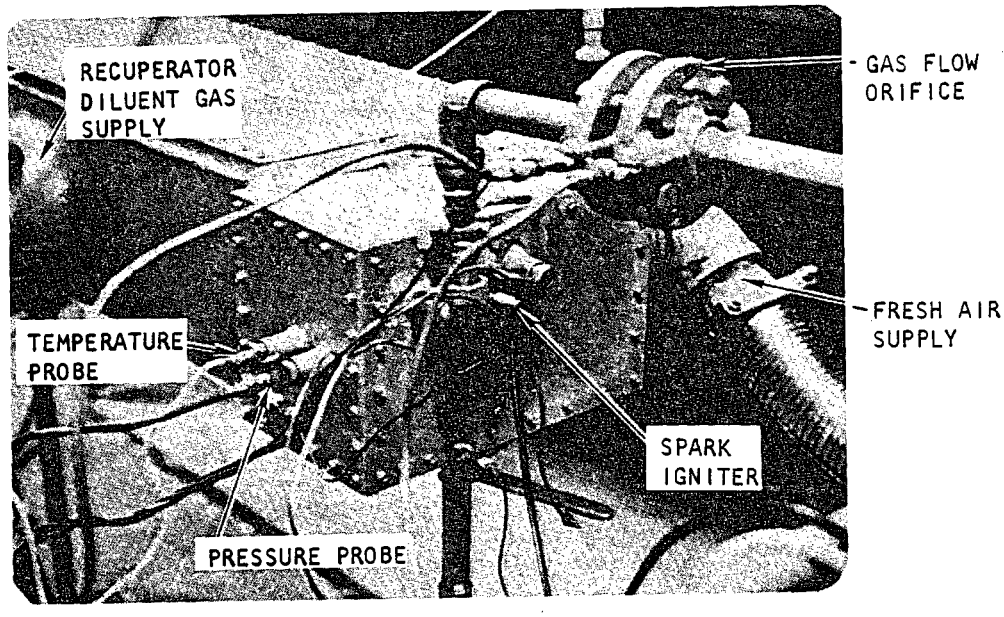

Figure 3-10. Prototype Combustor Test Setup

F-31175-A

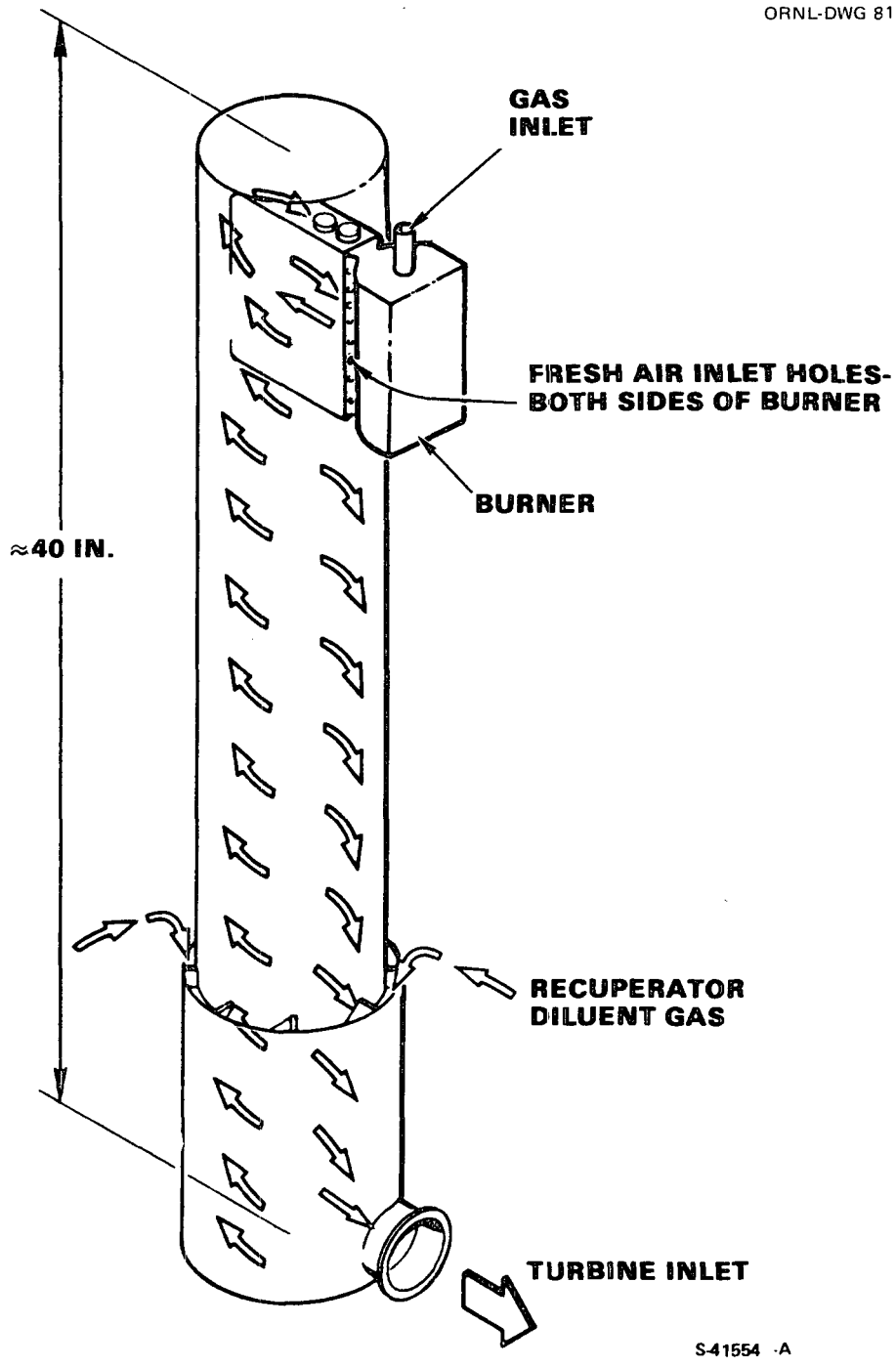

Figure 3-11. Flow Diagram of Prototype Combustor

ORNL-DWG 81-15023

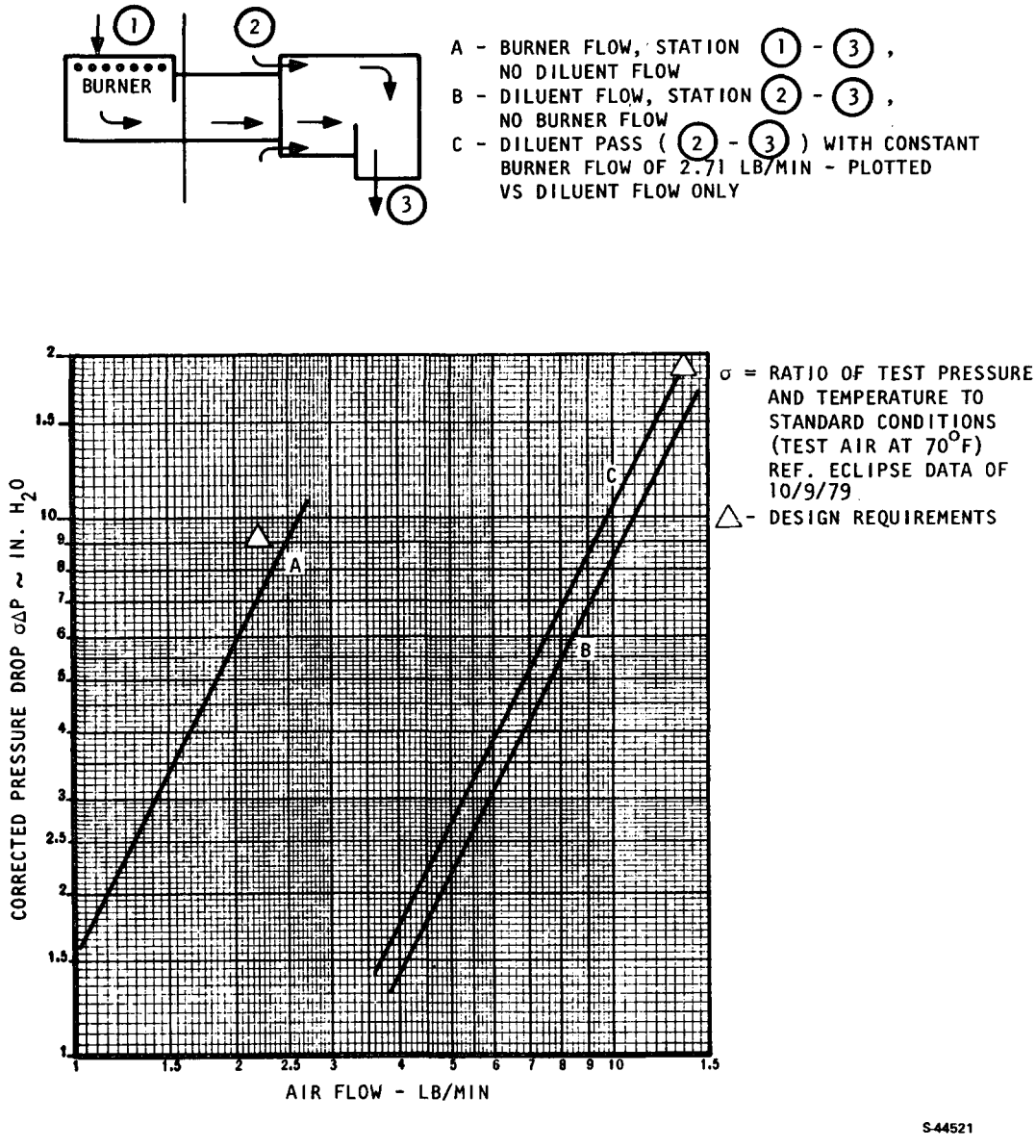

Figure 3-12. Combustor Pressure Loss Characteristics

ORNL-PHOTO 4607-81

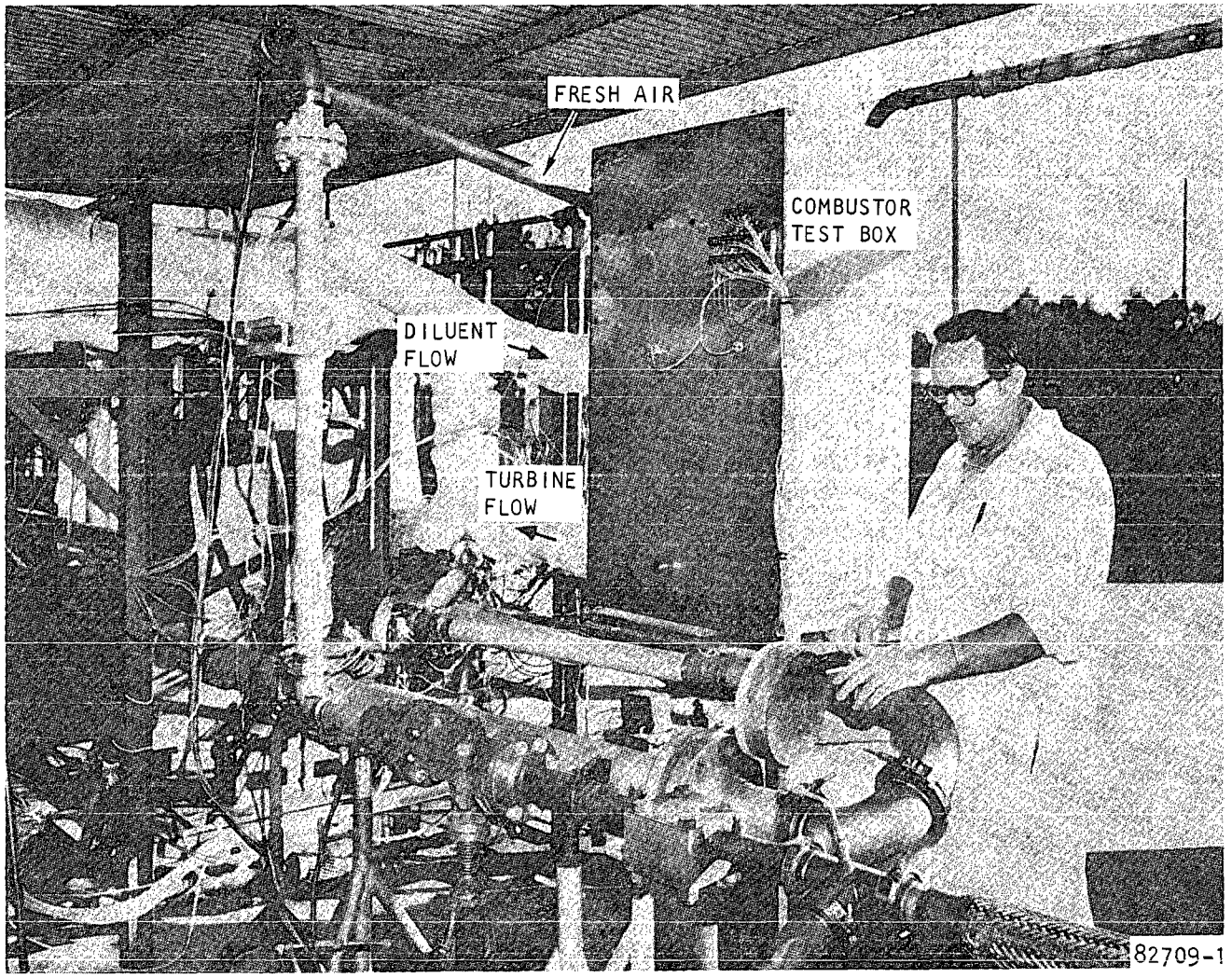

F-31446

Figure 3-13. Breadboard Test Setup of Combustor Test Enclosure

ORNL-PHOTO 4624-81

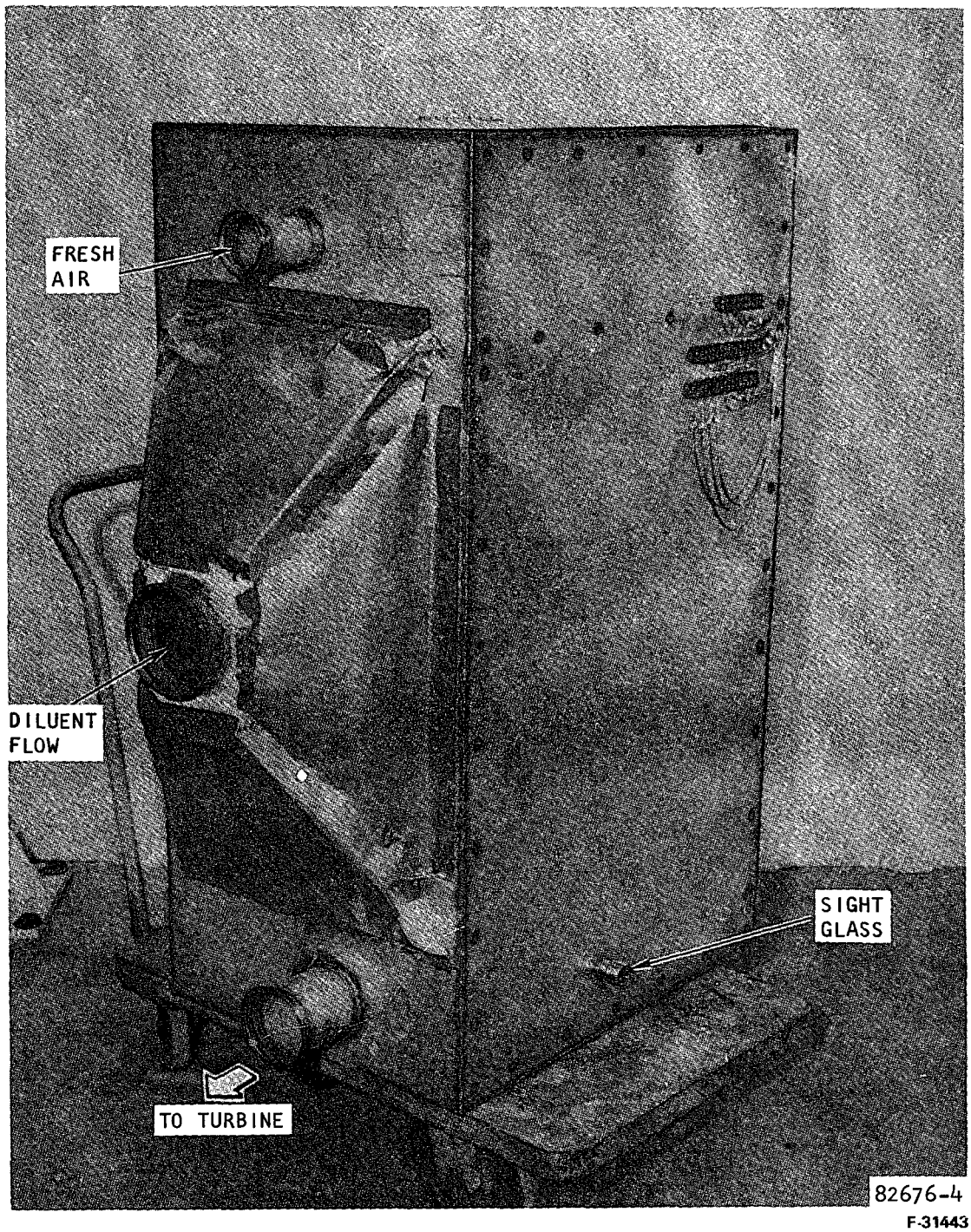

F-31443

Figure 3-14. Combustor Enclosure and Flow Connections

ORNL-PHOTO 4608-81

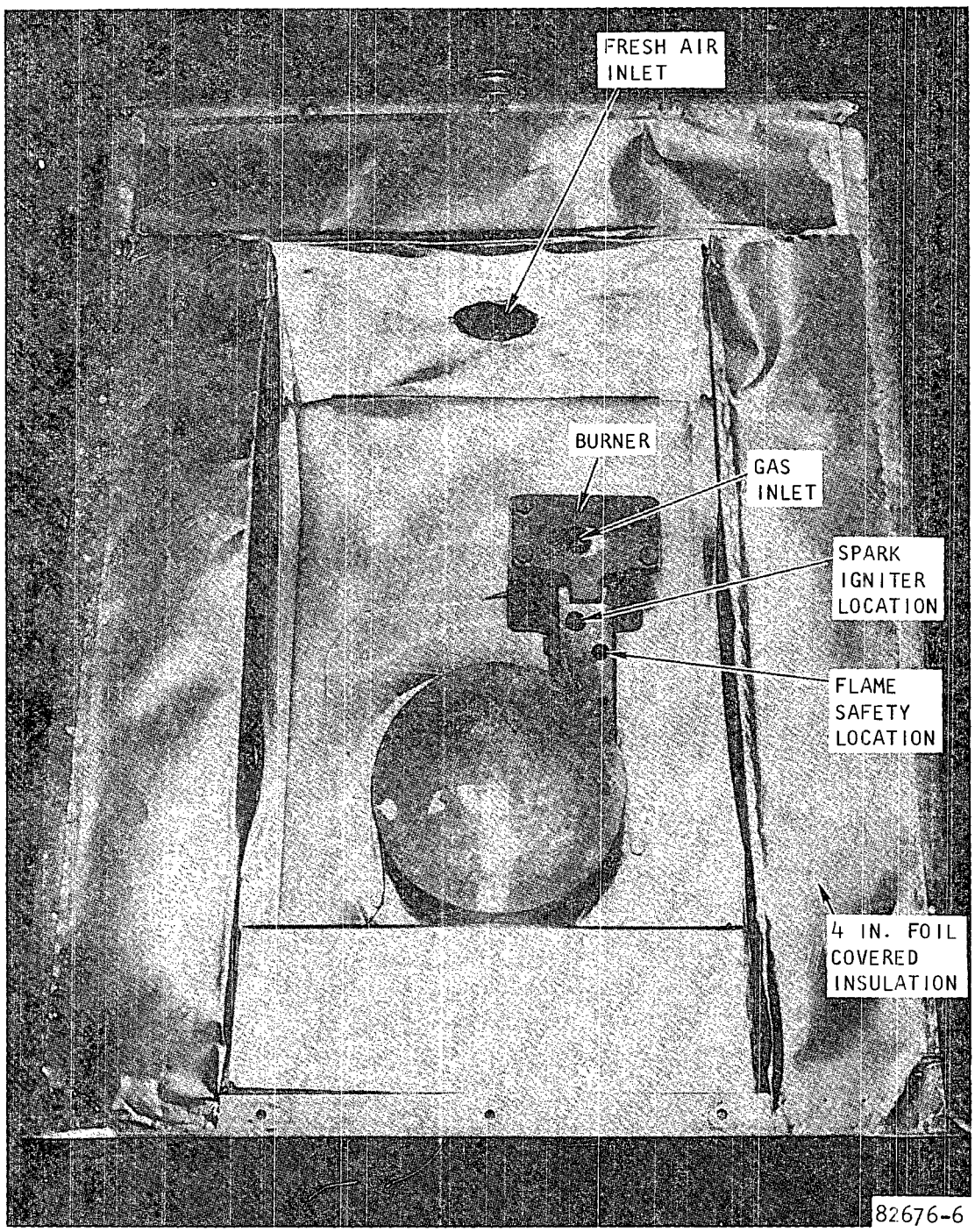

F-31445

Figure 3-13. Plan View of Combustor Showing Tangential Burner

ORNL-PHOTO 4609-81

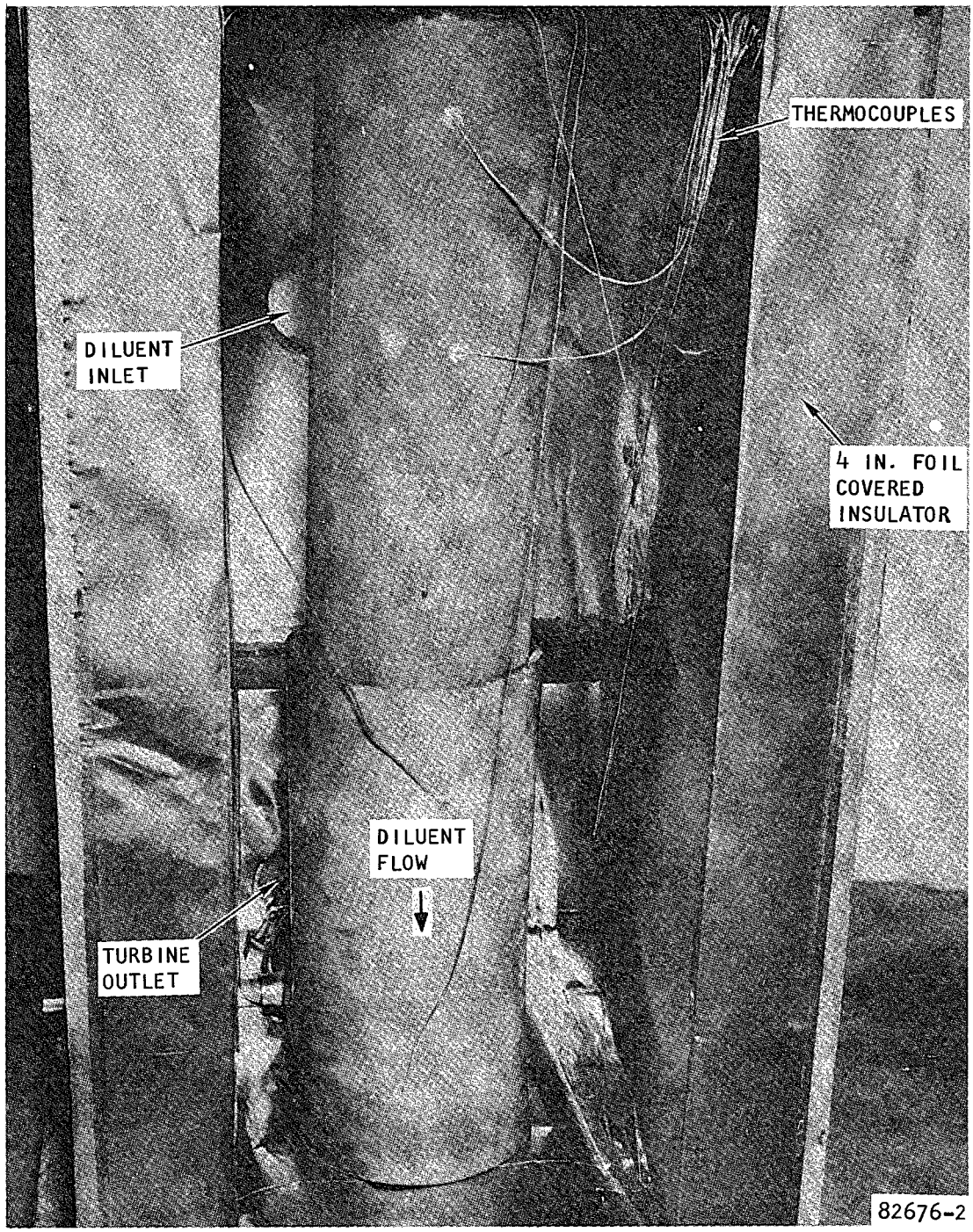

F-31444

Figure 3-16. Lower Section of Combustor Showing Diluent Inlet Scarf

After initial testing, several modifications were made to the combustor and combustion chamber, as described below.

(a) External insulation was added to the combustion chamber to eliminate excessive thermal losses through the upper section of the combustor box. The losses occurred because the internal panel between the fresh air and diluent chambers was in direct contact with the external panels.

(b) A longer diluent tube, shown in Figure 3-17, was added in the lower combustion chamber to reduce radiation effects on the box walls.

(c) The spark ignitor was redesigned and relocated to ensure fuel ignition during high gas flow startups.

(d) The flame safety sensor was relocated to increase the sensitivity of the monitoring circuits.

After relocation of the combustor flame sensor, nuisance tripping of the gas valve stopped. Combustor testing was continued to verify combustor pressure drop and efficiency with the combustor modified to simulate the final configuration (i.e., extended lower diluent tube). The measured pressure drop was well within the design limit. Efficiency was measured by use of a mobile emission analyzer (Figures 3-18 and 3-19). The analyzer data listed in Table 3-1 indicated almost 100-percent efficiency and a very low fuel-to-air ratio, which was attributed to system leakage from the ambient air. This leakage precluded verification of efficiency through a thermodynamic balance.

Design Optimization Studies

The source control drawing for the combustor was updated to the latest configuration (i.e., extended lower diluent tube, relocated flame sensor and spark ignitor) and forwarded to Eclipse for evaluation and design optimization.

Eclipse recommended that the burner material be changed to a high-temperature alloy to allow for an increased fresh air temperature. Eclipse also supplied cost data for development, prototype, and production units. Further design optimization will be required for reducing production costs to meet pricing goals. A combustor assembly for the development engine has been incorporated into the system breadboard test setup.

CONTROLS

Starting Method Selection

Several system starting concepts were initially investigated; these can be broadly classified according to the location of the starter on the Brayton turbocompressor shaft or the Rankine compressor shaft. In line with the investigation, a detailed analysis was made of the system starting torque characteristics, including torque-speed relationships for various inlet temperatures of the Brayton turbocompressor and its bearings and of the Rankine compressor and its bearings.

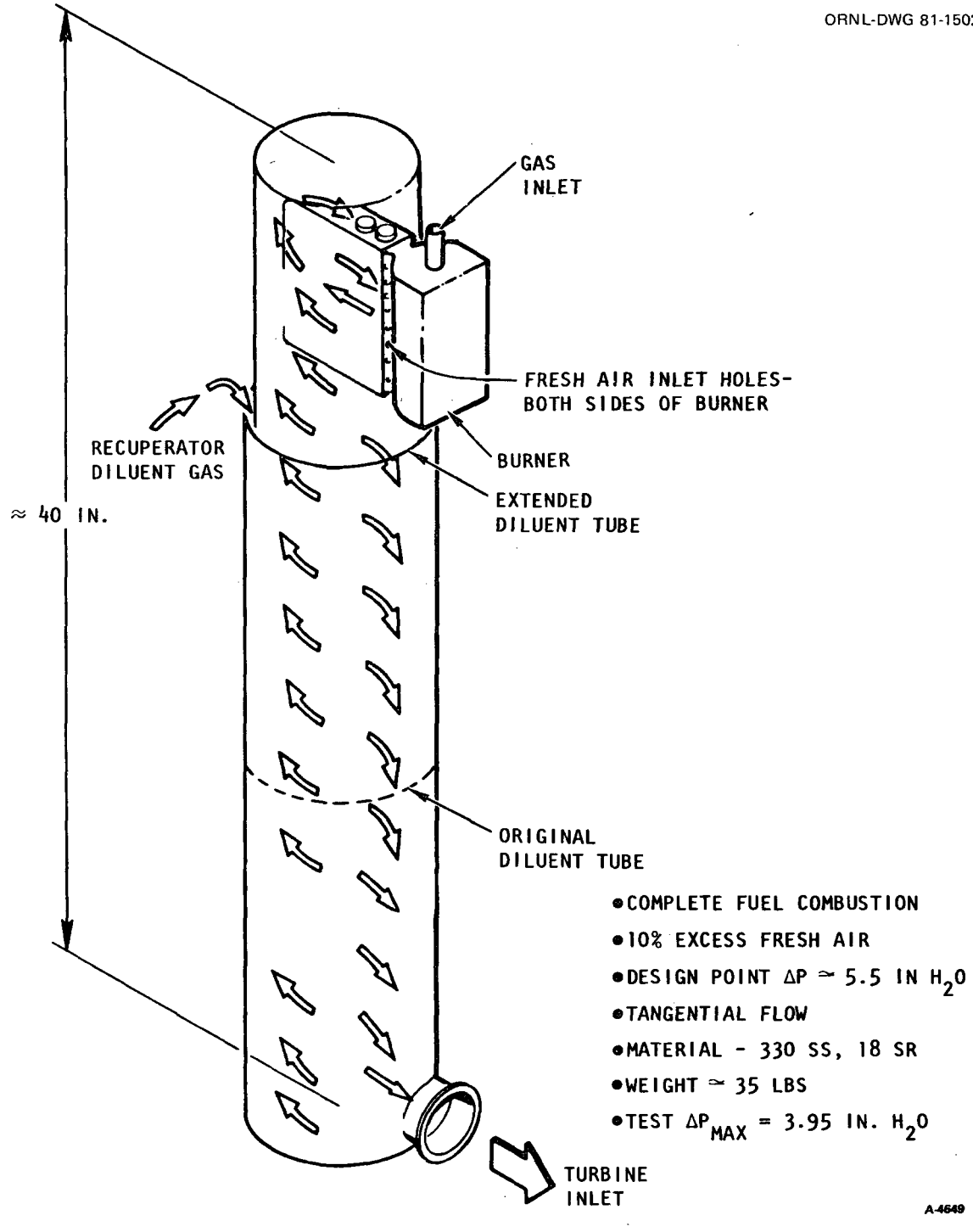

Figure 3-17. Flow Diagram of Prototype Combustor Showing Extended Diluent Tube

ORNL-PHOTO 4610-81

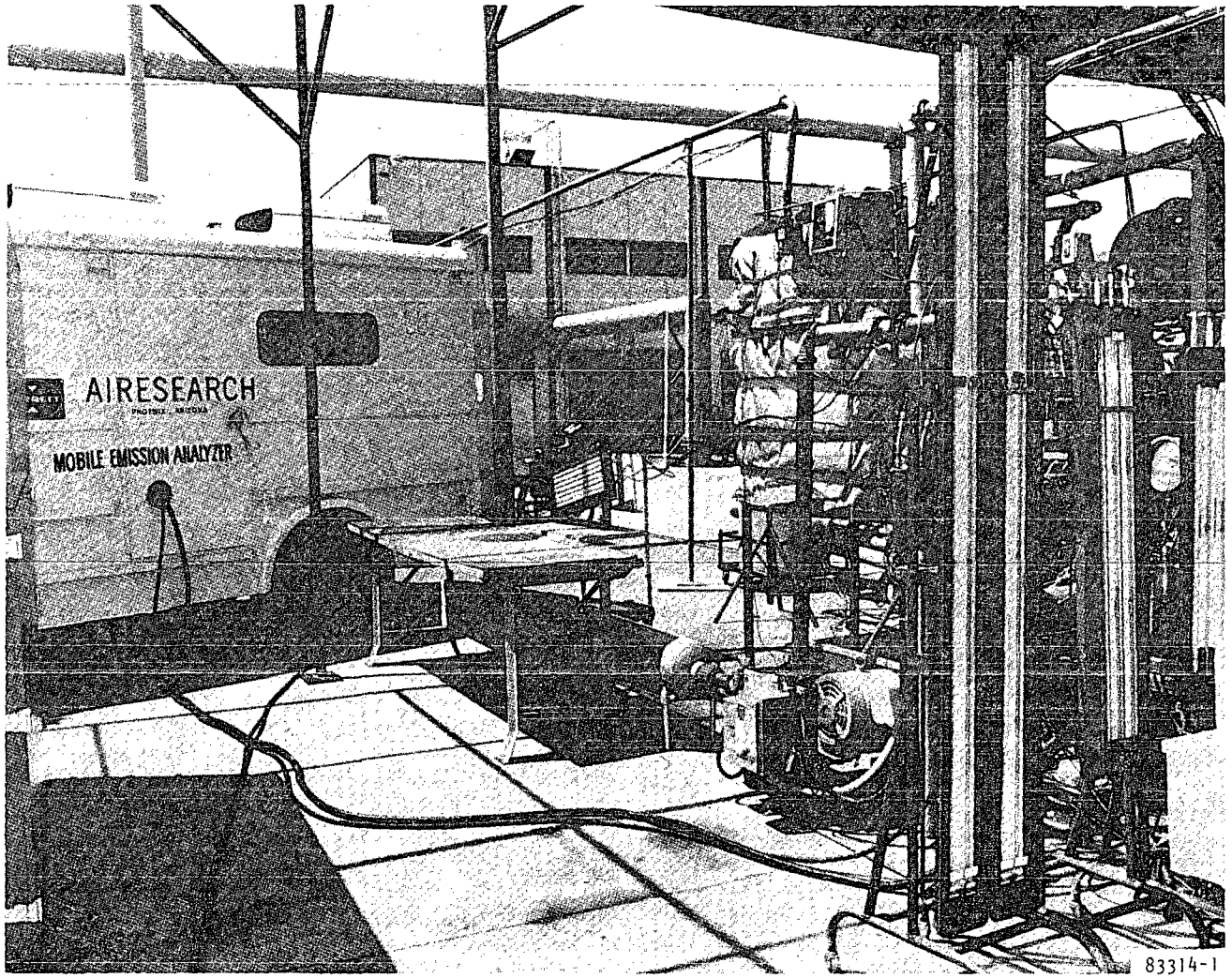

F-32688

Figure 3-18. Mobile Emission Analyzer Integrated with Breadboard Test

ORNL-PHOTO 4611-81

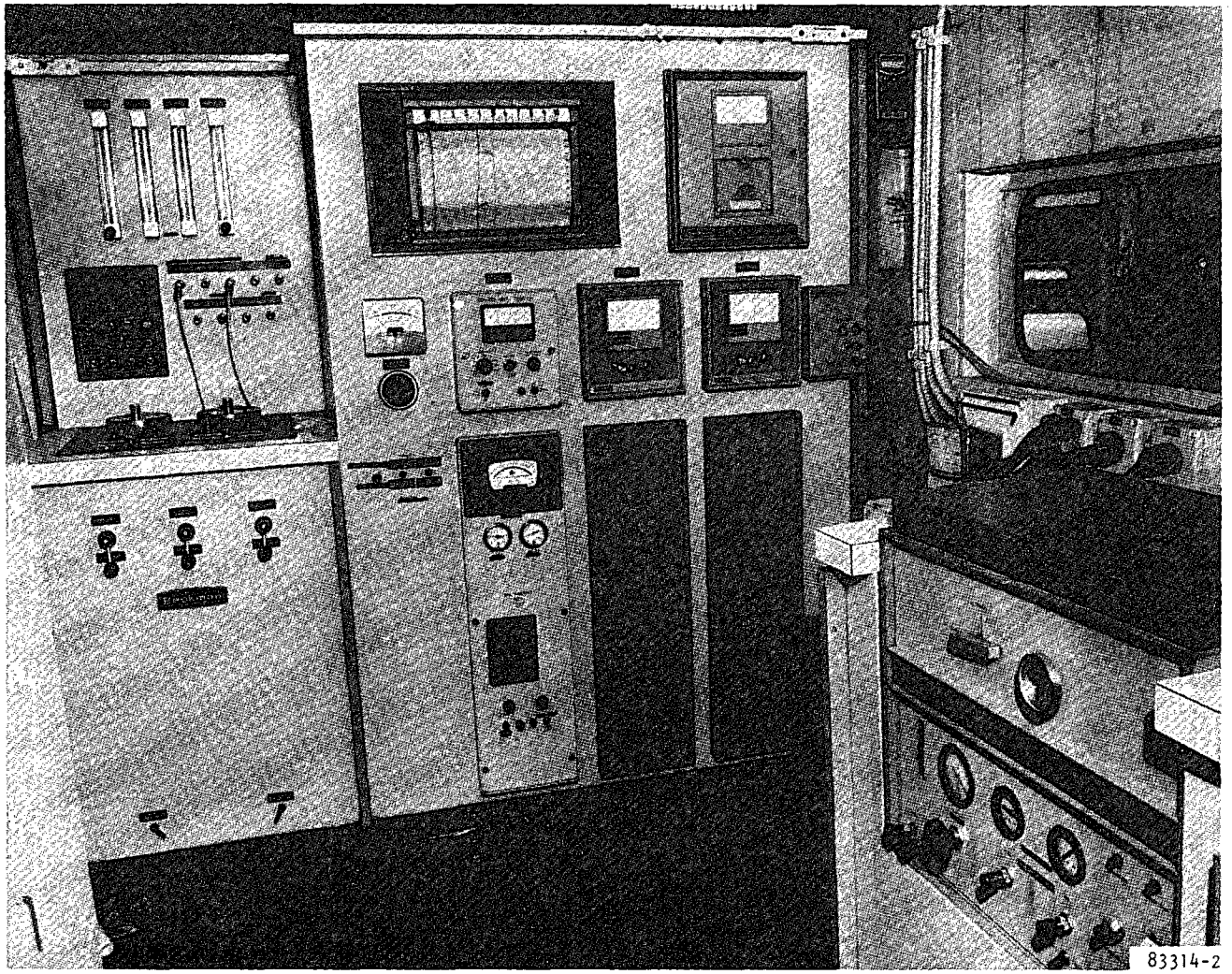

F-32687

Figure 3-19. Mobile Emission Analyzer--Gas Analysis Equipment

TABLE 3-1

EMISSION ANALYZER TEST DATA

**********GRI 10 TON HEAT PUMP EMISS TEST,6/27/80,SITE A **********

FUEL = GAS PBARO = 29.87 DEW PT,F = 78.00 RFL HUM = 60.00

FUEL H/C = 3.90 STOI F/A = .05848 L H V = 20201. SPEC HUM = .01853

DATA POINT NUMBER	AA	BB	CC	DD	EE
CORRECTED FUEL FLOW , LB/HR	6.3	6.3	6.3	5.9	6.0
FA RATIO CALC. FROM EMISSION	.0242	.0245	.0242	.0295	.0280
EQUIVALENCE RATIO	.414	.419	.414	.505	.479
COMB EFFIC FROM EMISSIONS	99.978	99.983	99.983	99.985	99.977

**********SUMMARY OF REDUCED EMISSION DATA**********

CARBON DIOXIDE					
PERCENT BY VOLUME, WET	4.22	4.26	4.22	5.09	4.84
PERCENT BY VOLUME, DRY	4.60	4.65	4.60	5.65	5.35
LB. CO2 PER LB. OF FUEL	2.76	2.76	2.76	2.76	2.76
WEIGHT FLOW, LB./HR.	17.4	17.4	17.4	16.3	16.6
CARBON MONOXIDE					
PPM BY VOLUME, WET	9.0	7.2	7.2	7.8	14.3
PPM BY VOLUME, DRY	9.8	7.8	7.8	8.6	15.8
LB. PER 1000 LB. OF FUEL	.375	.296	.299	.268	.519
WEIGHT FLOW, LB./HR.	.002	.002	.002	.002	.003
UNBURNED HYDROCARBONS- PPM AS CARBON, WEIGHTS AS CH4					
PPM BY VOLUME, WET	5.9	4.6	4.6	4.6	5.9
PPM BY VOLUME, DRY	6.4	5.0	5.0	5.1	6.5
LB. PER 1000 LB. OF FUEL	.139	.109	.110	.091	.121
WEIGHT FLOW, LB./HR.	.001	.001	.001	.001	.001
RATIO LB HC/LB CO	.3713	.3678	.3675	.3398	.2336
NITRIC OXIDE (NO) - WEIGHTS AS NO2					
PPM BY VOLUME, WET	37.0	41.1	36.0	23.1	21.6
PPM BY VOLUME, DRY	40.3	44.8	39.2	25.7	23.8
LB. PER 1000 LB. OF FUEL	2.529	2.783	2.459	1.309	1.284
WEIGHT FLOW, LB./HR.	.016	.018	.015	.008	.008
NITROGEN DIOXIDE (NO2)					
PPM BY VOLUME, WET	1.5	2.6	2.1	.5	.5
PPM BY VOLUME, DRY	1.7	2.8	2.2	.6	.6
LB. PER 1000 LB. OF FUEL	.105	.174	.141	.029	.031
WEIGHT FLOW, LB./HR.	.001	.001	.001	.000	.000
TOTAL OXIDES OF NITROGEN (NO+NO2) AS NO2					
PPM BY VOLUME, WET	38.5	43.7	38.0	23.6	22.1
PPM BY VOLUME, DRY	42.0	47.6	41.4	26.2	24.4
LB. PER 1000 LB. OF FUEL	2.635	2.957	2.600	1.338	1.315
WEIGHT FLOW, LB./HR.	.017	.019	.016	.008	.008

NOTES 1.ALL EMISSIONS CONCENTRATIONS CORRECTED TO CONCENTRATION IN WET OR DRY EXHAUST FROM COMBUSTION WITH DRY AIR.
2.EQUIVALENCE RATIO CALCULATED FROM CO2,CO,AND HC DATA AND FUEL COMPOSITION.
3.MASS EMISSIONS OF NO, NO2, AND NO+NO2 CALCULATED AS NO2 FROM CONCENTRATIONS WITH MOLECULAR WEIGHT OF NO2 (46.01).
4.COMBUSTION EFFICIENCY CALCULATED FROM CO,AND UHC AS VAPORIZED ORIGINAL FUEL ON LB/ LB FUEL BASIS.

Brayton Turbocompressor Starting Concepts

(a) Electric motor located asymmetric to mid-rotor

(b) Electric motor located symmetric with mid-rotor

(c) Electric motor at hot end

(d) Vacuum applied at compressor inlet

(e) Pressure applied at turbine inlet

Rankine Compressor Starting Concepts

(a) Electric motor at compressor end

(b) Thermal start turbine

(c) Bottoming cycle

The advantages and disadvantages of each starting mode were given a preliminary evaluation, and layout studies of the more promising concepts were made.

After design layout studies and pricing for the candidate systems were completed, an internal design review was conducted at which two primary rotating group starters were considered as likely candidates. These were: (a) the baseline rotating group with a vacuum start, and (b) a new "single spool" rotating group with a mechanical start.

As a result of the design review, the "single spool" rotating group concept was dropped because of the associated high development risk. Also, reinvestigation of the hot-end mechanical start for the baseline rotating group was initiated. Further analysis of vacuum start concepts included use of a simplified system without a boost vacuum tank and a combustor-assisted start. This concept was selected as the most cost-effective and technically risk-free method for use with the baseline rotating group. Figure 3-20 is a schematic representation of the integrated vacuum start method, which includes a vacuum pump (blower) and check valves at the Brayton cycle compressor outlet and blower inlet.

Using the simplified vacuum start concept, rotating group starter testing was conducted to confirm theoretical starting torque calculations. Testing was accomplished by using an aircraft turbocompressor as a vacuum pump, and measuring flow and differential pressure across the Brayton turbine at various temperatures. Data were recorded just as shaft rotation began. Test data corresponded very well with calculated values. Starting control parameters were also monitored and indicated that the present control logic would be adequate for automatic starting of the system.

Vacuum start testing was continued to optimize turbine starting characteristics and reduce component costs. The configuration tested utilized a small

ORNL-DWG 81-15025

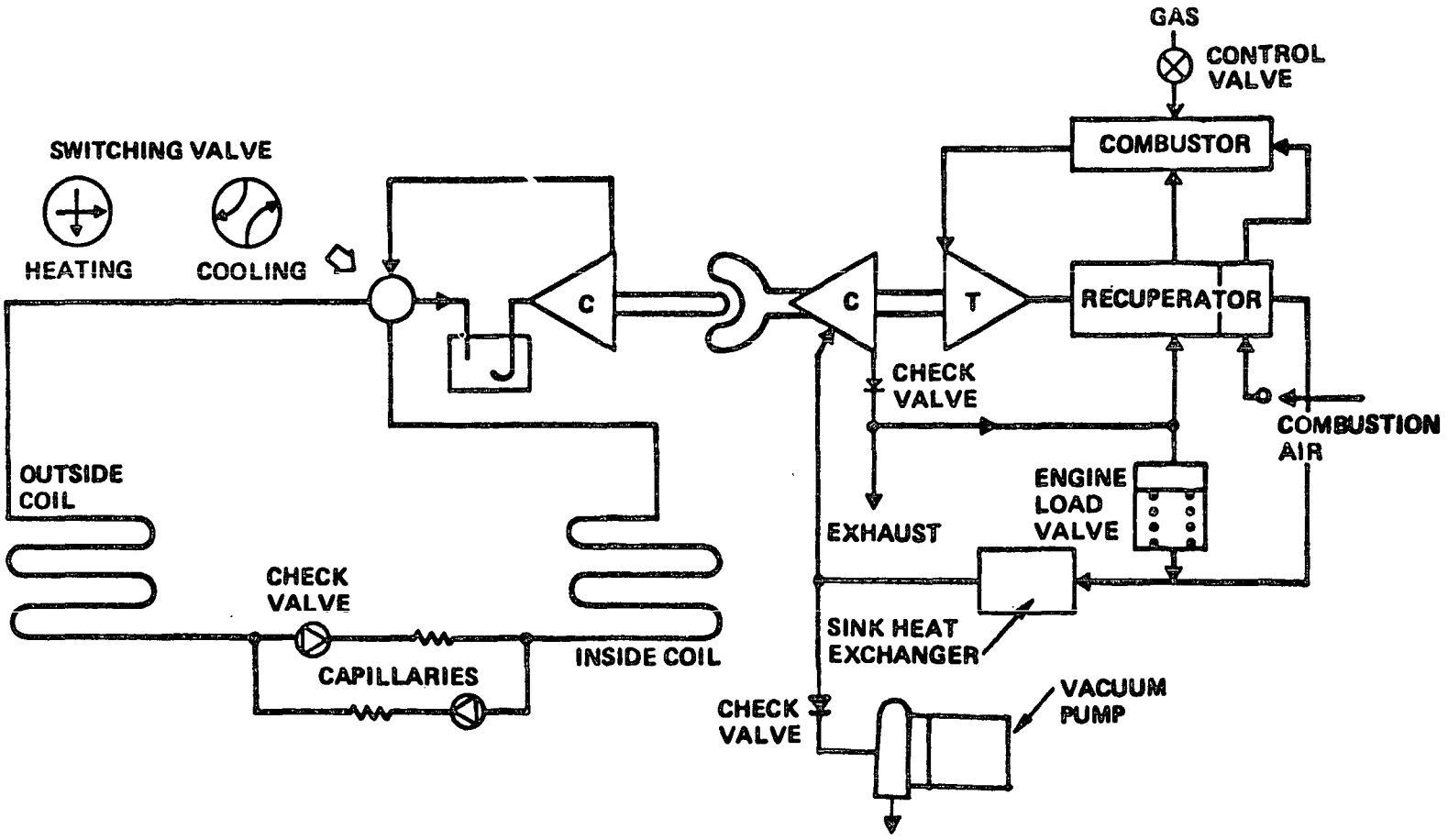

Figure 3-20. Vacuum Start Method for Baseline System

vacuum blower to allow purging of the system. The combustor was then ignited and turbine inlet temperature increased to approximately 1000°F. During this purge-and-preheat cycle, turbine flow was maintained at a low enough level so that the turbine did not rotate. This was necessary because the maximum wear on the turbine foil bearings occurs during initial rotation of the shaft, when mechanical contact is made between the shaft and the foils. When the turbine inlet temperature reached approximately 1000°F, an electric valve located on a vacuum tank was energized. The initial tank pressure was approximately 25 in. Hg vacuum. When the valve opened, a sudden increase in flow occurred across the turbine wheel, and the turbine accelerated to approximately 30,000 rpm instantaneously. The combustor continued to supply heat to the turbine, and after a drop in speed to approximately 21,000 rpm, the turbine became self-sustaining and the vacuum blower was deenergized. From this point, the turbine speed increased to the required operating speed as dictated by the gas flow to the combustor, which is controlled by a modulating gas valve.

Freon Circuit Controls

From the analysis of the Freon circuit controls, a suction pressure regulator was selected for surge control of the Rankine compressor. The defrost mode of the outside coil during heating was changed to use hot bypass gas from the compressor discharge to the outside coil, rather than the typical reversing at the four-way valve. This change eliminated the need for making the indoor coil serve as an evaporator during the defrost cycle, which causes a sharp decrease in supply air temperature.

Testing of the breadboard Freon circuit controls was conducted using the test setup shown in Figure 3-21. The controls were modified to include a thermostat and a gas valve, which modulates in response to indoor temperature. During the heating cycle, as indoor temperature decreases, the valve modulates toward the full open position. In the cooling mode, as indoor temperature decreases, the valve modulates toward the minimum open position. A calibration test was then conducted to verify gas flow versus indoor temperature in both the cooling and heating modes. The other Freon circuit controls operated satisfactorily for both modes of operation.

The breadboard Freon circuit test facility was then modified to incorporate the updated control configuration shown in Figure 3-22. The circuit was sequenced through all operating and failure modes. All controls sequenced properly and no feedback was encountered. The current was monitored during all modes, and the maximum current, as expected, was in the full heating mode with the defrost heater energized. In this mode, the current was 1.5 amp at a 24-vac control voltage.

A flow test was also conducted on the modulating gas valve using air. After correcting the test data for the density of natural gas, the flow was well within the operating range of the combustor. The temperature span on the thermostat was 5°F, which appeared to be adequate for the heat pump system.

The breadboard test facility was further modified to incorporate commercial heat pump controls and additional instrumentation to the Freon circuit. Testing then commenced with emphasis on Rankine compressor surge control and transient mode operation.

ORNL-PHOTO 4612-81

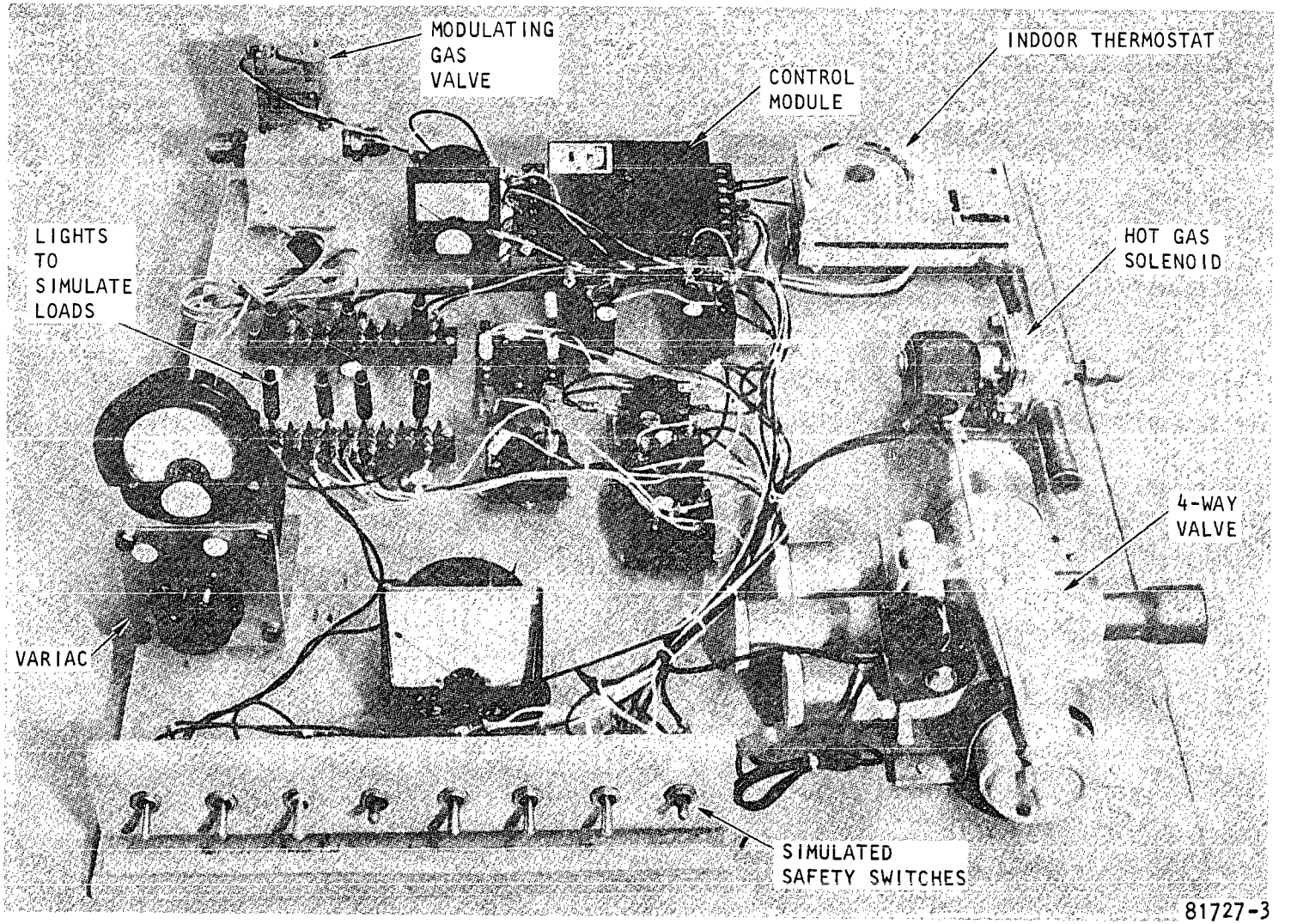

F-30256

Figure 3-21. Breadboard Controls Test Setup

ORNL-PHOTO 4613-81

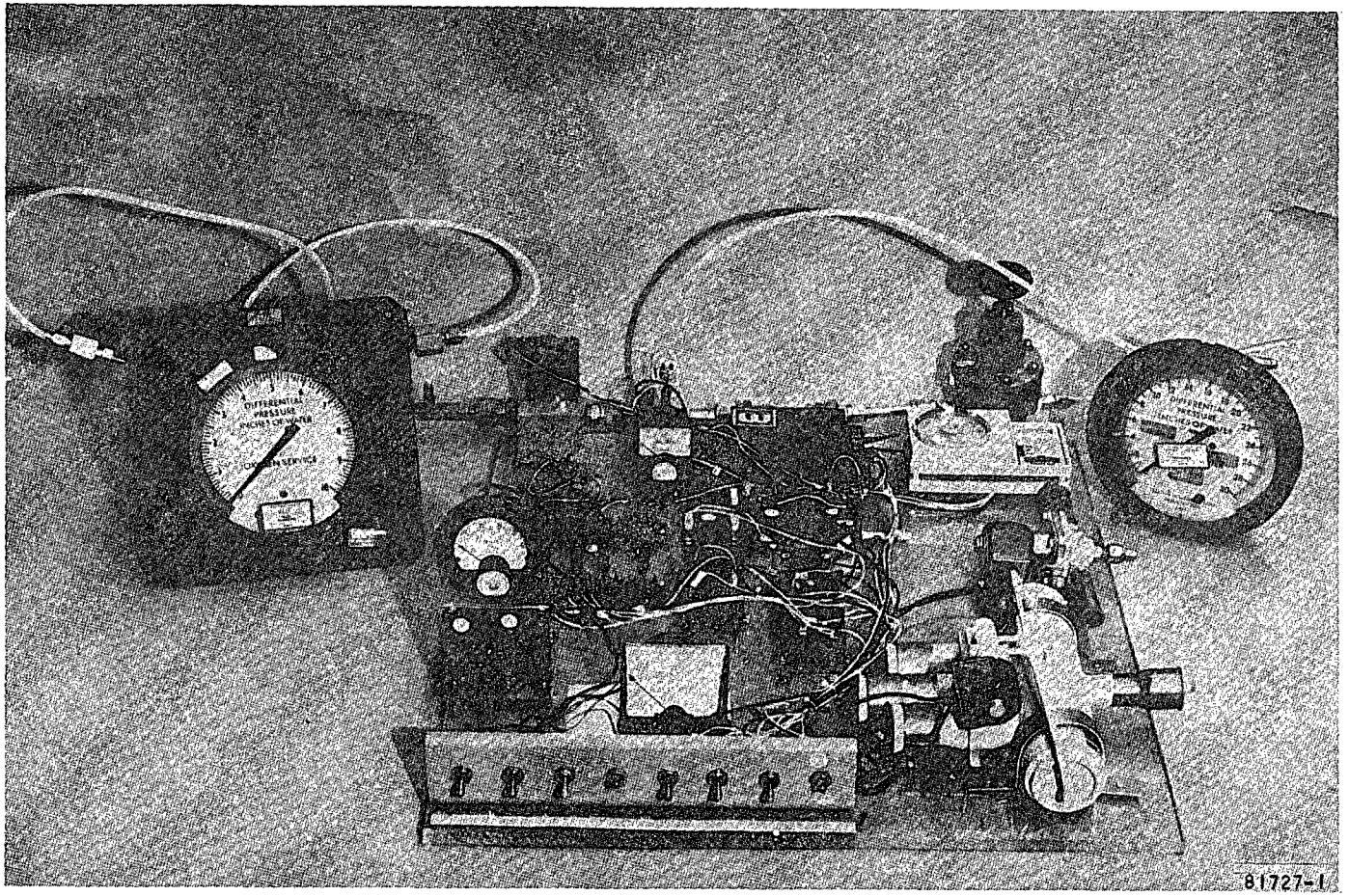

Figure 3-22. Breadboard Control Circuit Test Setup

Additional tests were conducted to establish a baseline for the new Freon circuit components operating in the cooling mode prior to the start of heating tests. All components were operationally tested and adjusted for optimum cooling mode performance. Heating tests were then conducted, with emphasis on component compatibility with respect to cooling mode operation. Refrigerant "slugging" of the compressor was encountered in the cooling mode during operation at speeds from 60,000 to 75,000 rpm. A larger accumulator was installed in the suction line, which solved the problem and also appeared to reduce compressor surge at low operating conditions. The Freon circuit charge and the expansion valve pressure setting were also determined at this time.

Calibration and testing of the Rankine compressor surge valve in the breadboard test facility were conducted using the Mark II compressor. The surge valve is an existing AiResearch part, used previously on another vapor cycle system. The valve prevents compressor surge by sensing compressor flow and differential pressure to maintain a minimum flow at low-load conditions by bypassing compressor discharge gas to the compressor suction side. The valve closes during medium- and high-load operation to ensure maximum system performance.

Engine Safety Controls

Sample high-temperature (1300°F) safety switches were incorporated into the breadboard Freon circuit in conjunction with the installation of the prototype combustor and its flame/ignitor safety circuit. Results of the flame safety tests were satisfactory during all modes of operation.

An overspeed valve was incorporated into the system, and preliminary testing indicated satisfactory operation for limiting turbine speed to a safe level. A control box containing the operating and safety controls needed for testing the breadboard Freon circuit with automatic control sequencing was then added to the system test facility. Safety control testing was successfully completed on the following safety parameters: turbine overspeed, recuperator overtemperature, flame safety, and sink overtemperature.

Alternate Microprocessor Control System

Investigation of a commercial microprocessor control system was made as a possible alternate for the baseline electromechanical control system. The preliminary microprocessor control logic diagram, shown in Figure 3-23, was generated and sent to Sylvania and Honeywell to compare costs with the existing system. In both cases, the cost comparisons still favored the electromagnetic controls.

SINK HEAT EXCHANGER

Early Design Activity

Early in the program, a design for the development sink exchanger core, with an accompanying cost estimate, was prepared. Using the computer analytical model, system performance with this unit incorporated was evaluated and found

ORNL-DWG 81-15026

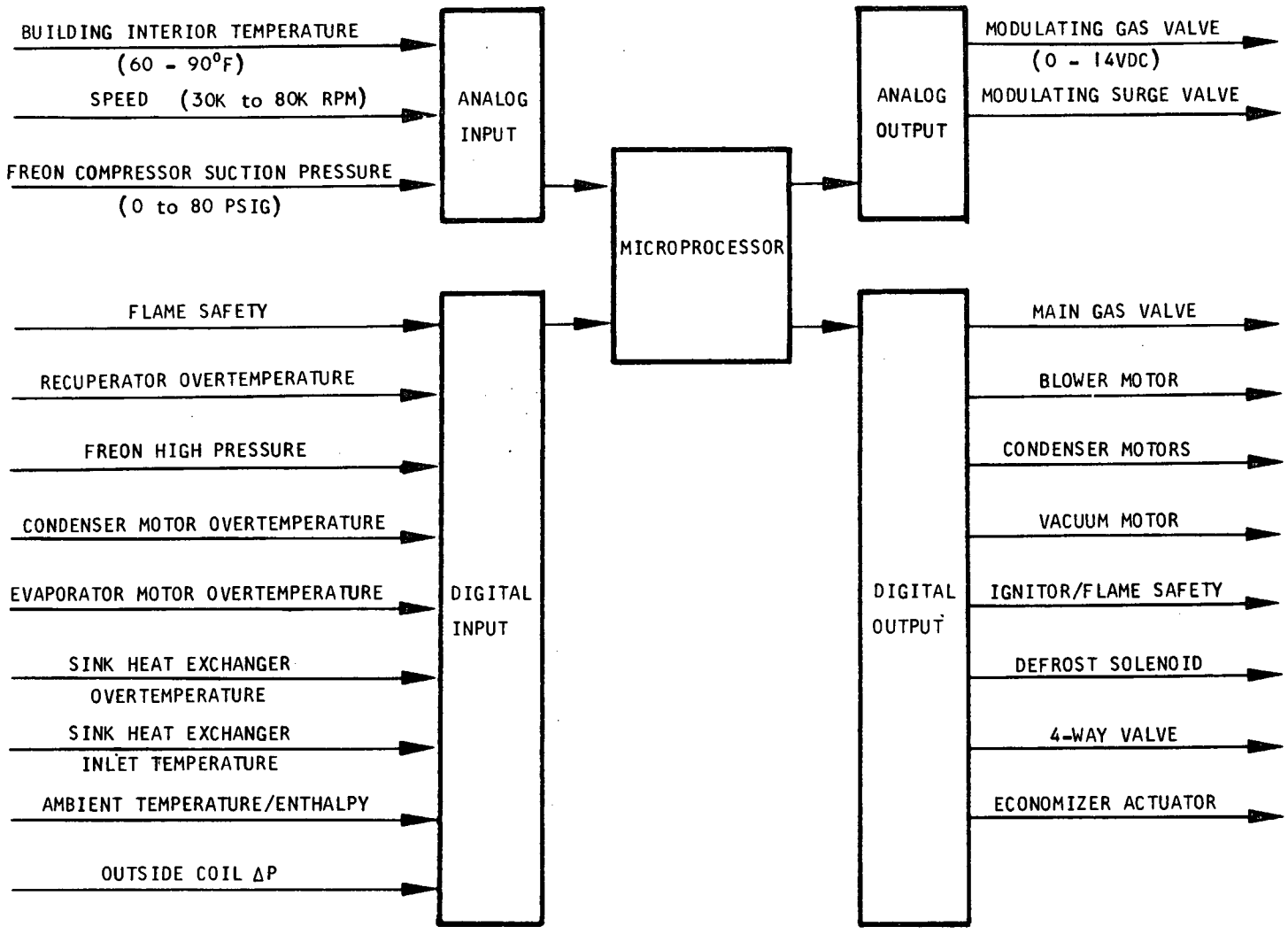

Figure 3-23. GRI Microprocessor Control Logic Diagram

to be acceptable. Based on the performance predictions of the new design, it was selected for the system, and layouts for installation in the engine assembly proceeded.

The layouts were for three engine installation configurations with the selected sink heat exchanger oriented differently in each case relative to the recuperator. Cost and weight data were also developed in support of the tradeoff study. A configuration with the sink heat exchanger oriented horizontally in the engine installation proved to be the preferred arrangement.

Results of Thermal Analysis

A finite-element thermal analysis of the sink heat exchanger tube plates and side plates was performed. The analysis focused on the number of operating cycles and maximum temperatures associated with each mode of operation. Also, the thermal stress within the heat exchanger and its effect on the operating life of the unit were determined.

Results of the analysis also showed that, with a hot-side gas inlet temperature of 750°F during a steady-state condition, the maximum tube plate temperature is 429°F. During this same condition, the peak temperature in the side plate is 446°F. Because the unit is made of mild steel, these temperatures and the resultant maximum stress levels should meet system life requirements considering both steady-state and cyclic operation.

Protective Coating Evaluation

Various protective coatings were evaluated for preventing corrosion externally and internally. Internally, corrosion can be caused by the high concentration of combustion products in the hot gas, which will form carbonic acid in the unit if condensation occurs during static cooldown. To protect the mild steel material from such corrosion, the heat exchanger core and inlet manifold are coated with FP-85, a silicone solution impregnated with aluminum particles. This coating has been used successfully on other heat exchangers with similar operating conditions. The outlet manifold, which is made of fiberglass, does not require a protective coating.

Manufacturing Processes and Techniques

Difficulties encountered while brazing the first core assembly were resolved by increasing the thickness of the tube plate. Differential thermal contraction between the header bar and the tube plate had caused buckling of the plate. By increasing the plate thickness, the differential contraction was reduced, but the no-flow length of the core was increased by 0.50 in. The development unit is of this configuration.

Two cores were built to support the development program and prove manufacturing processes and techniques. One core was constructed of two sections and the second of three sections along the no-flow dimension. The unit shown in Figure 3-24 is the three-section version. The two-section core, which was the primary design, was selected for performance testing because it was considerably better from a leakage standpoint.

ORNL-PHOTO 4614-81

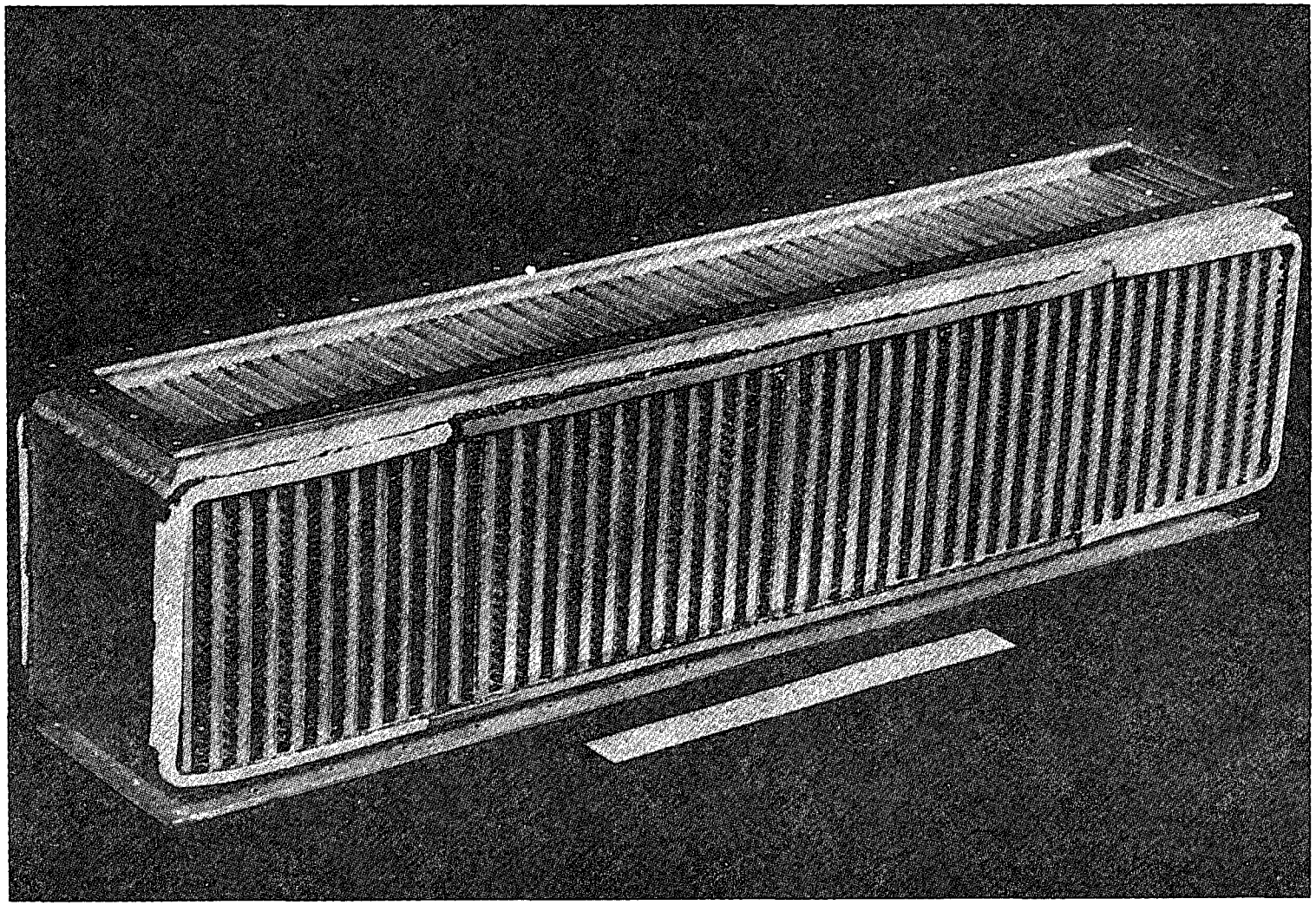

F-33153

Figure 3-24. Sink Heat Exchanger Development Core

Test Results

Isothermal pressure drop tests and performance tests at operating conditions were conducted in the test setup shown in Figures 3-25 and 3-26. The tests were conducted with the system inlet and outlet pans instrumented so that flow distribution through the core could be evaluated. Test results presented in Figures 3-27 and 3-28 showed that the pressure drops on both sides of the core were very close to expected values, but that hot-side effectiveness was approximately 2 percent less than predicted because of minor flow maldistribution on the hot side.

Prototype Design Changes

Heat exchanger optimization studies performed with the system analytical model indicated that a 10-percent reduction in the core size (no-flow dimension) could be implemented with minimal impact on system performance. The close correlation of predicted performance and test data supported the feasibility of this change, which has weight and cost-saving benefits. Also considered were changes for system optimization, cost reduction, and design improvement purposes. Potential cost-reduction changes (retaining the same core configuration) were evaluated relative to their impact on both engine and heat pump designs to determine net system cost reduction. It was decided that changes for the prototype configuration will consist of the previously mentioned core size reduction, the addition of mounting tabs for heat pump interfacing on the cold side, and the increased thickness of the protective coating on the inlet manifold. Figure 3-29 is a sketch of the prototype unit with manifolds attached.

Updated drawings reflecting the prototype design changes have been released, and hardware manufacture has commenced. In the meantime, alternate core design approaches and other cost-reduction changes will continue to be evaluated for possible implementation in the field test phase.

SYSTEM PACKAGING

Engine

1. Basic Design Approach

The design layout of the Brayton engine package began by consulting with thermodynamics, heat transfer, stress, and turbomachinery specialists at AiResearch. The turbine-to-recuperator and recuperator-to-sink heat exchanger interface designs were the major topics discussed. Thereafter, several engine assembly layout concepts were made and a cardboard half-scale mockup, shown in Figure 3-30, was fabricated to evaluate interfaces, ducting, and simplification of design. The various concepts were evaluated from cost as well as from technical aspects.

The basic engine package configuration that evolved is illustrated in the mockup of the Brayton cycle engine shown in Figure 3-31. Preliminary thermodynamic and stress analyses were performed to evaluate the initial designs, and changes resulting therefrom were incorporated. Completion of this initial

ORNL-PHOTO 4615-81

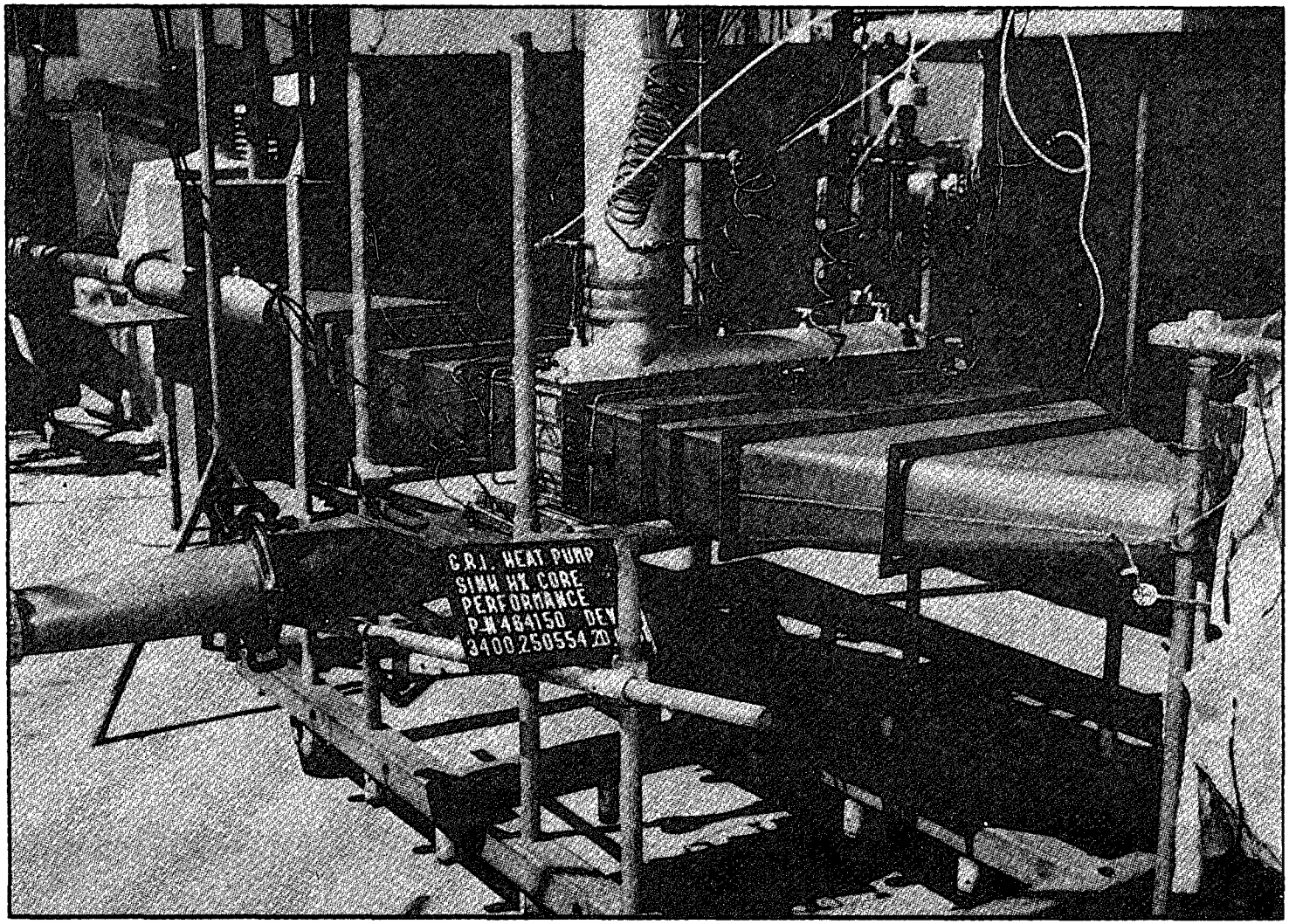

F-33152

Figure 3-25. Sink Heat Exchanger Performance Test Setup

ORNL-PHOTO 4616-81

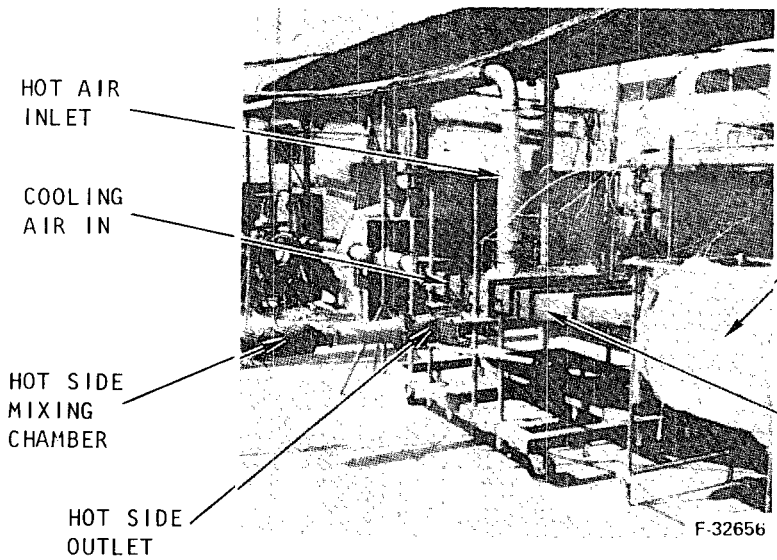

a. COMPLETE SETUP

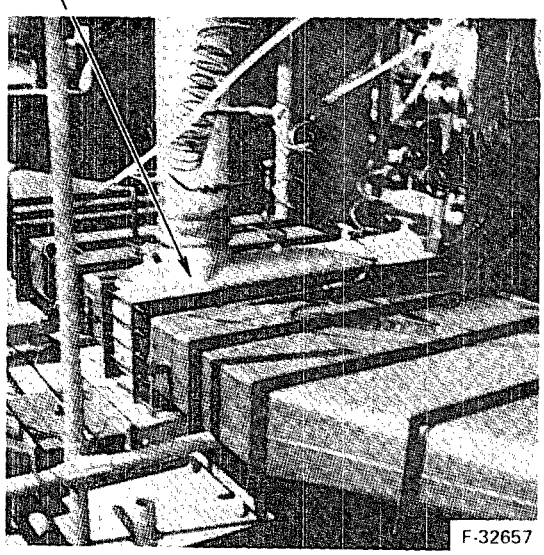

b. HOT-SIDE INLET

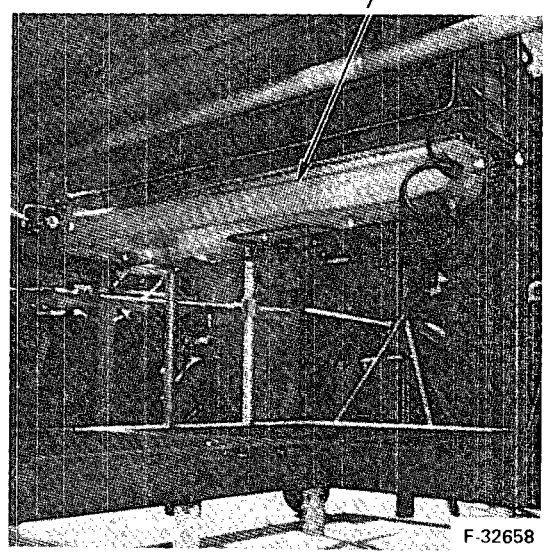

c. HOT-SIDE DISCHARGE

F-32661

Figure 3-26. Sink Heat Exchanger Performance Test Setup

NOTES:

1. $\sigma\Delta P$ BASED ON CORE INLET TOTAL PRESSURE MINUS CORE OUTLET TOTAL PRESSURE
2. σ = 17.35 P/T

   P = AVERAGE PRESSURE IN INTERCOOLER, IN. HG ABS

   T = AVERAGE TEMPERATURE IN INTERCOOLER, °R

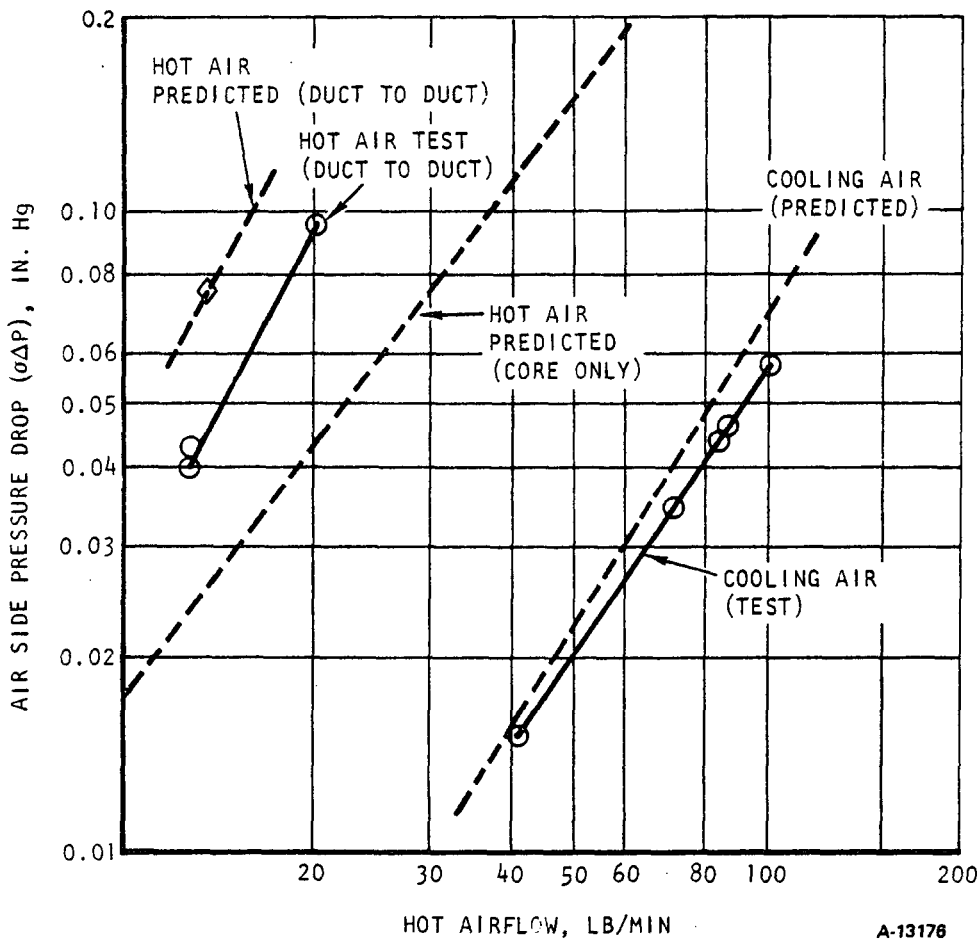

Figure 3-27. Sink Heat Exchanger Pressure Drop Characteristics

ORNL-DWG 81-15028

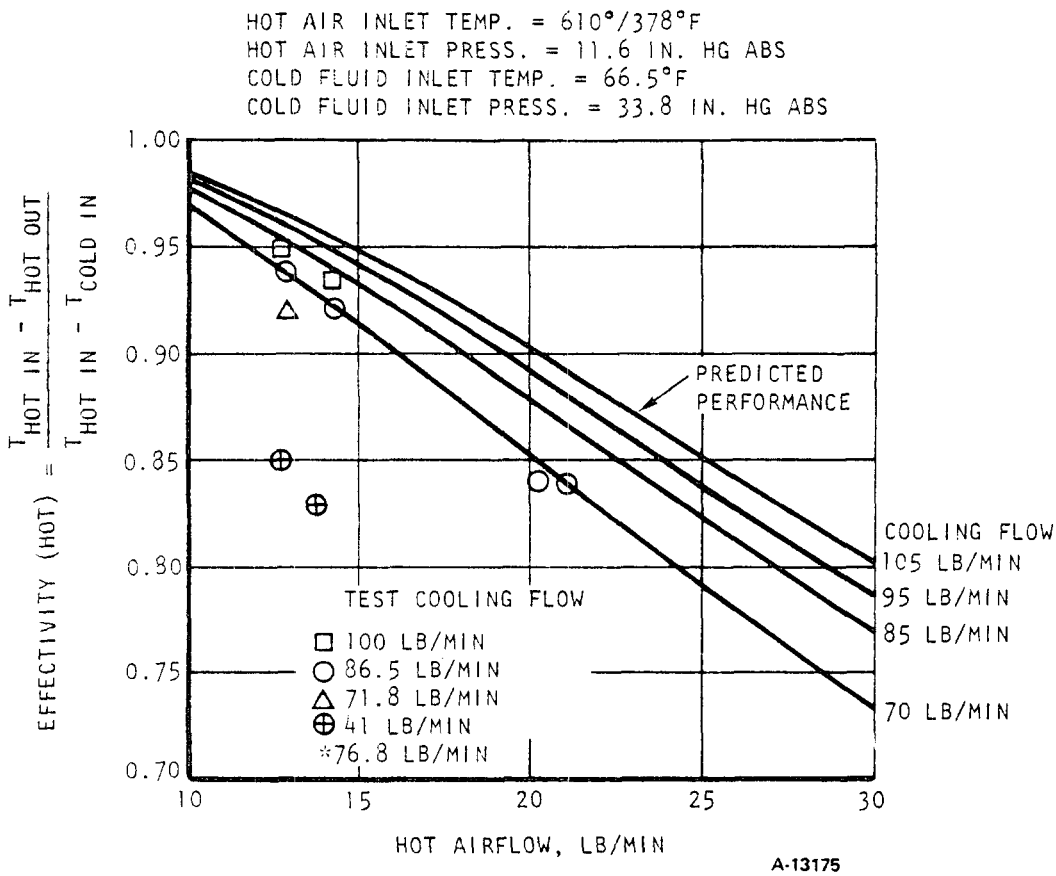

Figure 3-28. Sink Heat Exchanger Effectiveness (Hot)

ORNL-DWG 81-15029

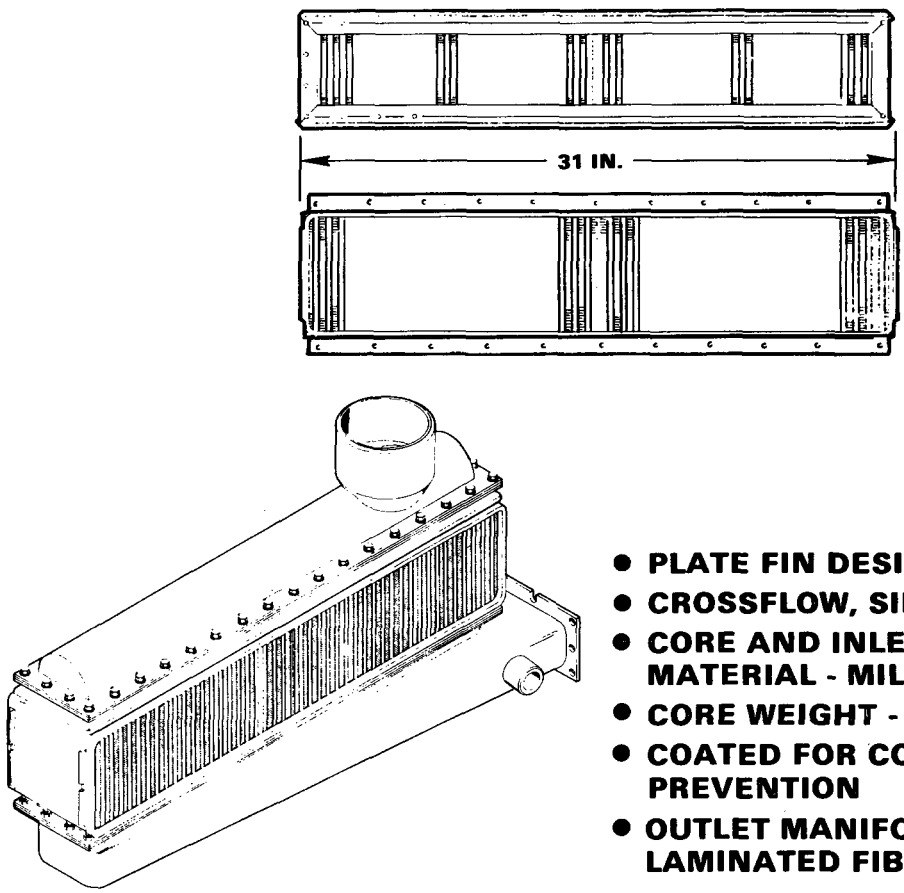

- PLATE FIN DESIGN
- CROSSFLOW, SINGLE PASS
- CORE AND INLET PAN MATERIAL - MILD STEEL
- CORE WEIGHT - 58 LBS
- COATED FOR CORROSION PREVENTION
- OUTLET MANIFOLD - LAMINATED FIBERGLASS

A-2471-A

Figure 3-29. Sketch of Prototype Sink Heat Exchanger

ORNL-PHOTO 1437-82

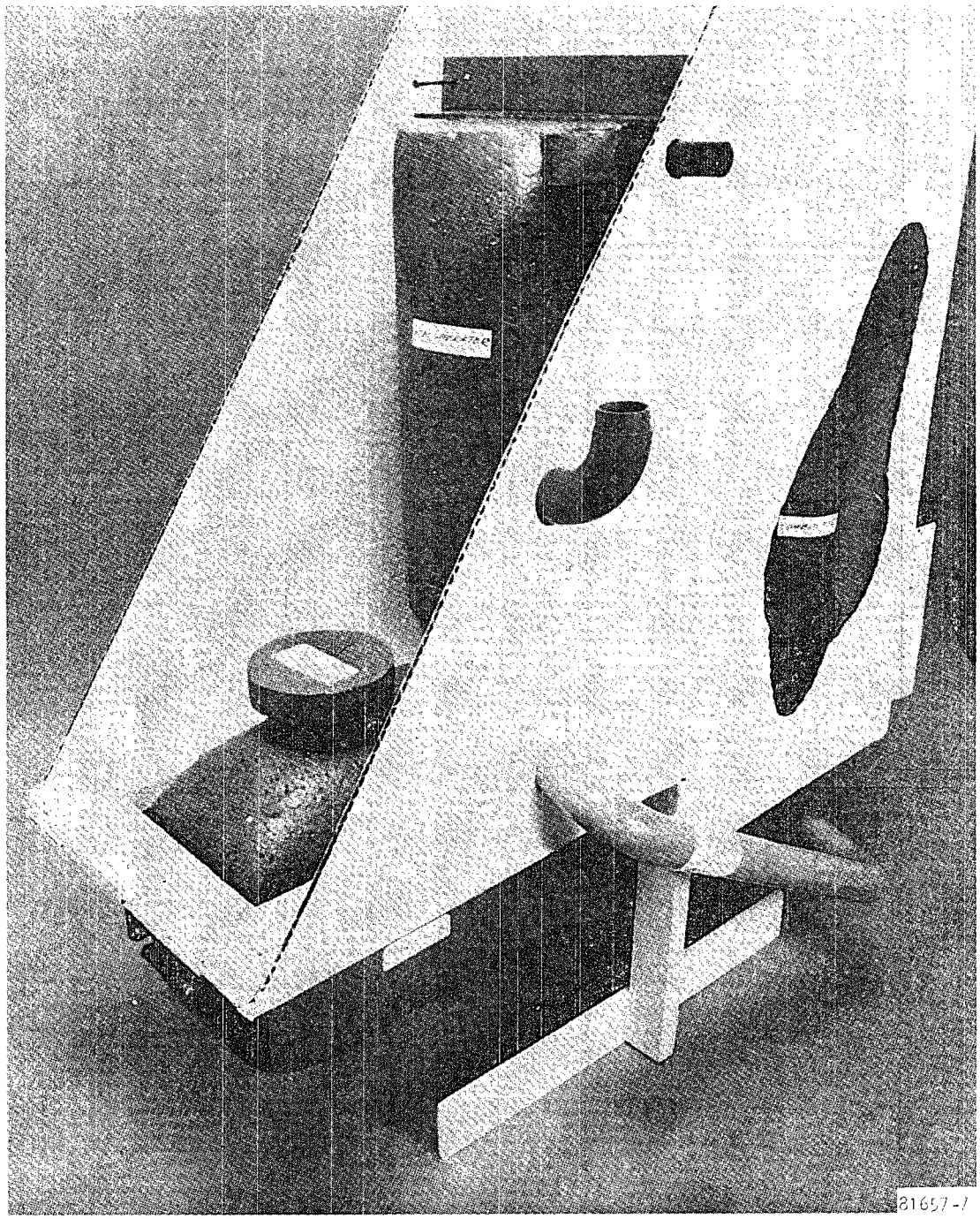

Figure 3-30. Mockup of Initial Engine Assembly

ORNL-PHOTO 4617-81

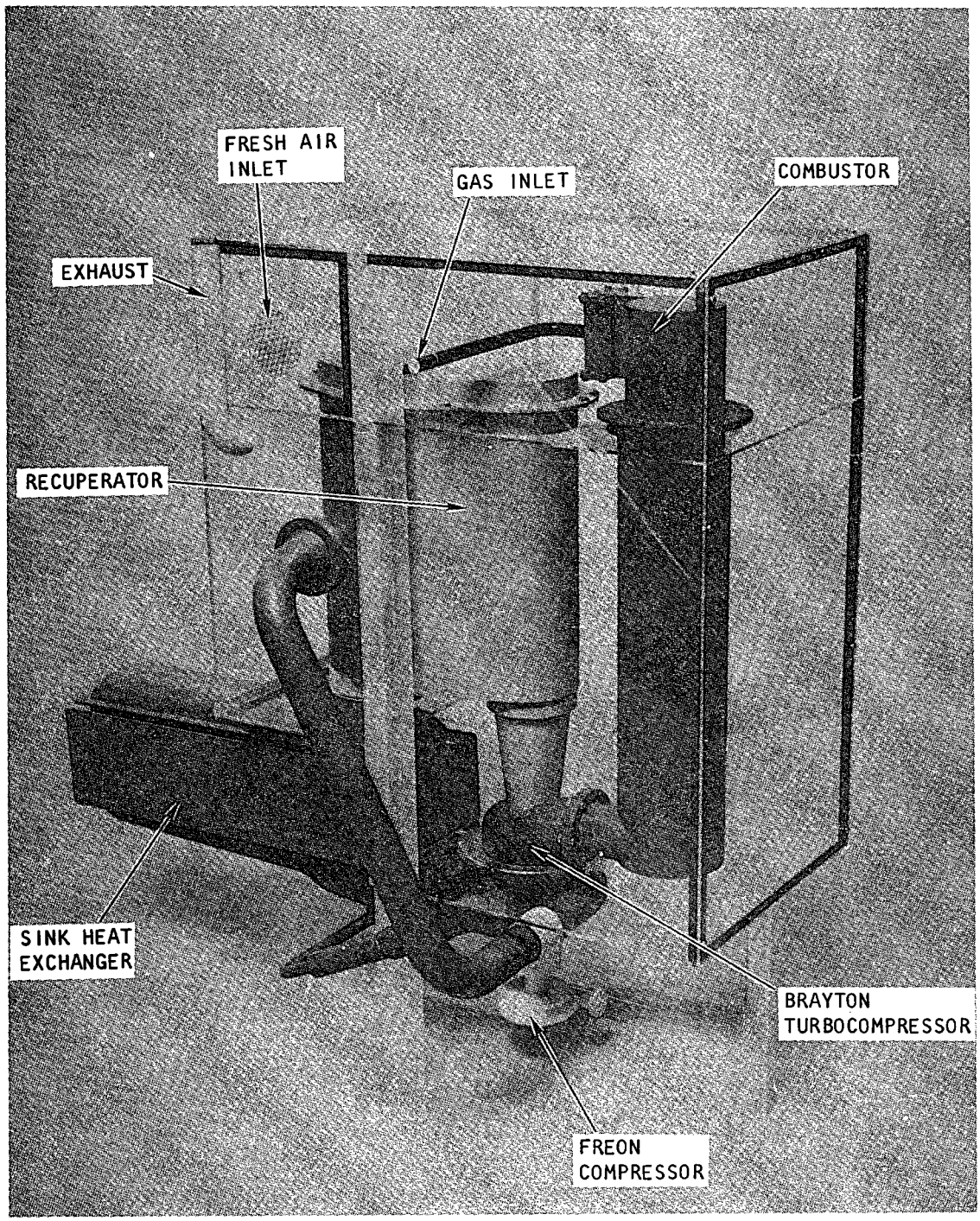

F-31442

Figure 3-31. Mockup of Prototype Engine Assembly

phase allowed initiation of (1) detail design of the heat pump assembly by Dunham-Bush, and (2) procurement/manufacture of a detail part set for a development engine.

2. Supporting Analyses

A thermal model for the Brayton engine package was developed, using results from the thermal analysis previously completed for the 95°F day design condition. Heat loss studies of the basic engine package design were made to investigate candidate insulation materials and methods. These studies provided a basis for a tradeoff study of insulation performance versus cost.

External structural loads were determined for the engine package, using estimated weight and center-of-gravity data. Internal load distribution was developed, and component panels were stress-analyzed for static loads and applied pressures from the operating loads as development modifications occurred.

The high-temperature interface between the turbine discharge and recuperator inlet was analyzed to determine the amount of thermal growth needing compensation. A piston ring seal evolved as the recommended solution to allow adequate axial and radial growth, while maintaining a positive seal on the vacuum circuit. After the sink heat exchanger orientation in the package was selected, the thermal growth characteristics of its interface with the recuperator were analyzed to determine if the same type of seal could also be used for this application.

Other thermodynamic and stress analyses were conducted to verify the structural integrity of the engine package design and its compatibility with thermal expansion characteristics over the full operating temperature range.

Pressure drop studies were made of several candidate design configurations for the diluent duct-to-turbine inlet transition elbow in an effort to decrease pressure losses. This effort was made in support of the AiResearch-developed components and the outside-developed combustor with respect to design and performance. These studies resulted in making new design layouts of the engine package to reflect the necessary component changes.

3. Engine/Component Interfaces

Problem statements for all valves, controls, and sensors of the engine assembly were generated, and parts were selected for use in the development program. In addition, production quantity cost estimates of these components were obtained.

The separation and sealing of the interface between the structure and the recuperator on surfaces exposed to ambient pressure was investigated. A high-temperature mastic resin was applied to a sample recuperator module to evaluate sealing characteristics. The resin proved to be unsatisfactory, cracking with time and applied temperatures. Other development tests are being undertaken to ascertain methods to provide a satisfactory seal and minimize costs. Promising sealing techniques will be evaluated during testing of the recuperator and engine package assembly.

An investigation of alternative schemes to separate the primary and service sections of the recuperator cold side was completed. A scrap recuperator core of identical construction was used so that all constraints or advantages inherent in the design would be considered. The preferred approach was the insertion of a separating flange into a peripheral slot between adjacent flow passages. The flange was not physically attached to the core, and clearance in the slot was provided to accommodate thermal expansion. To preclude intersection leakage, a pliable material compatible with the surface temperature was placed in the slot and compressed lightly between the flange and core. The addition of the recuperator primary/service separation flange resulted in a slight engine package reconfiguration. A benefit derived from this package change was a reduction of approximately 2 in. in overall height and a significant reduction in fresh air branch pressure drop.

4. Engine Mockup

Component and engine mockup drawings were completed and the half-size mockup of the Brayton cycle engine shown in Figure 3-31 was procured. The mockup reflects the current configuration of individual components, including recent changes to the combustor and recuperator, as well as the engine enclosure outline. The mockup was constructed with removable panels and separable interfaces to allow easy modification and additions.

5. Enclosure Design

System testing of a diluent chamber closely simulating the intended configuration for the breadboard system test combustor revealed some necessary changes related to the engine enclosure design. These were:

(a) The selected insulation will require encapsulation or a metallic outer wrap to prevent surface deterioration and ingestion of debris by the turbocompressor. Alternate materials with equal effectiveness are being investigated.

(b) The internal baffles that interface with the outer wall of the enclosure, even though of thin-gage material, must be thermally isolated.

(c) The large-area flat panels will require internal reinforcement, even though the pressure differential across the panels is only a few inches of water.

For cost reduction reasons, the present configuration of the engine package utilizes the external insulation blankets shown in Figure 3-32 on the hot side, rather than internal blankets. The external blankets are covered by fiberglass cloth on the inside against the hot walls, and by rubberized nylon on the outside. The more expensive high-temperature sheet metal cost required for the engine enclosure with this approach is offset by the combination of reduced blanket manufacturing costs and sheet metal quantity reduction. An additional benefit is derived from simplification of engine assembly operations.

Sheet-metal fabricators were contacted for suggestions regarding quantity production methods and costs for the engine enclosure. Cost estimates were received from the fabricators for the engine package sheet metal box and from

ORNL-DWG 81-15030

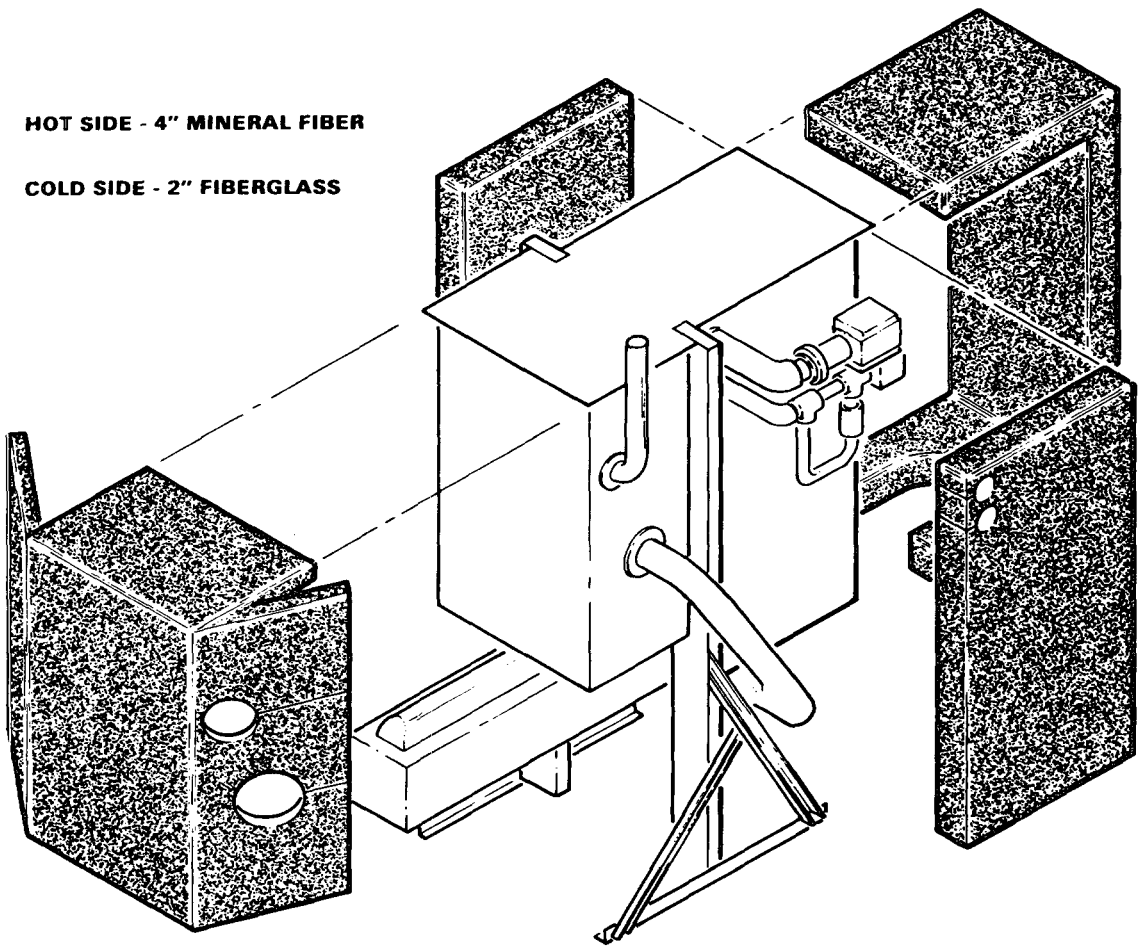

A-9211

Figure 3-32. Installation of Engine Insulation Blankets

suppliers for the package insulation provisions. Engine package cost estimate updating was a continuing effort throughout the program.

The development engine enclosure was fabricated and will be used as a test bed for the recuperator component development test. In addition, the full engine assembly (including the rotating assembly, combustor, sink heat exchanger, recuperator, and various valves and controls) will be installed in the enclosure, and development tests will be conducted to verify structural integrity, mechanical interfaces, thermal performance, pressure drop analysis, and control operation.

Figure 3-33 is a photograph of the enclosure. Figure 3-34 shows the recuperator mounted in the enclosure ready for development test.

6. Prototype Engine Configuration

Based on test data and analysis, alternate recuperator and sink heat exchanger designs were defined, which reduced their sizes by 16 percent and 10 percent, respectively. In turn, unit weights and costs were reduced.

The prototype engine enclosure assembly is designed to adapt to either the baseline or reduced-height recuperator. The configuration of the combustor discharge section, which is designed to preclude excessive radiation to the recuperator, will be determined by the choice of recuperator.

7. Special Adaptors for Test

Several special drawings for development unit modifications and adaptors for test purposes were completed. These drawings cover provisions for special instrumentation and adapting components that vary slightly from the prototype configuration.

Heat Pump

1. Basic Design Approach

At the start of the program, a meeting was held with Dunham-Bush regarding its participation in supplying the heat pump portion of the system. As a result of the meeting, a statement of work and purchase order were issued for the heat pump packaging and design effort. A preliminary layout of the engine assembly was sent to Dunham-Bush to allow initiation of the design effort. It was decided that AiResearch would build and develop the engine package, with Dunham-Bush incorporating this package into the heat pump. This would permit each company to concentrate on its area of expertise and readily permit system testing of related components. A conceptual mockup of the heat pump with the engine package incorporated was fabricated for use as a design aid. A photograph of the mockup is presented in Figure 3-35.

2. Selected Configuration

The selected heat pump arrangement is shown in Figure 3-36. The damper/blower relationship is shown in the airflow schematic of Figure 3-37. The airflow paths are visually depicted in Figures 3-38, 3-39, and 3-40. Desirable

ORNL-PHOTO 4618-81

Figure 3-33. Development Engine Enclosure Assembly

ORNL-PHOTO 4619-81

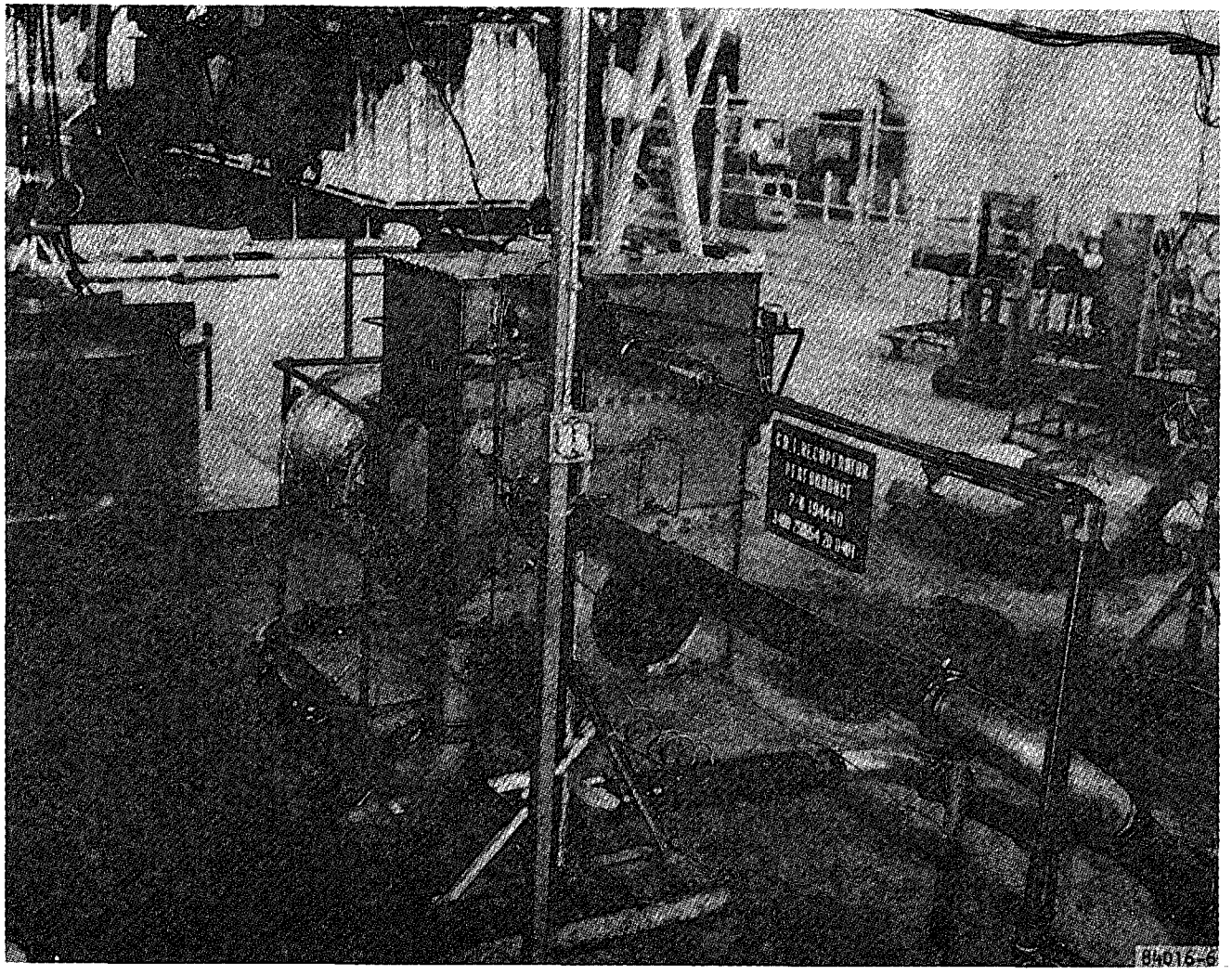

Figure 3-34. Recuperator and Engine Enclosure Test Setup--Uninsulated

ORNL-PHOTO 4620-81

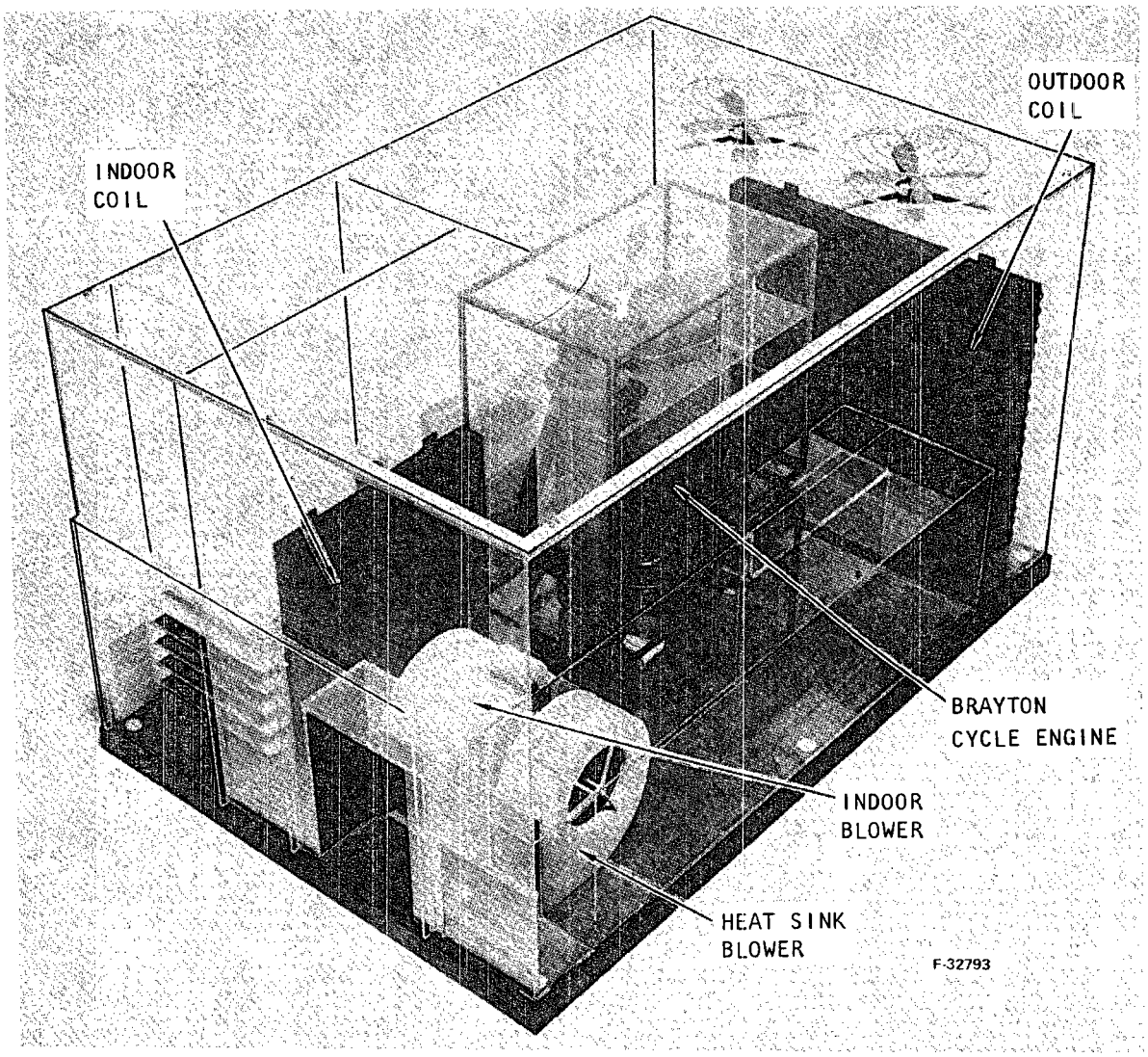

Figure 3-35. Conceptual Mockup of Heat Pump

ORNL-DWG 81-15031

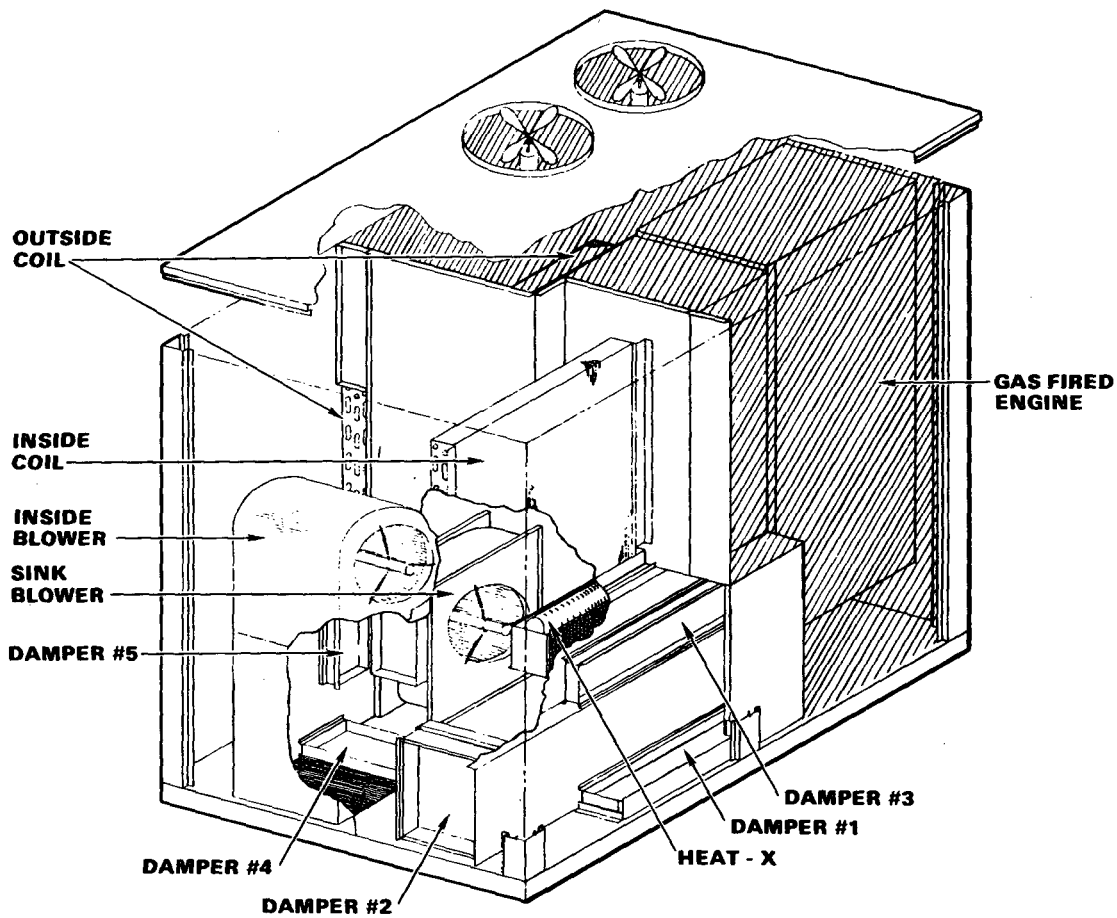

A-9179

Figure 3-36. Prototype Brayton/Rankine Heat Pump

ORNL-DWG 81-15032

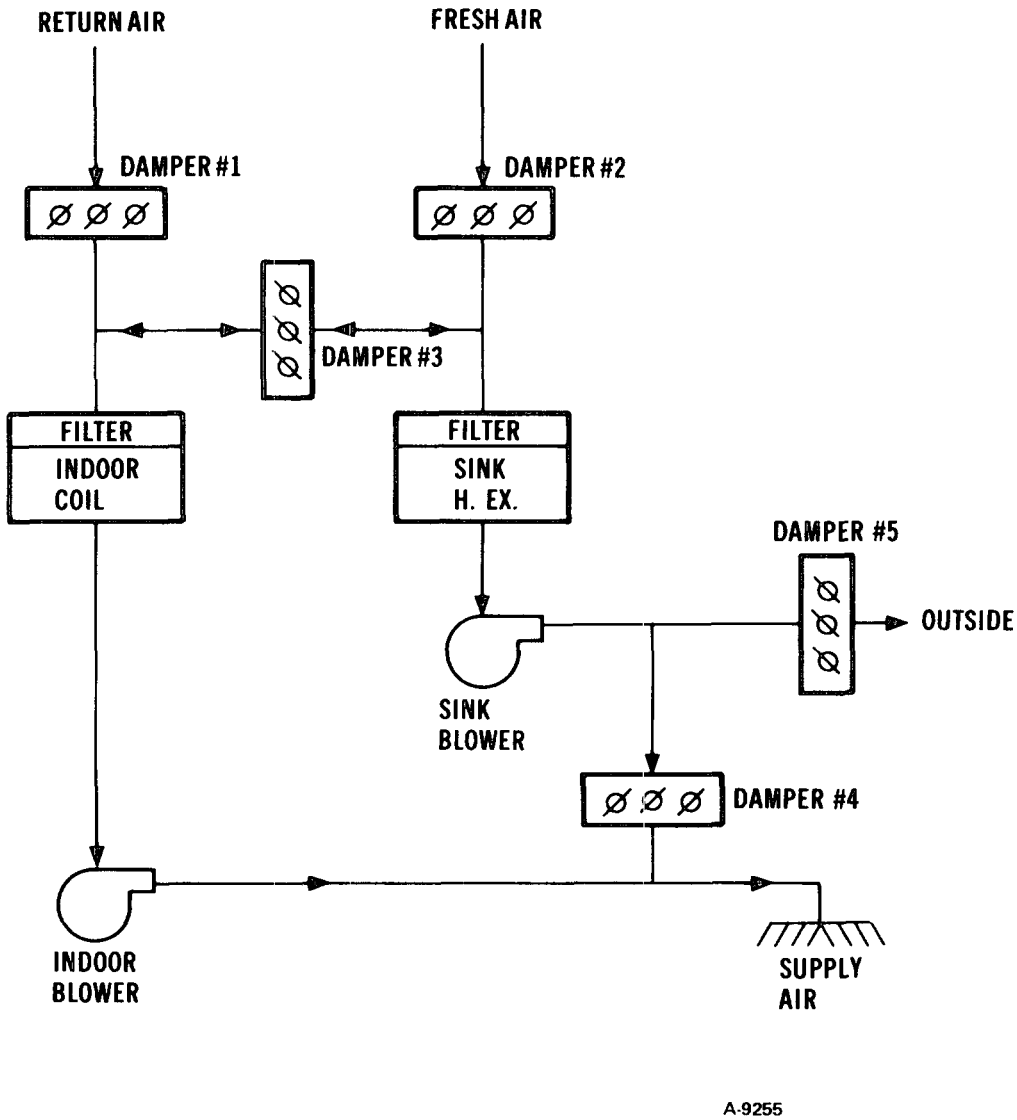

Figure 3-37. Airflow Schematic

ORNL–DWG 81-15033

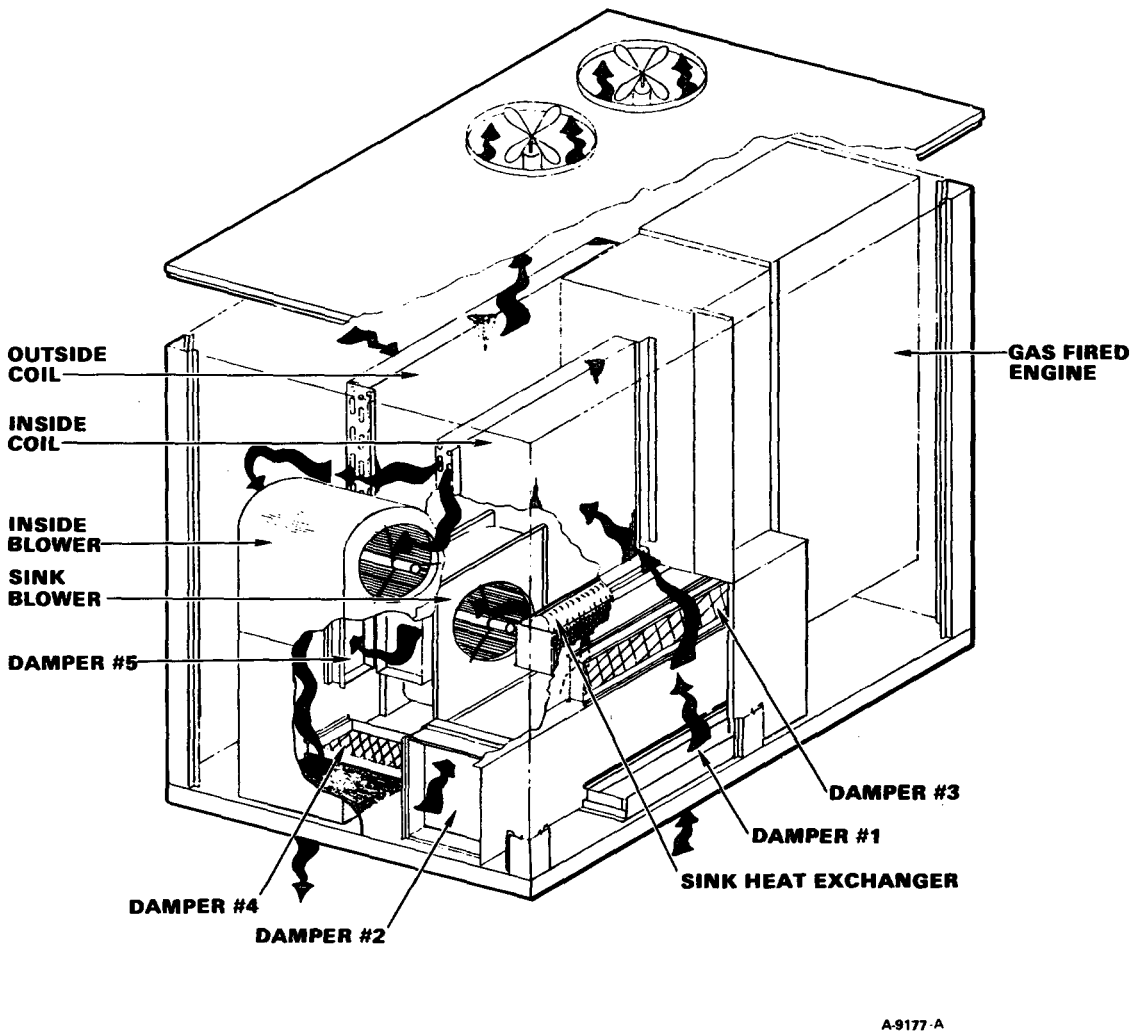

Figure 3-38. Cooling Mode Airflow Paths

ORNL-DWG 81-15034

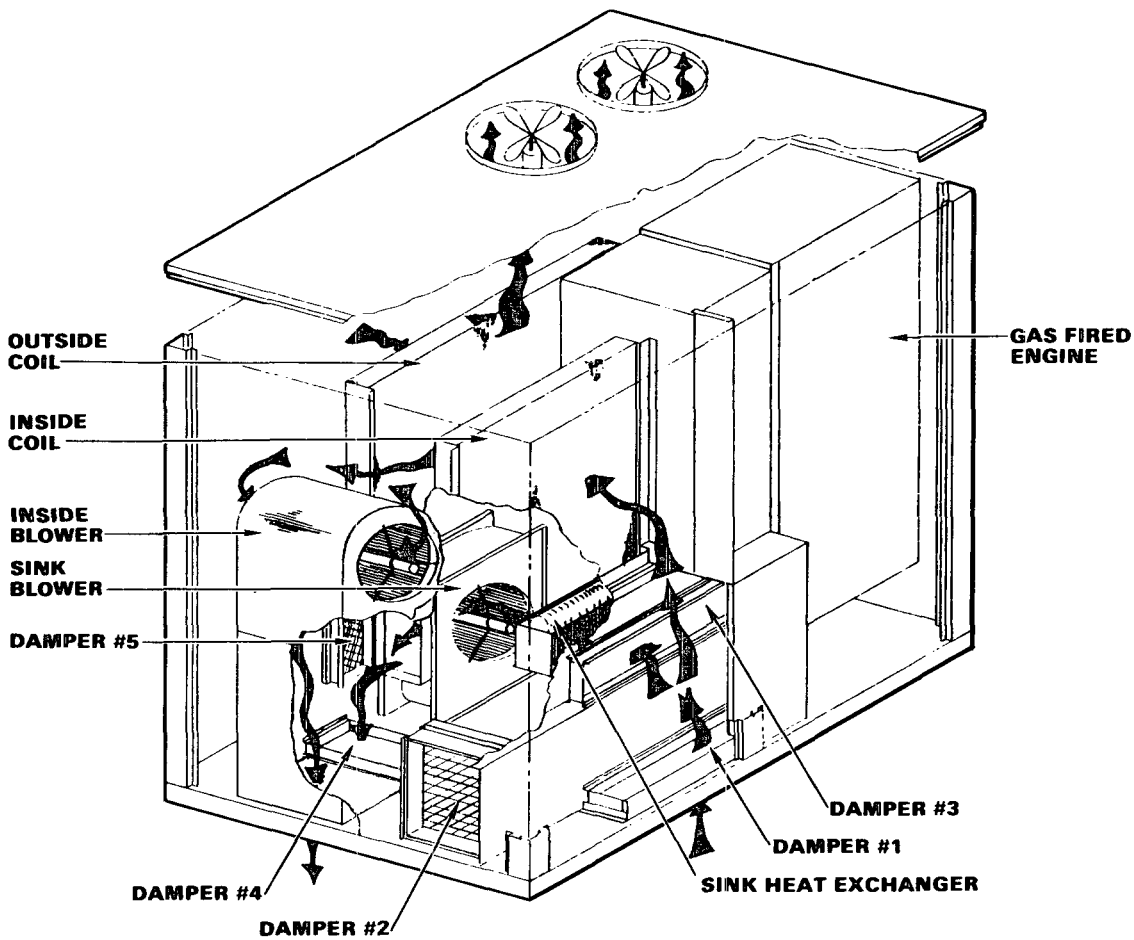

A-9178-A

Figure 3-39. Heating Mode Airflow Paths

ORNL-DWG 81-15041

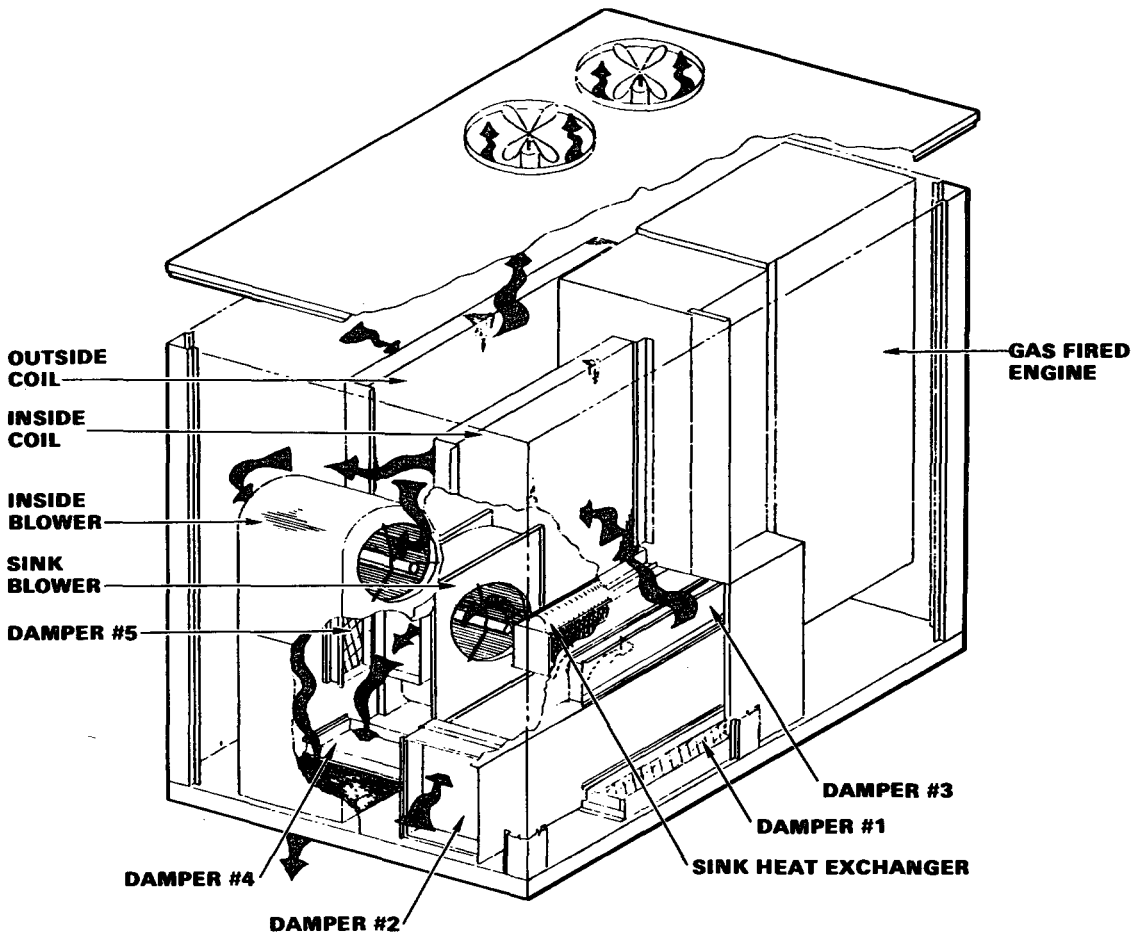

A-9176-A

Figure 3-40. Economizer Mode Airflow Paths

features of the selected design included minimum ductwork, the ability to vary each of the blower speeds from a single drive sheave, and complete separation of the outdoor coil air compartment and engine enclosure from the conditioned air section. The outdoor coil and engine enclosure sections are the shaded areas of Figure 3-36.

3. Engine/Heat Pump Interface Coordination

Several Dunham-Bush/AiResearch design coordination meetings were held to define special engine interface requirements for the heat pump and to discuss the overall design. These meetings and discussions culminated in completion of the layout activity and initiation of detail design for the heat pump package. Detail design is in progress.

SYSTEM BREADBOARD TESTING

Brayton Unit Testing in Facility No. 1

Breadboard testing was conducted in two separate test facilities. Test facility No. 1, the existing one, was modified to accommodate the Mark III Brayton turbocompressor and the dynamometer. In addition, a resistive load bank and a polyphase wattmeter were installed for the dynamometer, and a torque meter and load cell were installed for calibrating the Brayton turbine and compressor. Sample taps were added to the setup for emission testing in conjunction with other testing.

The Mark III Brayton engine breadboard test setup is shown schematically in Figure 3-41. Preliminary testing included air loading of the Brayton turbocompressor to check mechanical integrity throughout the operating range.

Continued testing of the Brayton turbocompressor showed performance data comparing very closely to predicted. However, a mechanical instability at high speed (75,000 rpm) was encountered. The machine was disassembled and found to have a slight shaft imbalance that was not being damped out by the foil bearings. The shaft was rebalanced and the bearings modified to improve dynamic stability. Performance and mechanical integrity testing is continuing.

Freon Circuit Testing in Facility No. 2

Test facility No. 2 was constructed for Freon circuit and engine demonstration testing (see Figures 3-42 and 3-43). As shown, totally contained climate chambers are used to simulate the indoor and outdoor sections of the heat pump. These chambers contain refrigeration coils and blowers similar to those intended for the production system. Using dampers and a variable output heater, a wide range of indoor and outdoor operating conditions can be simulated. An interior view of the indoor climate chamber is shown in Figure 3-44. The Freon circuit and components in the test setup are shown schematically in Figure 3-45. System controls and instrumentation shown in Figure 3-46 are housed in a trailer at the test site.

Freon circuit breadboard testing was conducted initially with the Mark II Rankine compressor being driven by a specially constructed air-driven turbine

ORNL-DWG 81-15035

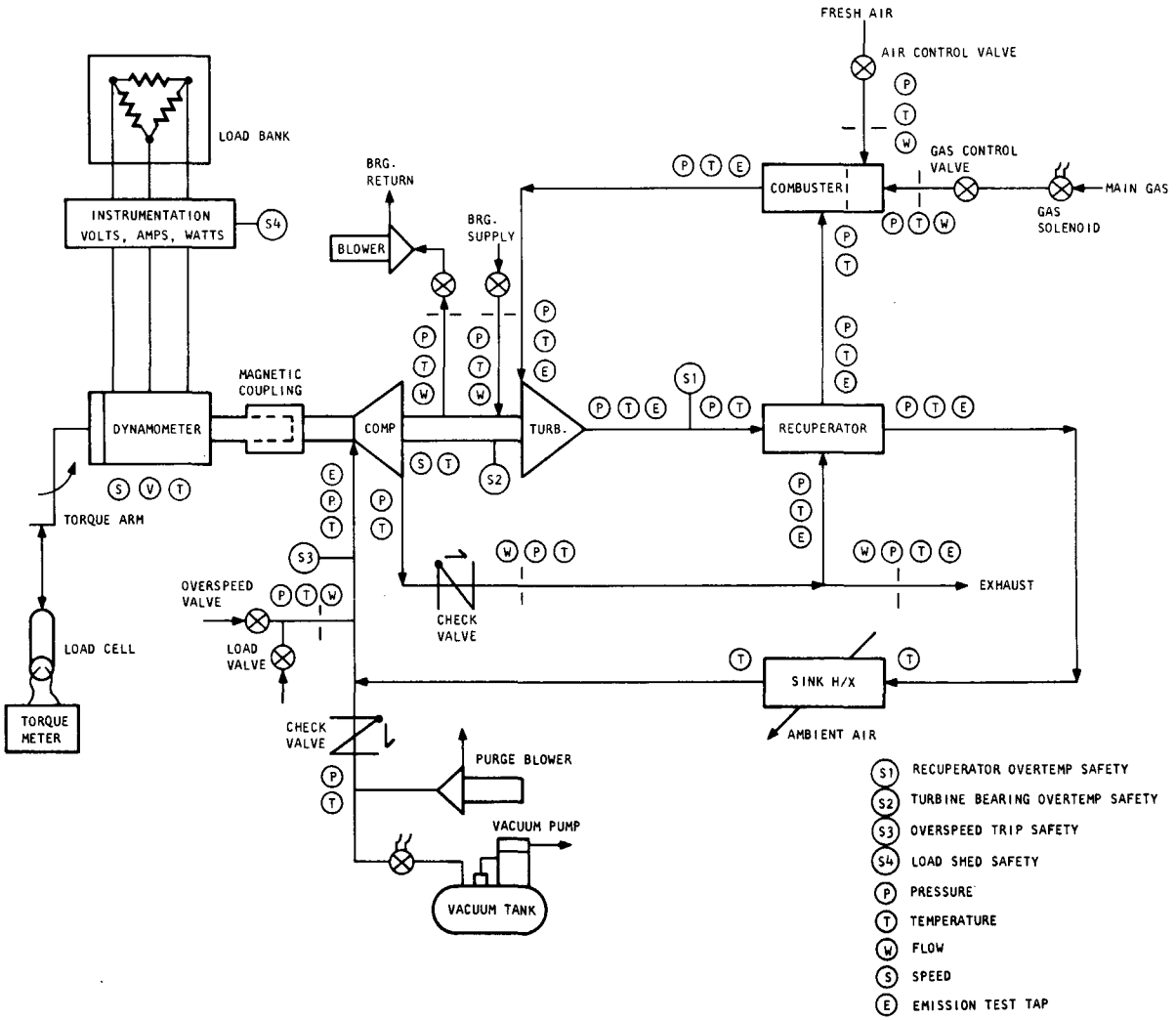

Figure 3-41. Mark III Brayton/Dynamometer Test Setup

ORNL-PHOTO 4621-81

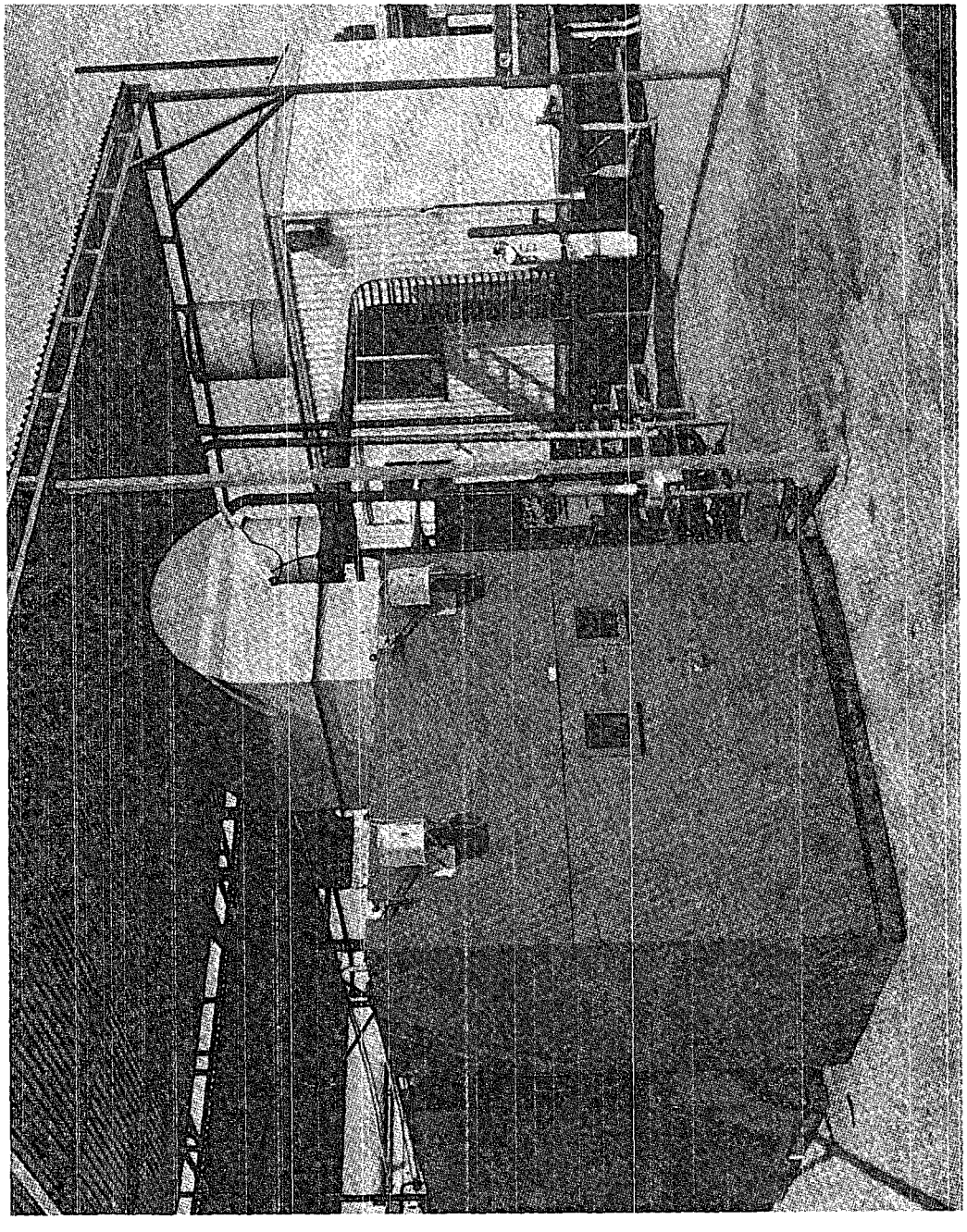

83592-15

Figure 3-42. Overall View of System Test Facility No. 2

ORNL-PHOTO 4622-81

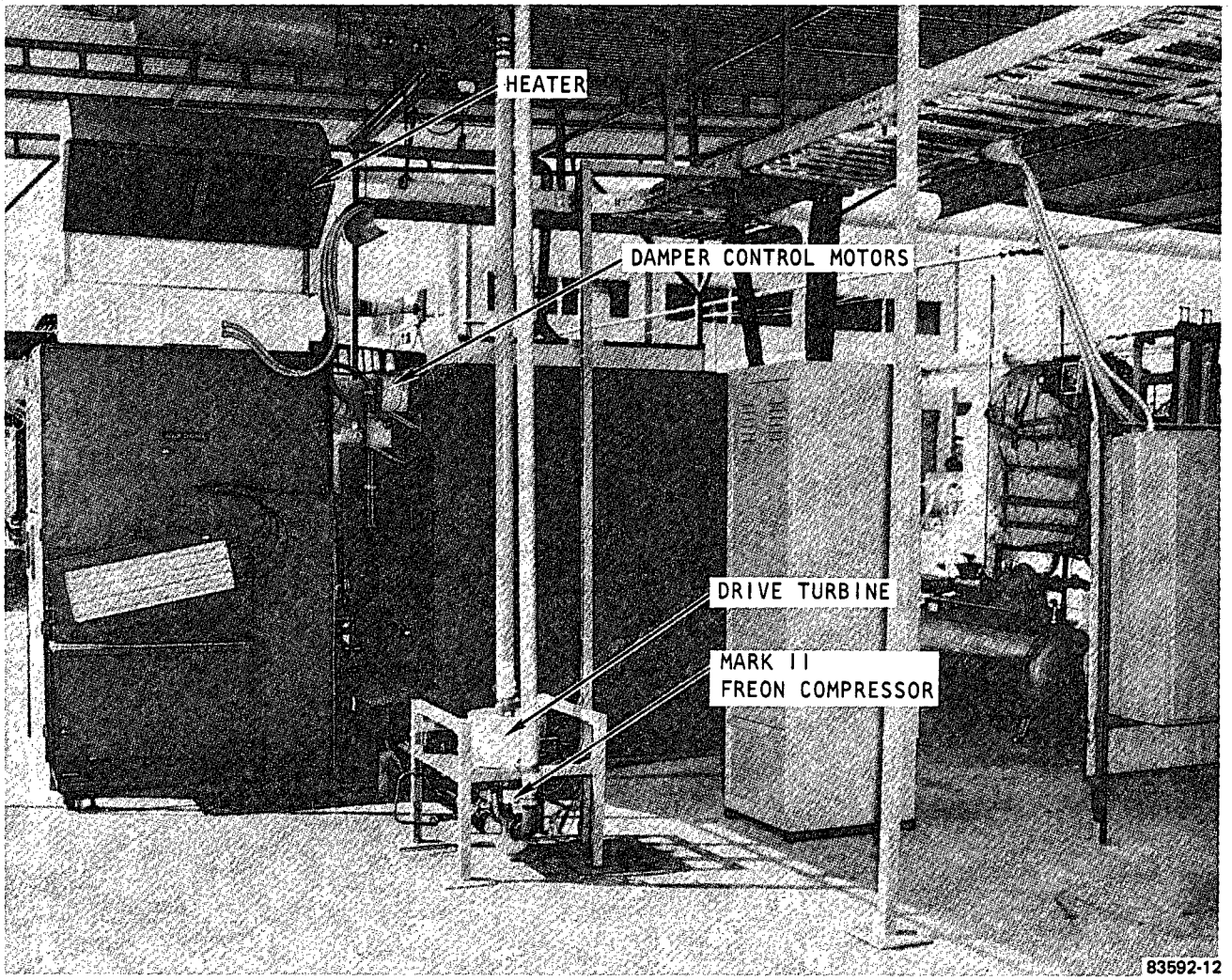

F-32796

Figure 3-43. Freon Compressor Test Setup

ORNL-PHOTO 4625-81

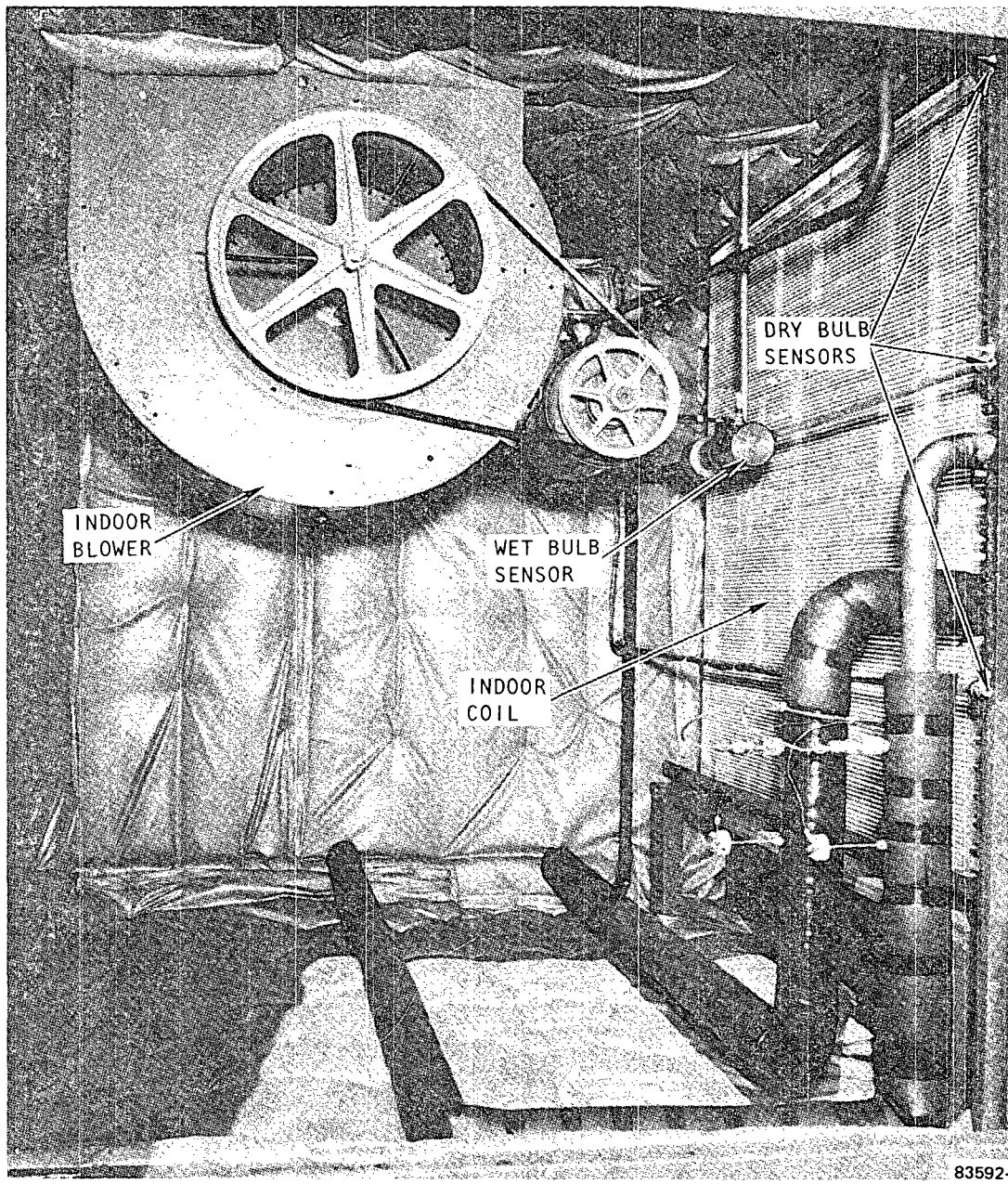

F-32794

Figure 3-44. Indoor Climate Chamber

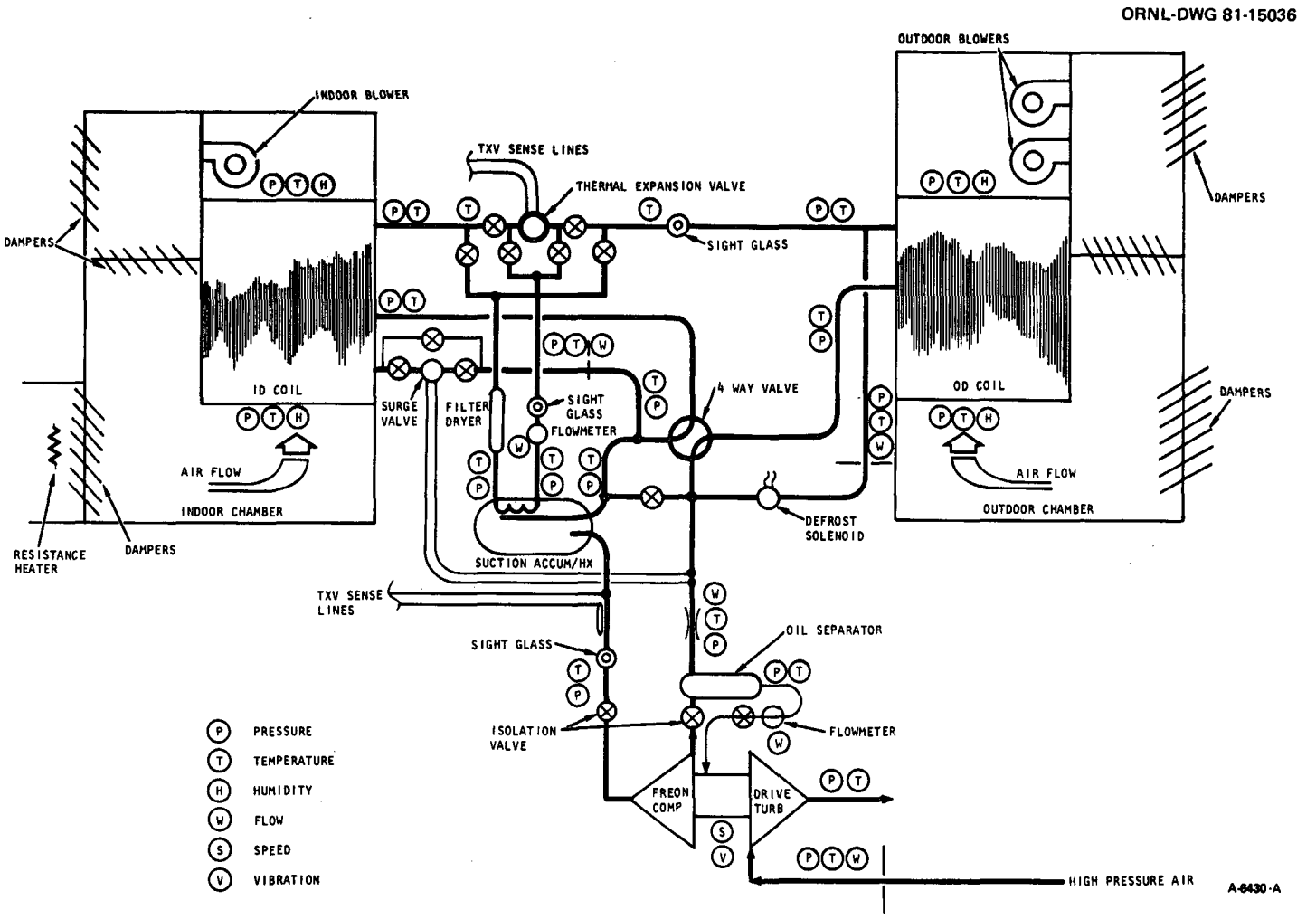

Figure 3-45. Mark III Freon Compressor Test Setup Schematic Diagram

ORNL-PHOTO 4627-81

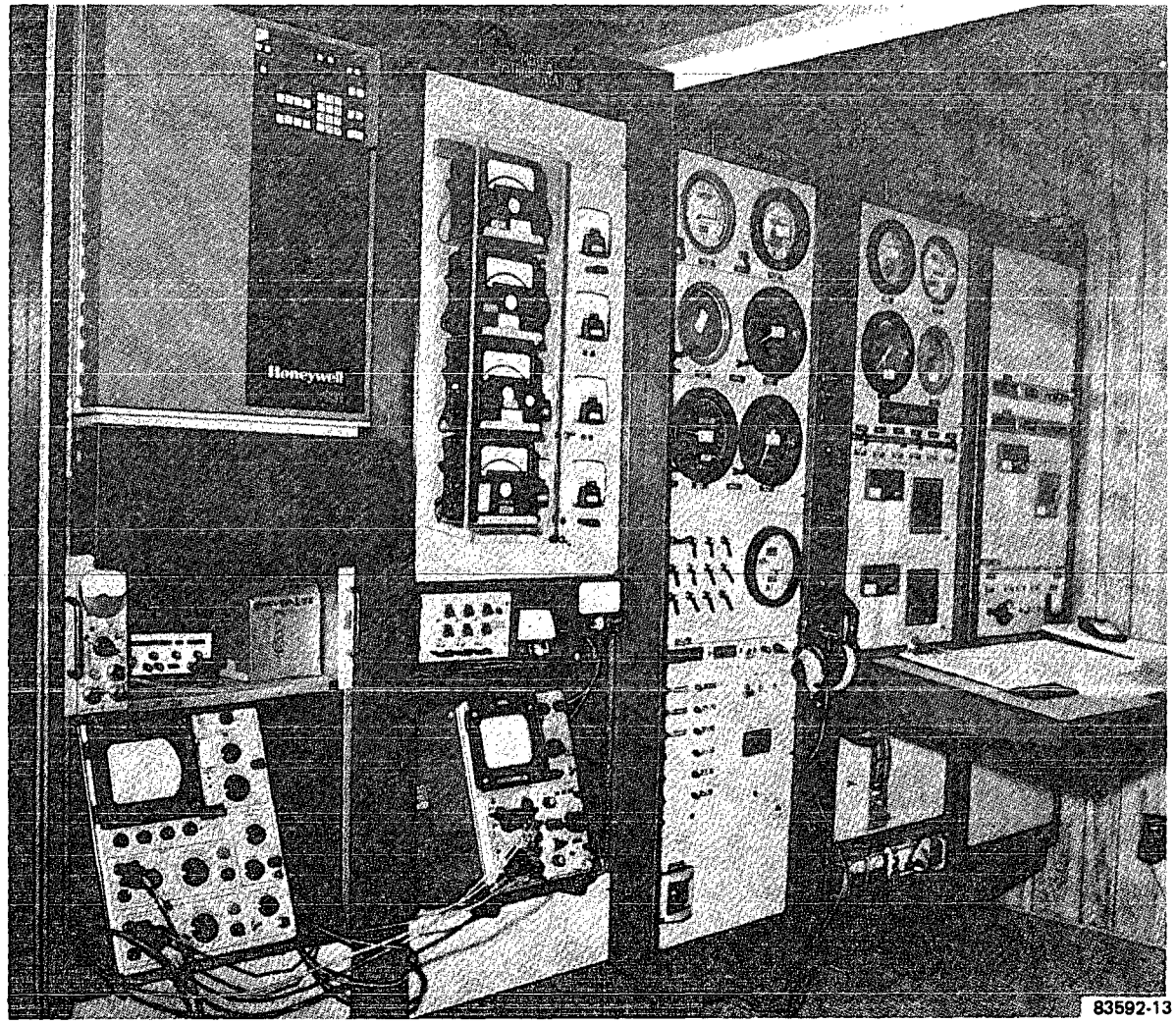

Figure 3-46. Freon Circuit Controls and Instrumentation

through a magnetic coupling (see Figure 3-43) similar to that of the Brayton turbocompressor. The tests were performed to:

(a) Verify component compatibility and system integrity.

(b) Verify that indoor and outdoor coil airflows and pressure drops meet design requirements.

(c) Measure indoor and outdoor coil Freon distribution in both the heating and cooling modes.

(d) Compare surge valve operation with that of previous tests.

(e) Verify that Freon piping and component pressure drops are within design limits.

After the above testing with the Mark II Rankine compressor was completed, the test setup was modified to incorporate the Mark III unit with a discharge oil separator for compressor bearing lubrication. Preliminary testing of the Mark III compressor revealed a lower-than-predicted performance level and an above-normal vibration level. The compressor was removed from the setup for a dimensional inspection and additional instrumentation.

Testing of the Mark III Rankine compressor continued after tightening tolerances and adding resilient bearing mounts to correct the problems encountered in preliminary testing. Verification of compressor performance and efficiency in conjunction with surge valve testing and overall system performance evaluation is continuing.

SECTION 4
SYSTEM ANALYSIS

SECTION 4

SYSTEM ANALYSIS

ANALYTICAL TASKS

The system analysis effort covered a variety of analytical tasks in support of functional and structural design of the system and its components. These tasks included the following:

(a) Prediction and optimization of system performance

(b) Thermodynamic and stress analyses

(c) Test data evaluation (correlation of actual and predicted performance)

(d) Various special analyses evaluating specific events or conditions

In addition, to evaluate total performance more fully and to compare the system with competitive equipment, fuel consumption and operational cost analyses were conducted.

The following paragraphs highlight each major analytical task and its relationship to the evolving system design.

PERFORMANCE PREDICTION/OPTIMIZATION

Prior to the start of the Phase II development program in March 1979, the basic configuration of the system had been defined and preliminary designs had been selected for the major items of the Brayton cycle engine. A Mark II rotating assembly, basically the same as the present Mark III in aerodynamic design, had been run in breadboard system tests. In support of both the preliminary design and test efforts, early analytical models of the Brayton and Rankine sides were separately developed for performance prediction and test data evaluation.

For maximum support and guidance of the design effort, the task of refining and optimizing the system design and the task of developing and refining the computer model were performed concurrently, with continual coordination between them. For example, as hardware selection was made based on analytical system evaluations of candidate designs, the actual or predicted performance data for that part was entered into the computer program. This, in turn, enhanced the evaluation of the next component design. Early in the hardware selection process, the separate analytical models for the Brayton and Rankine cycles were combined to form an integrated, commonly balanced, system program.

The initial baseline system, shown schematically in Figure 4-1, evolved gradually as the result of an extensive and systematic analytical study in which each component was individually evaluated. The study covered factors such as operational parameter variations, system/component configuration variations, and failure mode simulations. Climatic conditions were also varied as applicable. For each case, the effect upon predicted system performance and key internal

ORNL-DWG 81-15037

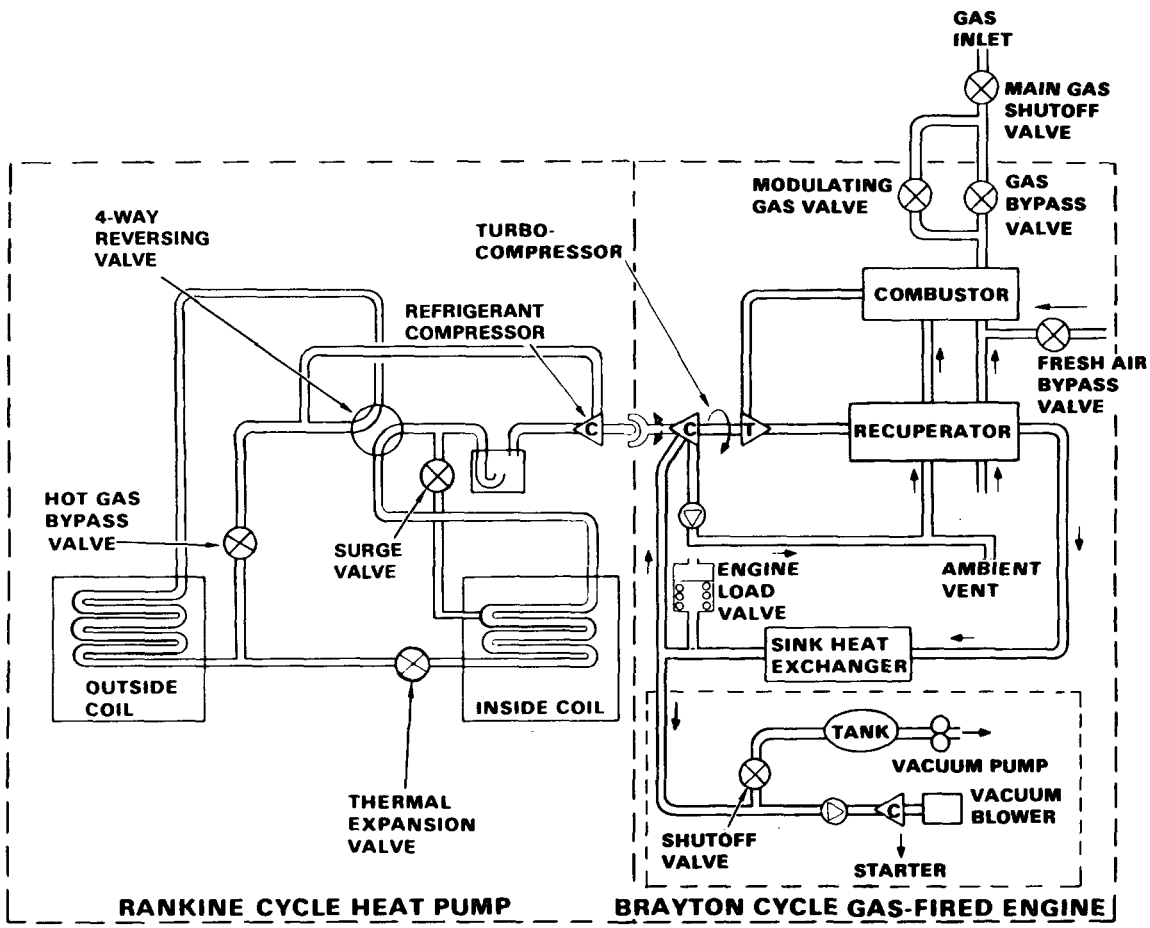

A-14245

Figure 4-1. Schematic Diagram of Brayton/Rankine Space Conditioning System

parameters, such as turbine speed or temperature, was evaluated. The end result satisfied the objective for the initial baseline configuration, which was an efficient, practically designed, conservatively optimized system to serve as a starting point for formal testing and a baseline for further design/cost optimization. The following are some of the highlights of the study:

(a) Several sink heat exchanger designs, which included variations in materials, construction, and shape, were evaluated. The selected unit is of plate-fin construction, made of mild steel, and specially coated for corrosion protection.

(b) The division of the cold-side recuperator passages (75 total) between primary and service sections had to be defined. Pressure drop balancing of the two sections was particularly important to ensure adequate fresh air flow to the combustor. The optimum split from the thermal and pressure drop standpoints was 69 primary and 6 service passages.

(c) Turbine speed, inlet temperature, and nozzle area were optimized for system performance and turbine life. Both criteria were best satisfied by a design speed (with related temperature) of 75,000 rpm, a reduction from the original design speed of 90,000 rpm. The turbine nozzle area selected was 1.45 sq in.

(d) The optimum gas flow modulation range was defined. The maximum flow reflects that required to produce 10 tons of cooling at the 95°F design point. In the determination of the minimum flow setting, COP vs gas flow characteristics at steady-state and at various flows with estimated cyclic degradation were considered. For field use, however, it could be more precisely optimized based on the site climate conditions.

(e) Two different approaches were evaluated for the low-temperature ambient (LTA) heating mode. For this mode, the sink heat exchanger must provide up to 90 percent of the total heat supplied to the building. Both candidate configurations involved the addition of special hardware and resulted in reduced efficiency. The selected approach, which achieves the capacity increase through increased fresh air and gas flow, was superior in all respects. The special hardware for this mode consists of two solenoid valves, identified as "fresh air bypass" and "gas bypass" in the Figure 4-1 schematic.

(f) In the Freon circuit, it was determined that surge protection is needed for the compressor in most heating conditions. This required the addition of the modulating surge valve shown in Figure 4-1 to recirculate vapor as needed to maintain a minimum compressor flow. To minimize coil mismatch in this condition, the recirculated vapor is extracted from within the indoor coil.

(g) Calibration points were defined for the surge valve and the hot gas bypass valve.

(h) Preliminary safety shutdown and control equipment settings were established.

Following the establishment of the initial baseline configuration, a series of performance prediction runs was made for ambient temperatures between 55° and 115°F in the cooling mode and between 47° and -10°F in the heating mode. Presented in Figures 4-2 and 4-3 is a performance summary of those runs in the cooling and heating modes, respectively. Steady-state system capacity and overall COP (without parasitics) are plotted over the gas flow modulation range. It should be noted that the COP values represent "source," and to obtain the equivalent "site" COP (as for an electrically driven heat pump), multiplication by 3.45 is required; i.e., a Brayton/Rankine COP of 1.0 is equivalent to an electrically driven heat pump COP of 3.45. The turbine speed over the gas flow modulation range is approximately 75,000 to 55,000 rpm in cooling, 80,000 to 60,000 rpm in heating, and 85,000 to 70,000 rpm in LTA heating.

Presented in Figures 4-4 and 4-5 is overall COP data, with and without parasitics, for selected ambient temperatures. Parasitic power consumption for the Brayton/Rankine system is approximately 2.15 kw in the normal heating and cooling modes, and approximately 1.35 kw in the LTA heating mode (no outdoor fans). At the 95 F ambient design point, the COP is 1.36 without parasitics and 1.07 with parasitics. This is equivalent to an electrically driven heat pump EER of 16.0 and 12.6, without and with parasitics, respectively--an improvement of more than 50 percent over existing conventional systems.

In Figure 4-6, the Brayton/Rankine COP is compared against various conventional units. As indicated, the Brayton/Rankine predicted system performance exceeds that of conventional systems, particularly in the heating mode.

Included in Table 4-1 is the computer program output for the 95 F ambient design point with the initial baseline system. Sheets 1 and 2 of the table cover the Freon circuit data and a system performance summary. Sheet 3 shows Brayton-cycle data and Sheet 4 is a summary of the exterior heat losses. The predicted Brayton-cycle efficiency is 0.303, 12 percent above the design point goal of 0.270.

System optimization was continued beyond the initial baseline configuration, with the effort concentrated primarily on heat exchanger effectiveness, size, and cost tradeoffs. Analysis indicates that with the number of hot passages in the primary section of the recuperator reduced from 70 to 58 (16 percent reduction in heat transfer area), very little component performance is sacrificed. This is due mainly to a reduction in total system flow (based on the original problem statement) and the combined effect of an increased heat-transfer coefficient and reduced axial conduction resulting from the higher flow per passage. Relating this to system performance at the cooling design point, the same total output is obtained with only a slight increase in turbine inlet temperature and a slight reduction in engine efficiency. The analysis also showed that while the 16-percent reduction had little impact on system conditions, extending the reduction further resulted in sharp increases in turbine temperature.

The sink heat exchanger was also evaluated for a possible reduction in size. Analysis indicated that with the reduced flow of the present system (based on the original problem statement) size could be reduced as much as 20 percent in the no-flow dimension, with essentially no performance impact.

ORNL-DWG 81-15038

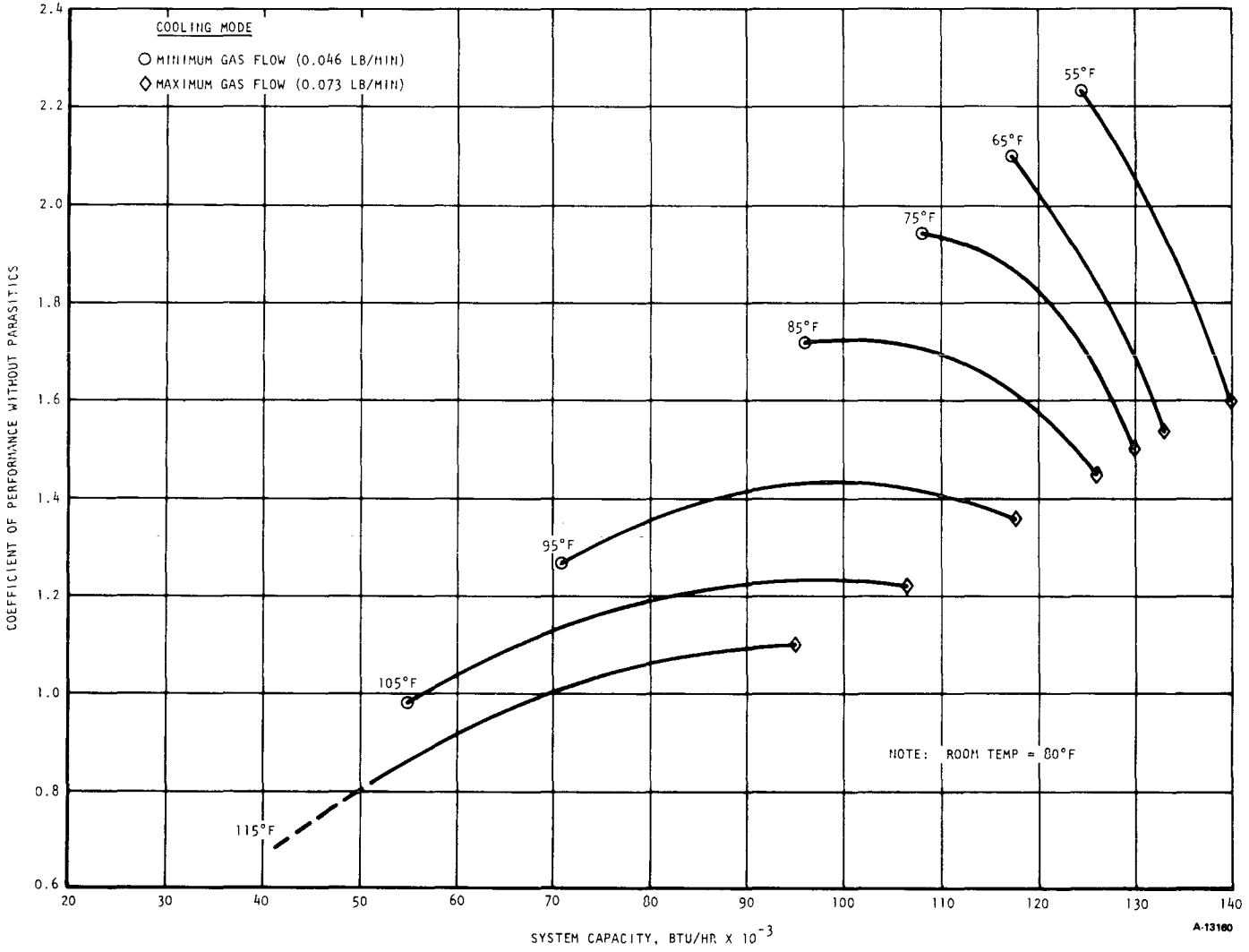

Figure 4-2. Predicted Cooling Mode Performance

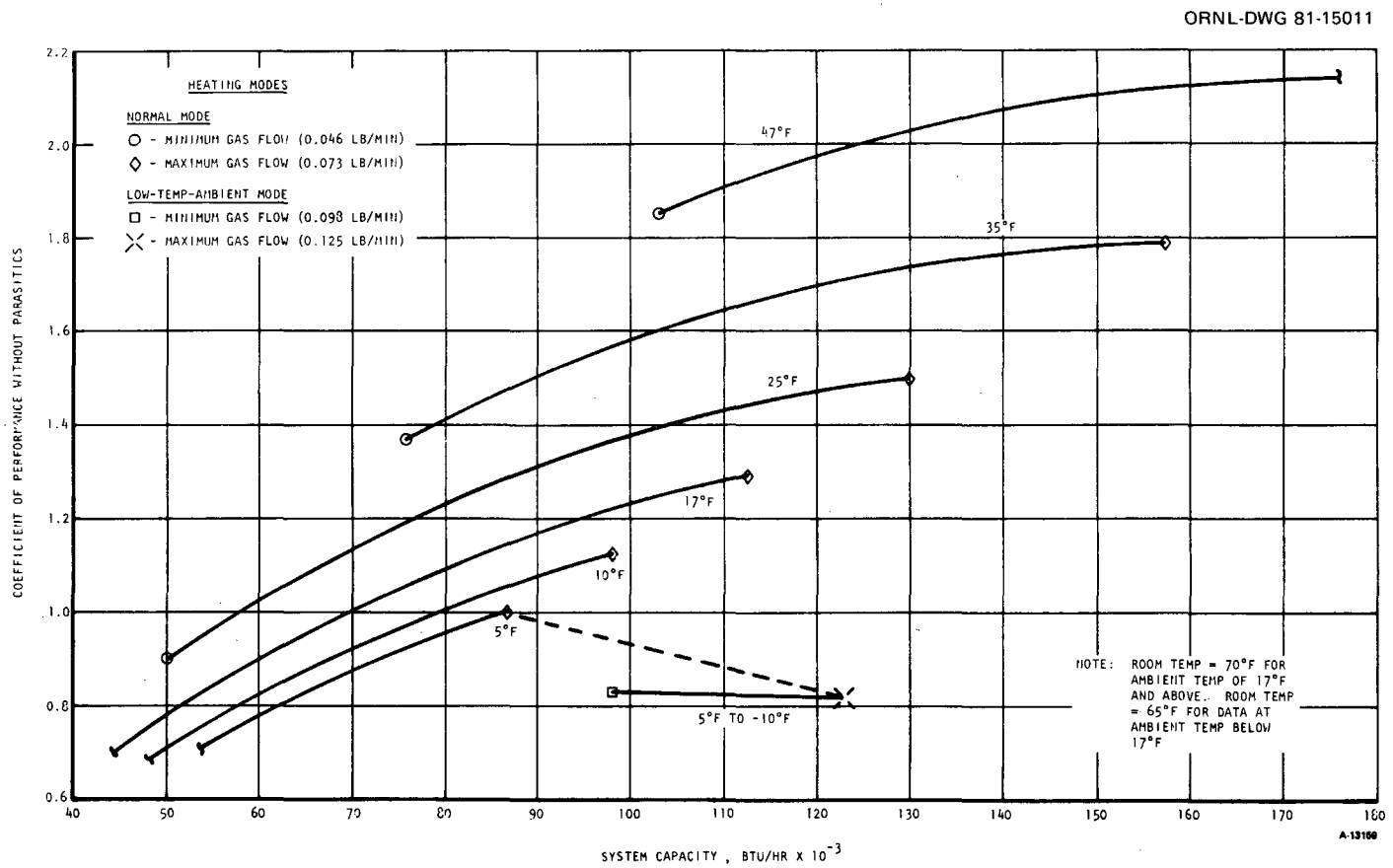

Figure 4-3. Predicted Heating Mode Performance

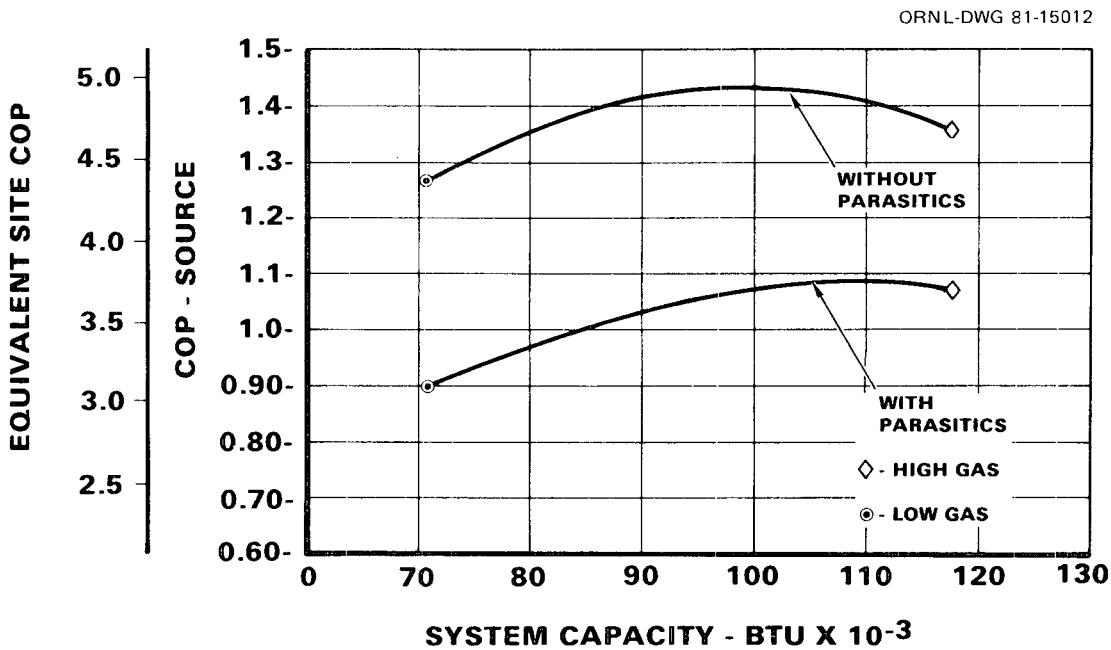

Figure 4-4. Steady-State Performance at Cooling Design Temperature (95°F Ambient)

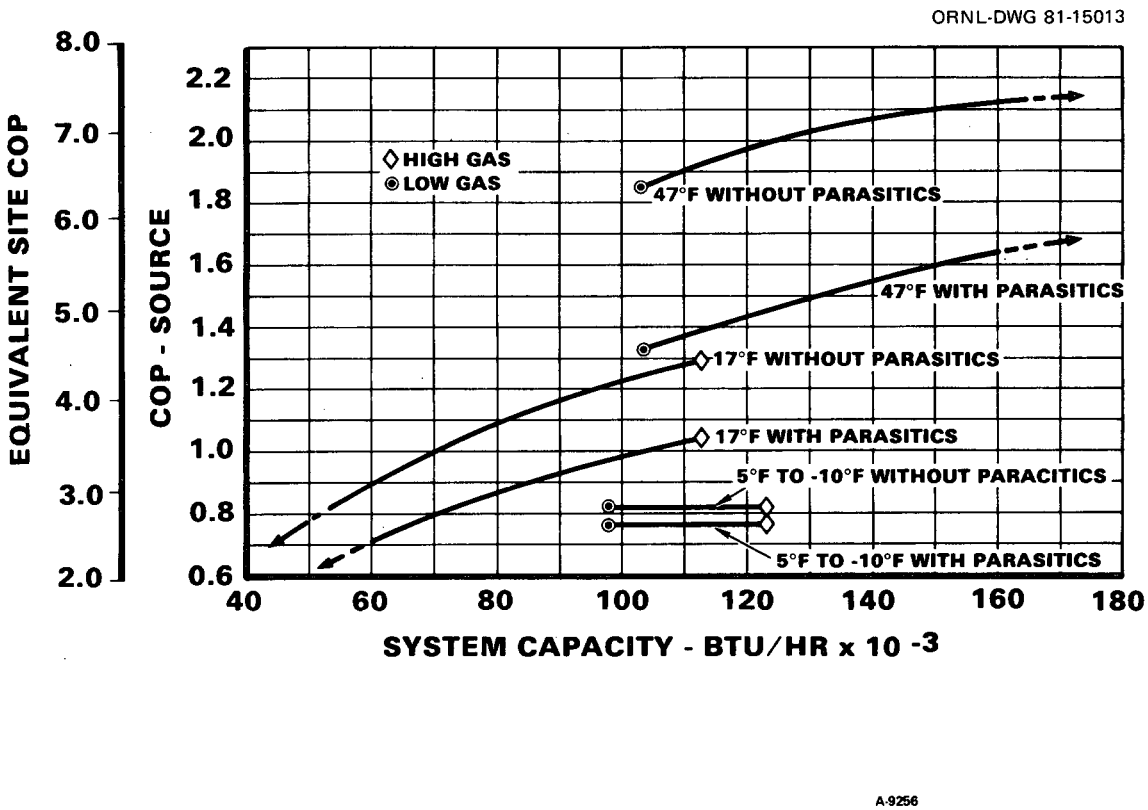

Figure 4-5. Steady-State Performance, Heating Mode

ORNL-DWG 81-15014

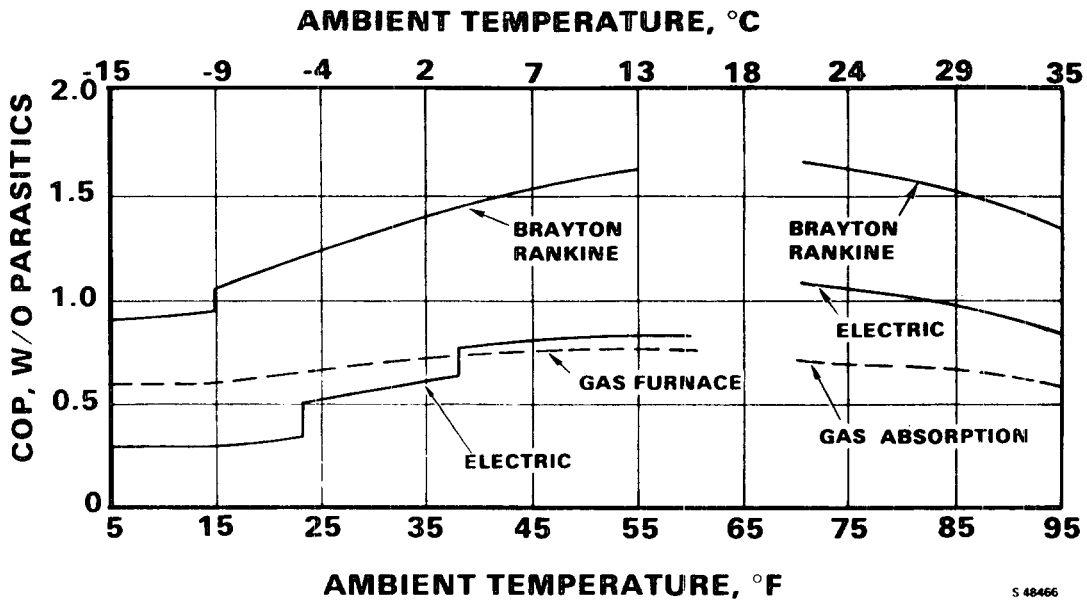

Figure 4-6. Comparative Performance

However, when the reduction was coupled with a recuperator change, 10 percent was found to be a more appropriate amount.

Table 4-2 includes comparative data for four candidate system baseline configurations: (1) the initial baseline, (2) with reduced size recuperator only, (3) with reduced-size recuperator and sink heat exchanger, and (4) the same as (3) but with an increase in turbine nozzle area. With both reduced-size units and the smaller turbine nozzle area, turbine inlet temperature increases only 40°F and cycle efficiency is down only 2 percent. If turbine inlet temperature should actually go higher because of other influences, full recovery to the original baseline temperature is possible with a turbine nozzle area increase. However, this change will result in a more pronounced impact on cycle efficiency and COP.

The proposed baseline configuration for the prototype system is with both heat exchangers reduced (16 percent for the recuperator and 10 percent for the sink) and the 1.45-sq-in. turbine nozzle area. If development testing indicates the need, the turbine nozzle area may be increased to 1.59 sq in. Reducing the size of the heat exchangers will not only reduce component costs, but will result in additional cost savings and size reductions for the engine and heat pump package assemblies, since they are both dependent on recuperator height.

TABLE 4-1

COMPUTER PROGRAM OUTPUT

```
* GARRETT * AIRESEARCH MANUFACTURING DIVISION  LOS ANGELES, CALIF.

GRI/GARRETT GAS FIRED SPACE CONDITIONING UNIT
                    RUN ON 21 JUL 80 AT 12:18:02                    PAGE 1 OF 4
  95 DEGREE DAY - COOLING MODE

   SYSTEM OPERATIONAL MODE  COOLING MODE
  UNITS IN PRINT OUT *** LENGTH=INCHES, AREA=SQ IN, SPEED=RPM, CORR SPEED=
  RPM/SQRT(T/TS), PRESS=PSIA, TEMP=DEG F, GAMMA=GRAINS/LB, ENTHALPY=BTU/LB,
  DENSITY=LB/CU. FT., FLOW=LB/MIN, VOL. FLOW=CFM, UA=BTU/(HR-F), CONDUC-
  TIVITY=BTU/(HR-FT-F), FILM COEFFICIENT=BTU/(HR-F**2-F)

                        * * * VAPOR CYCLE * * *
                              I N P U T   D A T A
                 DUCT PRESSURE LOSS COEFFICIENTS *10.*E+4
   .00000   .00000   .00000   .00040   .00200   .00054   .00001   .00093
   .00000  3.67000  1.17000   .01530   .04800   .01220  2.42000  5.81000

   SFC       SFCS      SFCW      SFF(1)    SFFW(1)   SFF(2)    SFFW(2)
  1.000     1.000     1.150     1.000     1.000     1.000     1.000
OUTHX AREA  INHX AREA     DTSH      DTSC    P SUCK
     2592.      1296.      10.0       2.0      61.2
                        * OPERATING CONDITION DATA *
 P AMB    T AMB   GA AMB   TAMB WB  P HOUSE  T HOUSE  GA HSE   THSE WB
 14.70    95.00   100.00    75.13    14.70    80.00    79.10    67.10

                          O U T P U T   D A T A
                         COMPRESSOR INFORMATION
    FREON FLOW                 40.257    INLET FLOW PARAMETER     31.389
    TEMPERATURE IN             59.544    TEMPERATURE OUT         153.627
    PRESSURE IN                60.935    PRESSURE OUT            173.528
    PRESSURE RATIO              2.848    EFFICIENCY                 .732
    SPEED                      75000.    CORRECTED SPEED         75000.
    ENTHALPY IN                 83.95    ENTHALPY OUT             94.67
    ENTROPY IN                  .1690    ENTROPY OUT              .1738

                      CONDENSER CIRCUIT INFORMATION
                         CONDENSER INFORMATION   (OUTSIDE COIL)
                                 AIR SIDE         FREON SIDE
    FLUID FLOW                   583.24             40.26
    INLET TEMPERATURE             95.00            153.58
    OUTLET TEMPERATURE           111.34            117.86
    PRESSURE IN                  14.700           173.326
    PRESSURE OUT                 14.692           172.621
    PRESSURE DROP                  .008              .705
    ENTHALPY IN                   38.51             94.67
    ENTHALPY OUT                  42.33             35.48
    SATURATED VAPOR TEMP                           120.01
    SATURATED VAPOR PRES                           172.97
    HEAT REJECTED                                 142983.
    NUMBER OF TUBES 192. TUBE LENGTH 54. NUMBER OF CIRCUITS 16.

                            DOWNSTREAM FAN
                 FAN INFORMATION (TWO FANS IN PARRALLEL)
    WEIGHT FLOW                 583.    VOLUMETRIC FLOW          8396.
    TEMP IN (DB/WB)   111.34/ 79.14     TEMP OUT (DB/WB) 111.64/ 79.24
    PRESSURE IN               14.692    PRESSURE OUT            14.712
    EFFICIENCY                  .608    HORSEPOWER                1.08
    EXIT PRESSURE             14.697
```

TABLE 4-1 (Continued)

```
* GARRETT * AIRESEARCH MANUFACTURING DIVISION  LOS ANGELES, CALIF.

GRI/GARRETT GAS FIRED SPACE CONDITIONING UNIT
                RUN ON 21 JUL 80 AT 12:18:02                    PAGE 2 OF 4
 95 DEGREE DAY - COOLING MODE

  SYSTEM OPERATIONAL MODE  COOLING MODE

                 EVAPORATOR CIRCUIT INFORMATION
                     EVAPORATOR INFORMATION   (INSIDE COIL)
                            AIR SIDE          FREON SIDE
  FLUID FLOW                 307.59              40.26
  INLET TEMP (DB/WB)     80.00/ 67.10            50.32
  OUTLET TEMP (DB/WB)    58.16/ 58.21            60.28
  PRESSURE IN               14.675            61.914
  PRESSURE OUT              14.661            61.440
  PRESSURE DROP               .014              .474
  ENTHALPY IN                31.55             35.48
  ENTHALPY OUT               25.19             84.04
  SATURATED VAPOR TEMP                         50.21
  SATURATED VAPOR PRES                         61.68
  HEAT REJECTED(SENS/LAT)        0./   117305.
  HEAT ABSORBED(SUPERHEAT/TOTAL)          3966./   117305.
  NUMBER OF TUBES 144. TUBE LENGTH 36. NUMBER OF CIRCUITS 36.
  COIL CALCULATED CAPACITY  117305.

                       DOWNSTREAM FAN
                      FAN INFORMATION
  WEIGHT FLOW                308.    VOLUMETRIC FLOW          4024.
  TEMP IN (DB/WB)    58.16/ 58.21    TEMP OUT (DB/WB)  58.89/ 58.51
  PRESSURE IN              14.561    PRESSURE OUT            14.701
  EFFICIENCY                .551    HORSEPOWER                 1.28
  EXIT PRESSURE            14.701

                    EXPANSION VALVE INFORMATION
  FLUID FLOW                40.26    VALVE CA                 .0109
  PRESSURE IN              172.62    PRESSURE OUT             61.91
  TEMPERATURE IN           117.36    TEMPERATURE OUT          50.32
  ENTHALPY IN               35.48    ENTHALPY OUT             35.48

                CONDENSER BYPASS/SURGE VALVE LOOP
  FLUID FLOW                 .00    VALVE CA                 .0000
  PRESSURE IN              172.37    PRESSURE OUT             61.44
  TEMPERATURE IN           120.01    TEMPERATURE OUT          87.57
  ENTHALPY IN               88.35    ENTHALPY OUT             88.35

                 OVERALL SYSTEM PERFORMANCE SUMMARY
  SYSTEM UTILIZABLE COMPRESSOR INPUT POWER (HP/BTUH)   10.33/26299.
  RANKINE COMPRESSOR BRG.,COUPLING/ROTOR WINDAGE LOSSES       1.5%
  THERMAL ENERGY REMOVED                                    117305.
  COP VAPOR CYCLE                                             4.498
  OVERALL COP WITHOUT PARASITICS                              1.364
  OVERALL COP                                                 1.042
```

TABLE 4-1 (Continued)

```
 * GARRETT * AIRESEARCH MANUFACTURING DIVISION  LOS ANGELES, CALIF.

GRI/GARRETT GAS FIRED SPACE CONDITIONING UNIT
                    RUN ON 21 JUL 80 AT 12:18:02                    PAGE 3 OF 4
  95 DEGREE DAY - COOLING MODE
   SYSTEM OPERATIONAL MODE  COOLING MODE
                        * * * POWER CYCLE * * *
                          PRESSURE LOSS Z*10**4
  1.5000    .6549    .1514    .1953    .0762    .7315   2.8594   7.5949
   .0195   3.2956   2.3280  16.9840    .0000    .0450    .0000    .0000
                          * SYSTEM CONSTANTS *
TURB NOZ    SINK HX A  TURB LK A   TURDN   COMDN    SFT     SFC    SFCW
  1.450        236.     77.0000    .000    .000   1.000   1.000   1.000
AF RATIO  DP REL  CPL EFF  GAS LHV  RPM MAX
 16.00     9.60     1.00   20000.   85000.
                  * OPERATING CONDITION DATA *
 P AMB    T AMB   GA AMB   TAMB WB  P HOUSE  T HOUSE  GA HSE   THSE WB
 14.70    95.00   100.00     .00    14.70    80.00    79.10     .00
                      O U T P U T   D A T A
                   PRESS    T DB   T DAR   GAMMA      H        W      W DRY
RECUP HX IN  69   14.750   297.3   297.3   100.0    88.37    12.35     .00
RECUP HX OUT 70   14.703  1188.8  1188.8   100.0   309.06    12.35     .00
BURNER IN    71   14.630  1181.3  1181.3   100.0   307.12    12.35     .00
BURNER OUT   54   14.484  1581.6  1581.6   100.0   412.34    13.68   13.49
TURBINE IN   55   14.435  1579.5  1579.5   100.0   411.73    13.68   13.49
TURBINE OUT  56    6.818  1272.8  1272.8   100.0   330.86    13.68   13.49
RECUP HX IN  57    6.798  1272.8  1272.8   100.0   330.89    12.52     .00
RECUP HX OUT 58    6.719   403.0   403.0   100.0   114.45    12.52     .00
SERVI HX IN  81    6.798  1272.8  1272.8   100.0   330.89     1.17     .00
SERVI HX OUT 82    6.715   182.4   182.4   100.0    60.05     1.17     .00
SINK HX IN   62    6.701   374.7   374.7   100.0   107.46    13.68     .00
SINK HX OUT  63    6.667   116.3   116.3   100.0    43.76    13.68     .00
COMPOR IN    64    6.606   115.6   116.3   100.0    43.76    14.08     .00
COMPOR OUT   65   14.833   301.4   299.7   100.0    88.93    14.08     .00
SINK AIR IN  77   14.718    95.6    95.6   100.0    38.67    77.37     .00
SINK AIR OUT 78   14.695   141.6   141.6   100.0    49.98    77.37     .00
SER HX A IN  51   14.700    95.0    95.0   100.0    38.51     1.26     .00
SER HX A OUT 52   14.651  1119.7  1119.7   100.0   291.42     1.26     .00
AIR COMPRESSOR BRG. COOLING FLOW = 0.4 LB/MIN
 RECUPERATOR  EH   .892  EC   .914  SHRH  1.000  SHRC  1.000

 SERVICE HX   EH   .926  EC   .870  SHRH  1.000  SHRC  1.000

 SINK HX      EH   .926  EC   .165  SHRH  1.000  SHRC  1.000  Q LOAD  52521.

 SINK FAN     CFM  1081.  P IN 14.700  P OUT 14.747  P/P  1.003  EFF   .677
              HP    .31

 TURBINE      ETA  .845  PRT  2.117  FF    .92  U/C  .95  NCOR  37823.

 COMPRESSOR   ETA  .787  PRC  2.227  WCOR 33.009  NCOR 71206.  N  75000.

 BURNER       ETA 1.000   HEAT INPUT  85974.   GAS FLOW  .072
                COMBUSTOR AIR FLOW  1.26   EXCESS AIR 1.100
 POWER        HPT   26.11  HPC   15.00  HPS   10.25  PBF  .967

 PRESS LOSS   DPHI   .315   DPLO   .212   DPTOT   .528   BETA   .951
              DPHI/DPTOT    .60
 ENGINE       CYCLE EFF  .303   POWER  10.25
```

TABLE 4-1 (Continued)

* GARRETT * AIRESEARCH MANUFACTURING DIVISION LOS ANGELES, CALIF.

GRI/GARRETT GAS FIRED SPACE CONDITIONING UNIT
RUN ON 21 JUL 80 AT 12:18:02 PAGE 4 OF 4
95 DEGREE DAY - COOLING MODE
SYSTEM OPERATIONAL MODE COOLING MODE

SYSTEM DUCTS HEAT TRANSFER

	1 AIRCOMP/ RECUPER	2 COMBSTR/ TURBINE	3 RECUPER/ COMBSTR	4	5	6
TEMPERATURES:						
FLUID	298.5	1580.6	1186.0			
INNER WALL	280.8	1424.4	1050.4			
TUBE/INSUL	280.7	1424.4	1050.4			
OUTER SURFACE	102.2	158.3	136.4			
AMBIENT	95.0	95.0	95.0			
FILM COEFFICIENT						
INNER WALL	.934	1.243	.787			
OUTER WALL	.408	.689	.606			
RADIATIVE	1.110	1.291	1.217			
TOTAL OUTSIDE	1.517	1.980	1.823			
OVERALL HEAT TRNSFR COEFF UA	1.98	.33	1.32			
WIND	0.	0.	0.			
SYSTEM FLUID						
TEMP LOSS	2.35	2.16	7.53			
HEAT LOSS	403.2	493.1	1438.6			
DUCT CONSTANTS						
LENGTH	90.24	8.88	39.48			
DIAMETER	12.42	13.18	15.72			
TUBE THCKNESS	.032	.032	.032			
TUBE CNDCTVTY	10.151	25.163	20.461			
INSL THCKNESS	3.162	3.557	3.206			
INSL CNDCTVTY	.020	.036	.026			
SRFC EMISSVTY	.930	.930	.930			

TABLE 4-2

COMPARISON OF CANDIDATE SYSTEM BASELINE CONFIGURATION
AT COOLING DESIGN POINT, 95°F AMBIENT

Parameter ↓	Recuperator → / Sink Heat Exchanger → / Turbine Nozzle →	Large* / Large / Small	Small / Large / Small	Small** / Small / Small	Small / Small / Large
System capacity, Btu/hr		117,305	117,305	117,305	117,305
Rotating group speed, rpm		75,000	75,000	75,000	75,000
Turbine inlet temperature, °F		1580	1602	1621	1570
Turbine nozzle area, sq in.		1.45	1.45	1.45	1.59
Recuperator inlet temperature, °F		1273	1294	1309	1275
Recuperator effectiveness (hot)		0.892	0.886	0.886	0.885
Gas flow, lb/min		0.072	0.074	0.074	0.078
Brayton output, hp		10.25	10.26	10.44	10.29
Brayton efficiency		0.303	0.294	0.298	0.280
Vapor cycle, COP		4.498	4.494	4.141	4.478
Overall COP, without parasitics		1.364	1.319	1.313	1.255
Overall COP		1.042	1.015	1.015	0.976

*Initial baseline configuration
**Proposed prototype configuration

ENGINE THERMODYNAMIC AND STRESS ANALYSES

A thermal model of the Brayton-cycle engine was prepared to define and evaluate thermal transients during startup and cyclic operation. Then, using the model and the AiResearch thermal analyzer computer program, an engine transient thermal analysis was performed. The primary objectives of this analysis were (1) to determine the startup characteristics of the engine, (2) to provide transient operating conditions for detailed transient thermal stress analysis of the recuperator and turbine, and (3) to identify the design or operating condition modifications required to prevent excessive heat loss or internal heat bypass.

The engine components are shown in Figure 4-7, together with a schematic for the conceptual approach of the Brayton/Rankine system. This effort was confined to a study of the Brayton cycle engine only. The fluid node numbers shown represent a comprehensive analysis of the entire engine. The event sequence and parametric control for the analysis simulated the anticipated operation profile. The cooling mode design point, 95°F ambient temperature, was the operating condition analyzed.

Predicted interface temperature vs. time is presented in Figure 4-8. The dashed lines reflect an initial minimum natural gas flow setting, then a switch to the maximum gas flow after 6 min. The solid-line profiles depict the transient going directly to the maximum gas flow. The control system will be configured for the faster transient, since it is most desirable for turbine starting and overall efficiency, yet is mild from the thermal stress standpoint.

Several engine packaging design improvements also resulted from the thermal analysis. For example, insulation was added to the outside of the engine enclosure in some areas to reduce external heat loss. In addition, to suppress radiation to the recuperator inlet manifold and to ambient through the adjacent wall, the combustor outlet section was extended in length to be near the mounting flange.

Because of the structural nature of the engine package assembly, stress analyses were an ongoing effort during the package design phase.

LABORATORY TEST SUPPORT

Part of they system analysis effort involved laboratory tests. Utilizing the breadboard system as a test bed, specific system/component characteristics and functions wre evaluated for correlation with anaytical predictions and for obtaining data to improve the analytical computer model. These evaluations included the following:

(a) Combustor Efficiency--System combustor performance was thoroughly evaluated to verify predictions based on component tests. In addition, special tests included a quantitative constituent analysis of the system exhaust gas at various combustor fuel/air ratios. The data indicated that contaminant levels were significantly lower than allowable. This test will be repeated during system development. A heat-loss analysis also generally confirmed the combustor efficiency.

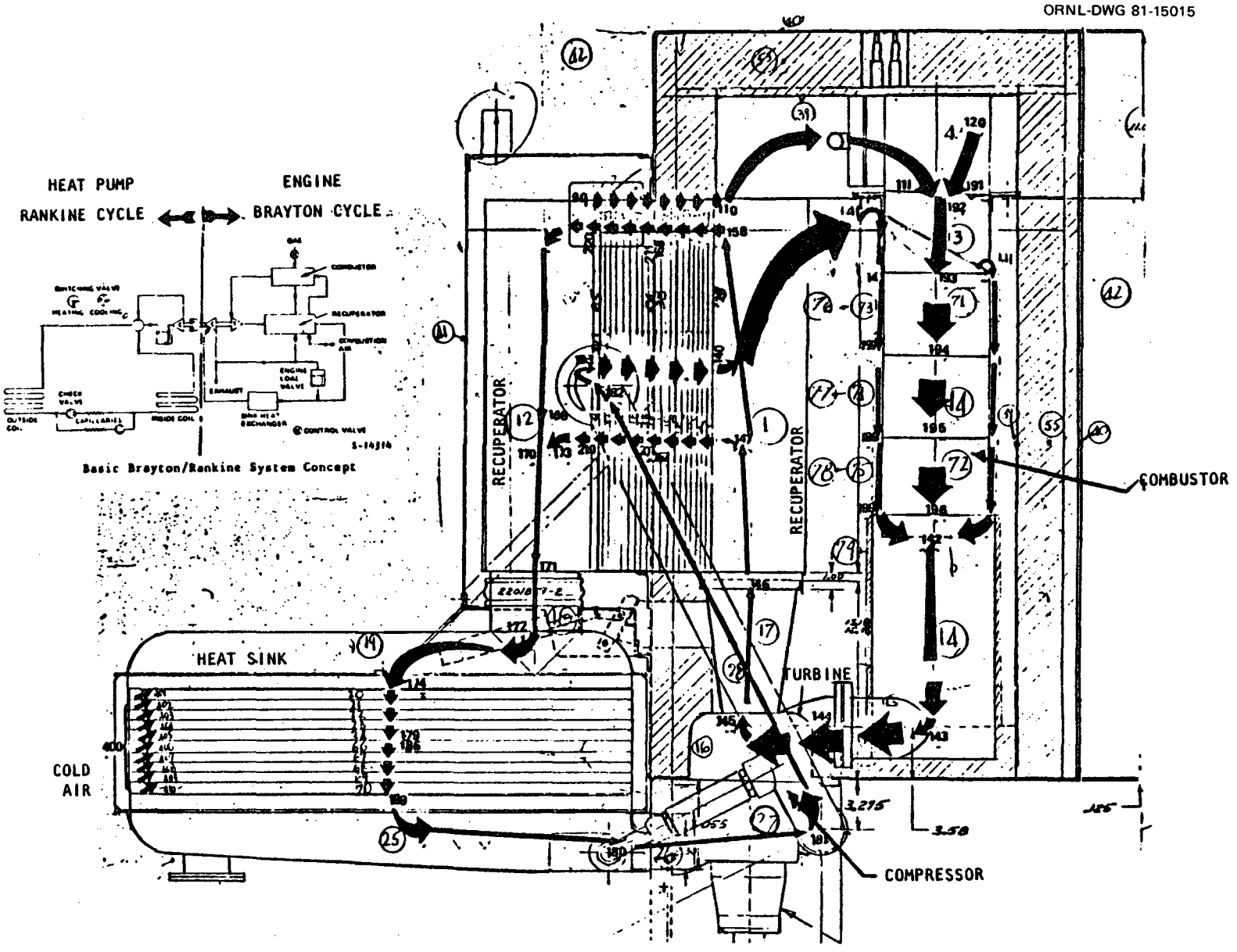

Figure 4-7. Station Points for Thermal Analysis of Brayton Cycle Engine

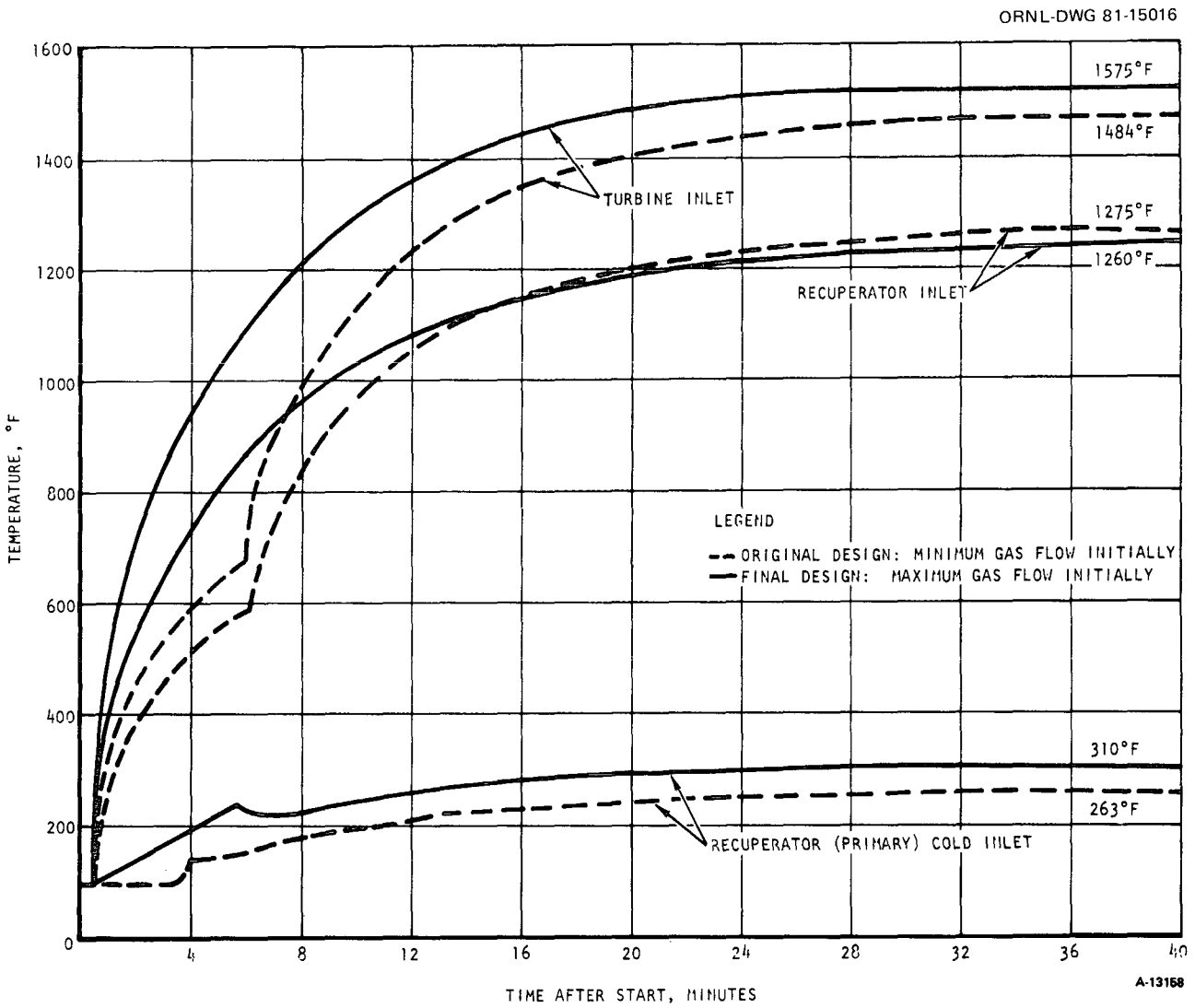

Figure 4-8. Predicted Values of Engine Interface Temperature During Start Cycle

(b) Startup Transients--Variations of the vacuum start concept were simulated to optimize the prototype starter for cost/performance. Laboratory equipment was obtained to evaluate further the vacuum-boost approach to starting and to correlate results with the analysis.

(c) Surge Valve--The Freon compressor surge valve was functionally evaluated on both the component and system levels. The computer model was modified to evaluate prototype system performance with actual valve characteristics.

General data analysis support was provided as required for all laboratory breadboard system and component testing.

MISCELLANEOUS ANALYSES

Several special analyses were performed in support of system and component design, or in support of other analyses. These are briefly described below.

(a) Corrosion due to condensation was analyzed. Condensation could occur at the sink heat exchanger outlet under certain conditions. Sulfurous acid formation is not considered a problem because of its minute quantity. Carbonic acid, which would be more prevalent with condensate, will not be a problem if the aluminum alloy and mild steel surfaces are suitably protected.

(b) Various turbine start systems were evaluated. The vacuum-boost configuration selected for prototype testing was optimized relative to vacuum tank size and blower steady-state flow rate.

(c) In support of turbine and recuperator life cycle analyses, annual duty cycles were established. The annual duty cycle for the turbine, in terms of speed and temperature vs. exposure time, is shown in Table 4-3.

(d) An analytical determination of annual system operation was made (including steady-state, cyclic, and economizer) using the DOE-North and DOE-South load and climatic data.

FUEL CONSUMPTION AND COST ANALYSIS

A separate computer program was developed to evaluate fuel consumption and operating costs for the Brayton/Rankine system and for competitive hardware, both current units and future high-efficiency units. The DOE North and DOE-South load lines (see Figure 4-9) were used. Brayton/Rankine steady-state performance was based on the data in Figures 4-2 and 4-3. Included in the analysis were degradation factors* for on-off cycling losses and for defrost. Competitive systems for this evaluation were:

*Didion, D. A., and G. E. Kelly, "New Testing and Rating Procedure for Seasonal Performance of Heat Pumps," ASHRAE Journal, September 1979, Vol. 21, No. 9, pp. 40-44.

TABLE 4-3

TURBINE ANNUAL DUTY CYCLE

Operating Mode	Turbine Inlet Temperature, °F	Turbine Speed, rpm	Total Operating Hours	
			North	South
Cooling	1340	60,000	1151	1823
	1420	65,000	195	350
	1500	70,000	178	237
	1580	75,000	84	103
Heating (normal)	1100	65,000	1795	1320
	1210	70,000	539	270
	1320	75,000	603	77
	1430	80,000	176	24
Heating (LTA)*	1200	75,000	0	0
	1320	80,000	127	10
	1440	85,000	211	3

*Special heating mode at low temperatures ambient (below 10°F)

(a) Future all-electric heat pump with EER of 11.5 at 95°F.

(b) Future year-round air conditioner incorporating pulse-combustion gas furnace with overall efficiency of 90 percent, and electric cooling EER of 11.5 at 95°F.

Figures 4-10 and 4-11 are comparative annual energy consumption data for both competitive systems and the Brayton/Rankine system. In Figures 4-12 and 4-13 fuel consumption is translated into dollars at various energy rates. As with the performance comparisons, the Brayton/Rankine system again is superior to competitive systems, even though the estimated performance of the latter is approximately 30 percent better than today's units.

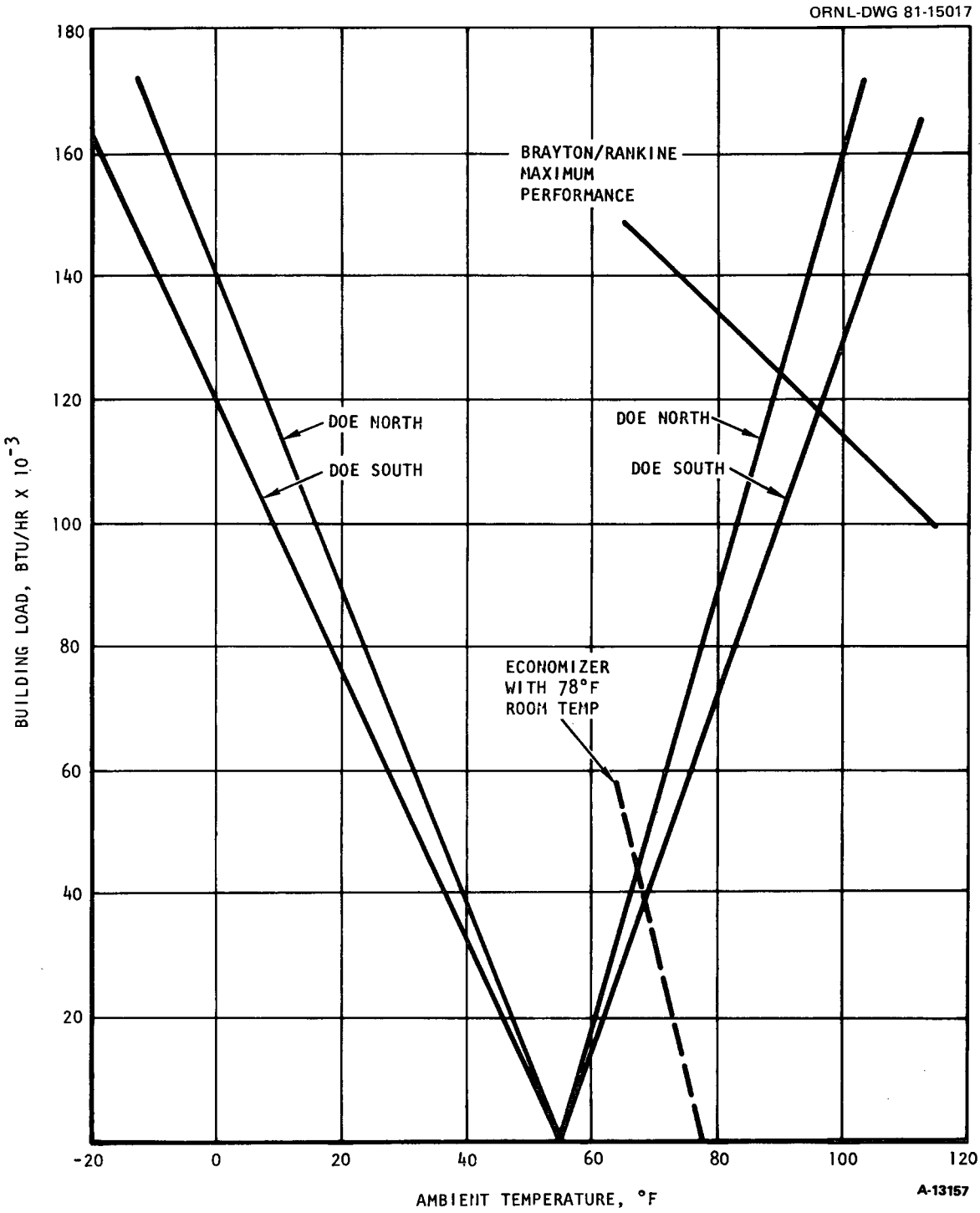

Figure 4-9. Building Loads at Various Ambient Temperatures

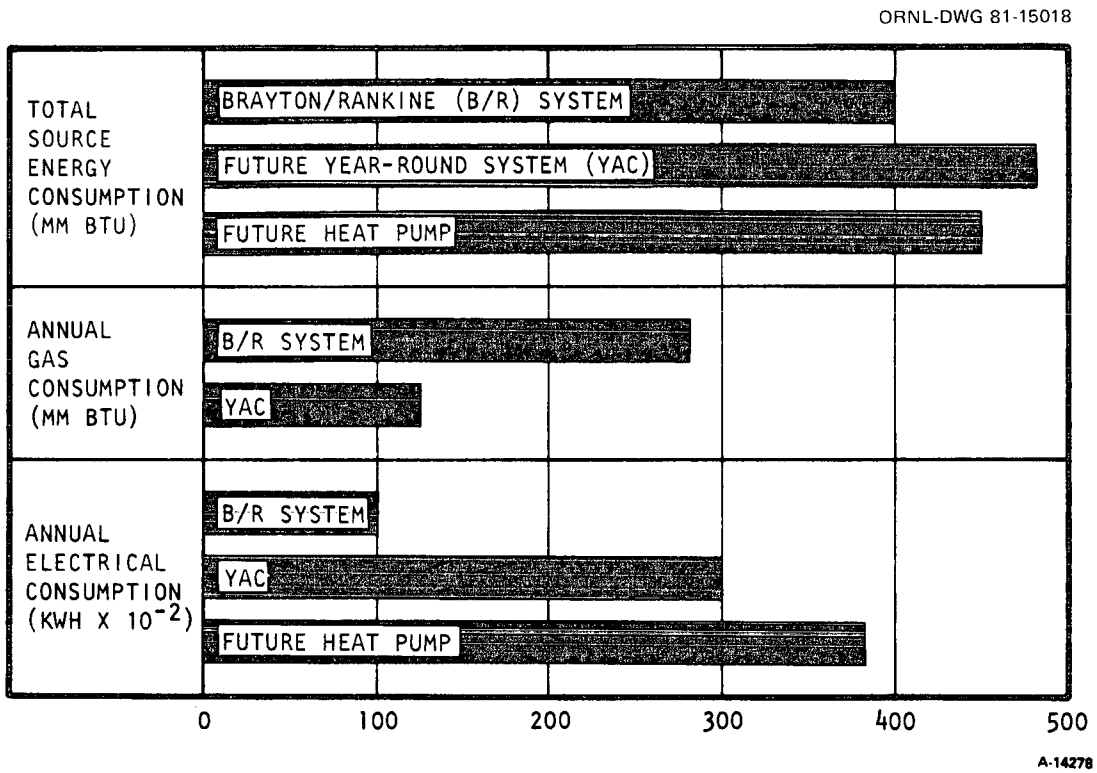

Figure 4-10. Comparative Annual Energy Consumption (DOE North)

AIRESEARCH MANUFACTURING COMPANY

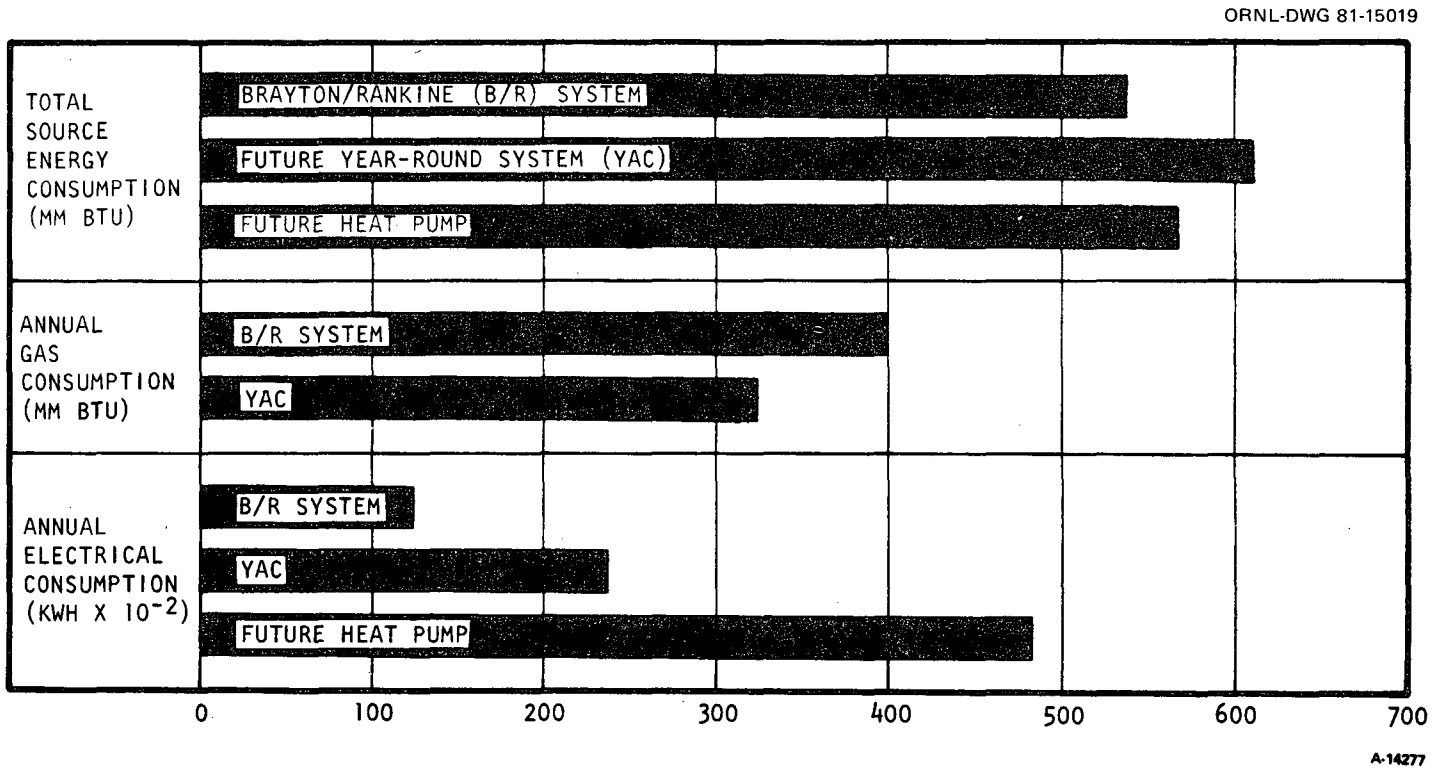

Figure 4-11. Comparative Annual Energy Consumption (DOE South)

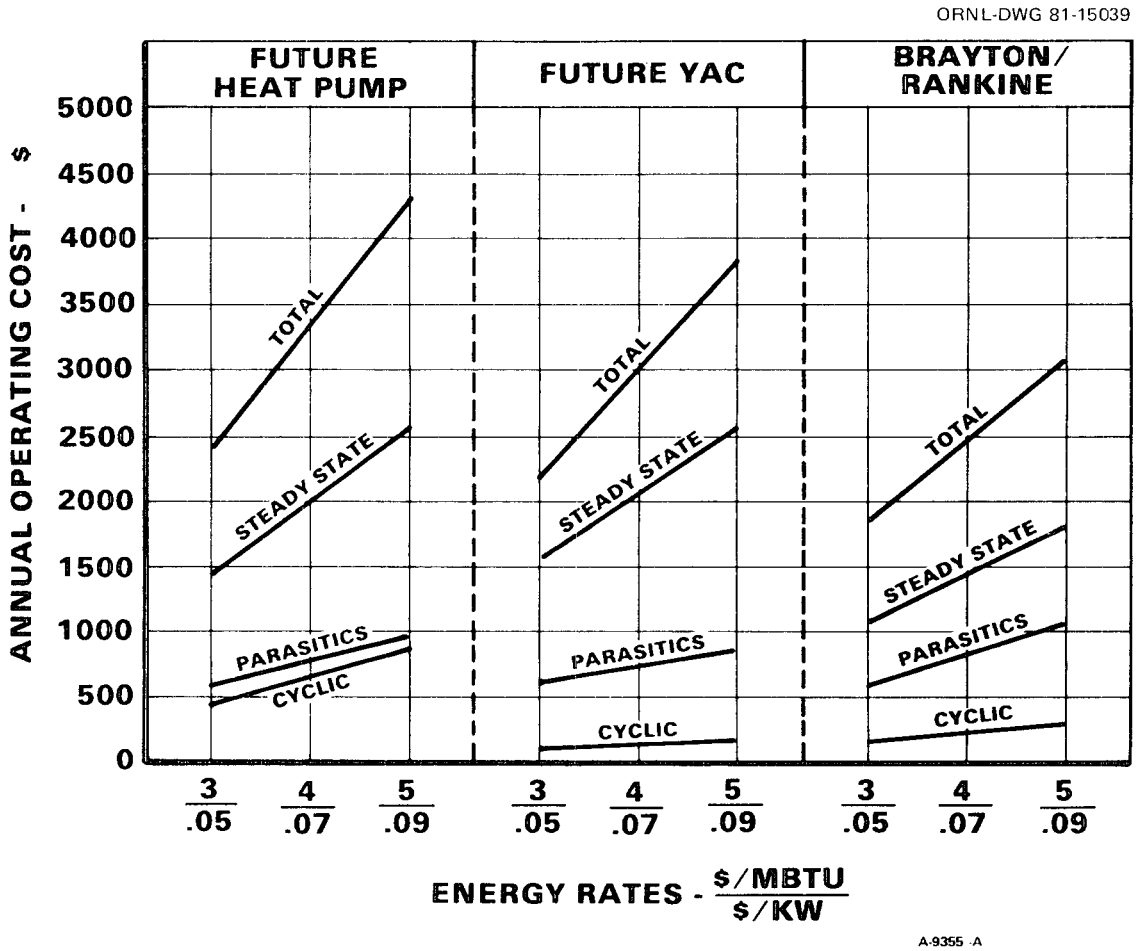

Figure 4-12. Comparative Annual Operating Cost (DOE North)

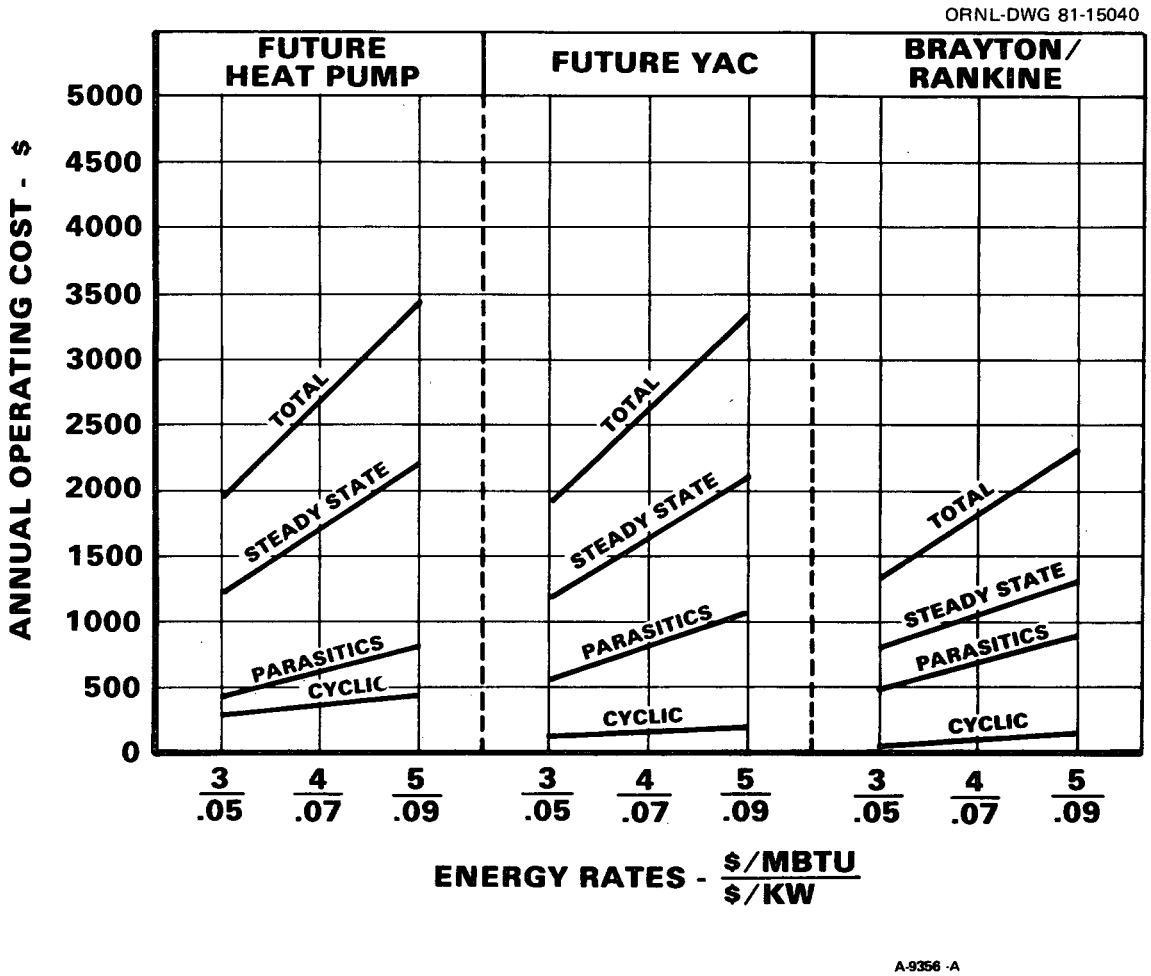

Figure 4-13. Comparative Annual Operating Cost (DOE South)

INTERNAL DISTRIBUTION

1. V. D. Baxter
2. R. S. Carlsmith
3. W. L. Cooper, Jr.
4. F. A. Creswick
5. R. C. DeVault
6. P. D. Fairchild
7. W. Fulkerson
8. R. E. Goodson, Consultant
9. G. Grossman
10. D. M. Hamblin
11. G. E. Kamp
12. M. A. Karnitz
13. T. R. LaPorte, Consultant
14. V. C. Mei
15. J. W. Michel
16. W. R. Mixon
17. L. I. Moss, Consultant
18. G. T. Privon
19. R. C. Robertson
20. I. A. Tag
21. L. F. Truett
22. T. J. Wilbanks
23-24. Central Research Library
25. Document Reference Section
26. Center for Energy and Environmental Information
27. Laboratory Records - RC
28-29. Laboratory Records Department
30. ORNL Patent Section

EXTERNAL DISTRIBUTION

31. C. A. Allen, Energy Information Administration, EI-60, Federal Building, 1200 Pennsylvania Avenue N.W., Washington DC 20461
32. Kent Anderson, The Trane Company, 2020 14th Street, Arlington, VA 22101
33. John Andrews, Solar Technology Group, Building 701, Brookhaven National Laboratory, Upton, NY 11973
34. B. Backstrom, Chalmers University of Technology, S-41296, Goteborg, Sweden
35. James Bard, Executive Vice-President, Bard Manufacturing Co., Inc., P.O. Box 607, Bryan, OH 43506
36. E. K. Bastress, Energy Conversion & Utilization Technology Div., CS-142, Forrestal Building, Department of Energy, Washington DC 20585
37. William Beale, Sunpower, Inc., 6 Byard Road, Athens, OH 45701
38. Warren Beeton, Vice-President-Engineering, Bristol Corporation, 649 Industrial Park Road, Bristol, VA 24201
39. J. Berghmans, Universitiet Leuven, Instituut Mechanica, Celestynen Laan 300A, B3030 Heverlee, Belgium
40. J. E. Bose, Director, School of Technology, Oklahoma State University, Stillwater, OK 74078
41. T. Bostrom, Swedish Council for Building Research, St. Goransgatan 66, S-11233 Stockholm, Sweden
42. W. R. Coleman, Residential & Commercial Services, American Elec. Power Services, 100 E. Broad, Columbus, Ohio 43201
43. Gerard Coyne, General Electric Company, Central Air Conditioning Dept., Troup Highway, Tyler, TX 75711
44. Kenneth Cuccinelli, Division of Marketing Services, American Gas Association, 1515 Wilson Blvd., Arlington, VA 22209

45. J. J. Cuttica, Manager, Fuel Cell Energy Systems, Gas Research Institute, 8600 W. Bryn Mawr Avenue, Chicago, ILL 60631
46. Nicholas D'Aleandro, Vice-President, A/C Engineering, Fedders Corporation, Woodbridge Avenue, Edison, NJ 08817
47. Jerry Dapper, BDP Company, Div. of Carrier Corporation, 7310 W. Morris Street, Indianapolis, IN 46231
48. Douglas DeWerth, Project Manager, Utilization Technology, Research & Development, 8501 East Pleasant Valley Road, Cleveland, OH 44131
49. R. J. Denny, Air-Conditioning & Refrigeration Institute, 1815 N. Fort Meyer Drive, Arlington, VA 22209
50. Richard Dougall, University of Pittsburg, Dept. of Mechanical Eng., Pittsburg, PA 15261
51. G. D. Duffy, Air Conditioning News, 700 East Maple, Birmingham, AL 48011
52. Richard English, Energy Systems Division, Carrier Corporation, Carrier Parkway, P.O. Box 4895, Syracuse, NY 13221
53. V. A. Eustace, IRD Co. Ltd., Fossway, Newcastle upon Tyne, Great Britain
54. J. N. Eustis, Department of Energy, Office of Industrial Programs, CE-121.1, 1000 Independence Avenue, S.W., Washington, DC 20585
55. Bernard D. Ferrao, Resource Engineer, Pacific Gas & Electric Company, 245 Market Street, Room 1330, San Francisco, CA 94106
56. R. J. Fiskum, Energy Conversion Equipment Branch, CE-113.2, Department of Energy, 1000 Independence Avenue S.W., Washington DC 20585
57. J. H. Gibbons, Office of Technology Assessment, U.S. Congress, 600 Pennsylvania Avenue S.E., Washington DC 20510
58. P. V. Gilli, Graz University of Technology, Kopernikusgasse 24, A-8010, Graz, Austria
59. Victor Goldschmidt, Purdue University, Ray W. Herrick Laboratories, West Lafayette, IN 47907
60. Peter Gorike, Abt. Anwendungstechnik, Rheinish-Westfakuscges, Krupstrasse 5, 4300 Essen 1, Federal Republic of Germany
61. D. E. Grether, Friedrich Air Conditioning & Refrigeration, P.O. Box 1540, San Antonio, TX 78295
62. James E. Griffith, Senior Research Engineer, PSE&G Research Corporation, Energy Laboratory, 200 Boyden Avenue, Maplewood, NJ 07040
63. G. C. Groff, Research Division, Carrier Corporation, Syracuse, NY 13201
64. Ronald D. Grose, Northern Natural Gas Company, Research Center, 4830 F Street, Omaha, NE 68117, a
65. Marvin Gunn, Energy Conversion & Utilization Technology Div., CS-142, Forrestal Building, Department of Energy, Washington DC 20585
66. James Harnish, Chief Engineer, Advanced Products, Unitary Products Engineering, York Division, Borg-Warner Corporation, York, PA 17405
67. D. J. Harrje, Princeton University, Energy & Environment, Von Neuman Building, Princeton, NJ 08544
68. Floyd Hayes, Thermal Systems, The Trane Company, 3600 Pammell Creek Road, LaCrosse, WI 54601

69. Robert Hemphill, Deputy Manager of Power, 546 Chestnut Street Tower II, Tennessee Valley Authority, Chattanooga, TN 37401
70. R. J. Hemphill, Gas Research Institute, 8600 Bryn Mawr Avenue, Residential & Commercial Util., Chicago, IL 60631
71. Ralph Hise, Consolidated Natural Gas Service Company, 11001 Cedar Avenue, Cleveland, OH 44106
72. Larry Hobart, American Public Power Association, 2000 Virginia Avenue N.W., Washington DC 20037
73. Tina Hobson, Building Equipment Division, CE-113.2, Department of Energy, 1000 Independence Avenue S.W., Washington DC 20585
74. Robert Holtz, Program Manager, Closed Cycle Systems, Argonne National Laboratory, 9700 S. Cass Avenue, Argonne, IL 60439
75. John Hughes, Commonwealth Edison Company, P.O. Box 767, Chicago, IL 60690
76. S. R. Jackbsen, Danish Ministry of Energy, Energy R&D Secretariat, Strandgage 29 DK 1401, Copenhagen, Denmark
77. H. Jaster, General Electric Corporate Research & Development, General Electric Company, P.O. Box 43, Schenectady, NY 13201
78. P. L. Johnson, Oak Ridge Associated Universities, Executive Office, Administration Building, Oak Ridge, TN 37830
79. F. R. Kalhammer, Energy Management and Utilization Division, Electric Power Research Inst., 3412 Hillview Avenue, P.O. Box 10412, Palo Alto, CA 94303
80. Ted Kapus, Office of Buildings Energy Research & Development, CE-11, Department of Energy, 1000 Independence Avenue S.W., Washington DC 20585
81. Herbert Kaufman, Empire State Electric Energy Research Corp., 1271 Avenue of the Americas, New York, NY 10002
82. George Kelly, Building Environment Division, IAT, National Bureau of Standards, Building 226, Washington DC 20234
83. R. W. King, Manager, Advanced Engineering, Copeland Corporation, Sydney, OH 45365
84. Milton Kosfeld, Vice-President, Engineering Compressors, Fedders Corporation, Woodbridge Avenue, Edison, NJ 08817
85. P. Kuppers, Kernforschungsanlage/Ple, Postfache 1913, D-5170, Julich 1, Germany
86. Gary Laden, Deputy Assistant Director, Div. of Energy & Product Inf., Bureau of Consumer Protection, Federal Trade Commission, Washington DC 20580
87. J. Langmead, Director of Technical Services, Gas Appliance Man. Assoc., 1901 N. Ft. Meyer Drive, P.O. Box 9245, Arlington, VA 22209
88. Arvo Lannus, Residential & Commercial Applications, Electric Power Research Inst., 3412 Hillview Avenue, P.O. Box 10412, Palo Alto, CA 94303
89. D. C. Lim, Energy Conversion Equipment Branch, CE-113.2, Department of Energy, 1000 Independence Avenue S.W., Washington DC 20585
90. George Long, Director of Research, Northern Illinois Gas Company, P.O. Box 190, Aurora, IL 60507
91. Nance Lovvorn, Alabama Power Company, 15 South 20th Street, P.O. Box 2641, Birmingham, AL 35291
92. H. P. Luckett, Editor in Chief, Popular Science, 380 Madison Avenue, New York, NY 10017

93. R. A. Macriss, Associate Director, Energy Conservation Research, Institute of Gas Technology, 3424 South State Street, Chicago, IL 60616
94. J. C. Major, Swiss Federal Institut for Reactor Research, CH-5303 Wurenlingen, Switzerland
95. Martin McCall, Consumers' Gas, 1 First Canadian Place, P.O. Box 90, Toronto, Ontario M5X, 1C5, Canada
96. Jim McCallum, Executive Editor, Air Cond. & Refrig. Bus., 614 Superior Avenue W., Cleveland, OH 44113
97. Alessio Mezzina, Solar Technology Group, Brookhaven National Laboratory, Building 701, Upton, NY 11973
98. J. P. Millhone, Office of Buildings Energy Research & Development, CE-11, Department of Energy, 1000 Independence Avenue S.W., Washington DC 20585
99. Eugene E. Moran, Washington Gas Light Company, 6801 Industrial Road, Springfield, VA 22151
100. F. H. Morse, Office of Solar Heat Technologies, CE-31, Department of Energy, 1000 Independence Avenue S.W., Washington DC 20585
101. T. Mukai, Permanent Delegation-Japan, 7, Avenue Hoche, 75008, Paris, France
102. W. E. Murphy, Department of Mechanical Engineering, Texas Engineering Exp. Sta., Texas A&M University, College Station, TX 77843
103. R. W. Newell, Vice President, Research & Development, City Investing Company, 5600 Old Greenwood Road, Fort Smith, AR 72903
104. Eric Nimke, Brooklyn Union Gas Company, 195 Montague Street, Brooklyn, NY 11201
105. Joe Pietsch, Northrup, Inc., 302 Nichols Drive, Hutchins, TX 75141
106. T. Ratchford, Committee on Science and Technology, Subcommittee on Energy R & D, House of Representatives, Washington DC 20515
107. V. Recchi, National Research Council, % O. T. B. Zona Industriale, Contrada del Parco, Bari, Italy
108. Robert Reid, Department of Mechanical & Aerospace Eng., Environment & Resource Center, University of Tennessee, 329 South Stadium Hall, Knoxville, TN 37916
109. Edward A. Reid, Jr., Manager, Utilization Research, Columbia Gas System Service, 1600 Dublin Road, Columbus, OH 43215
110. Hal Rhea, Director of Engineering, Lennox Industries, Inc., P.O. Box 877, 1600 Metro Drive, Carrollton, TX 75006
111. Bill Riley, Advance Development, Heil Quaker Corporation, 647 Thompson Lane, P.O. Box 40566, Nashville, TN 37204
112. J. M. Rivera, Research Project Manager, Southern California Gas Co., Terminal Annex, P.O. Box 3249, Los Angeles CA 90051
113. J. Rizzuto, New York State Energy Research & Development Auth., Agency Building No. 2, Empire State Plaza, Albany, NY 12223
114. Arthur Rosenfeld, Lawrence Berkeley Laboratory, Building 90, Room 3058, 1 Cyclotron Road, University of California, Berkeley, CA 94720
115. J. H. Rothenburg, Utilities Systems, Dept. of Housing & Urban Dev., 451 Seventh Street S.W., Washington DC 20410
116. William Rudoy, University of Pittsburg, Dept. of Mechanical Eng., Pittsburg, PA 15261
117. J. D. Ryan, Energy Conversion Equipment Branch, CE-113.2, Department of Energy, 1000 Independence Avenue S.W., Washington DC 20545

118. L. A. Sarkes, American Gas Association, 1515 Wilson Boulevard, Arlington, VA 22209
119. M. L. Savitz, Deputy Assistant Secretary for Conservation, CE-10, Department of Energy, 1000 Independence Avenue S.W., Washington DC 20585
120. James Schultze, Technology Program Manager, General Electric Company, Appliance Park, Building 6, Room 208, Louisville, KY 40225
121. J. L. Schulze, General Electric Company, Appliance Park, Louisville, KY 40225
122. Charles Sepsy, Ohio State University, Dept. of Mèchanical Eng., Room 2075 - Robinson Lab, 206 West 18th Avenue, Columbus, OH 43210
123. Warren Severin, Natural Gas Pipeline Company, 122 South Michigan Avenue, Chicago, IL 60603
124. James Shaw, Public Service Company of Oklahoma, P.O. Box 201, Tulsa, OK 74102
125. Neil Sher, Technology Strategy Center, Honeywell Control Systems, 1700 West Highway 36, St. Paul, MN 55113
126. D. E. Sherpereel, Research and Engineering Center, Whirlpool Corporation, Benton Harbor, MI 49022
127. J. A. Smith, Test and Evaluation Branch, CE-113.2, Department of Energy, 1000 Independence Avenue S.W., Washington DC 20585
128. Mason Somerville, Department of Mechanical Engineering, University of Arkansas, Fayetteville, AR 72701
129. E. W. Spannhake, White Consolidated Industries, Inc., 11770 Berea Road, Cleveland, OH 44111
130. Ing. F. Steimle, Angewandte Thermodynamik & Kimatechnik, Fachbereich 13, Universitatsstr. 15, 4300 Essen 1, West Germany
131. Mike Stenback, Michigan Consolidated Gas Company, One Woodward Avenue, Detroit, MI 48226
132. Don Stephenson, National Research Council, Division of Buildings Res., Montreal Road, Ottawa, Canada KIA 0R6
133. L. Hunt Sutherland, Vice-President, R&D, Lone Star Gas Company, 301 South Harwood Street, Dallas, TX 75201
134. P. F. Swenson, Consolidated Natural Gas Service Company, 11001 Cedar Avenue, Cleveland, OH 44106
135. C. J. Swet, 7040 Woodville Road, Mt. Airy, MD 21771
136. W. D. Syniuta, Advanced Mechanical Technology, Inc., 141 California Street, Newton, MA 02158
137. C. C. Thiel, Jr., Division of Advanced Technology Applications, National Science Foundation, 1800 G Street N.W., Washington DC 20550
138. W. H. Thielbahr, Energy Conservation Branch, Department of Energy, Idaho Operations Office, 550 Second Street, Idaho Falls, ID 83401
139. Tommy Thompson, Vice-President, Engineering, BDP Company, Div. of Carrier Corporation, 7310 W. Morris Street, Indianapolis, IN 46231
140. E. L. Tramel, Residential Technical Applications, Conservation & Energy Mgmt., Chattanooga Power Service Cnt., Chattanooga, TN 37401
141. S. S. Waddle, Department of Energy, Oak Ridge Operations, Federal Building, CS-2039, Oak Ridge, TN 37830
142. Michael Wahlig, Lawrence Berkeley Laboratory, Building 90, Room 2024, 1 Cyclotron Road, University of California, Berkeley, CA 94720

143. D. J. Walukas, Foster-Miller Associates, Inc., 795 Oak Ridge Turnpike, Oak Ridge, TN 37830
144. Eugene West, Sr. Vice President, Engineering, Amana Refrigeration, Inc., Amana, IA 52204
145. G. W. Wiener, Manager, Materials Science Division, Westinghouse R&D Center, 1310 Beulah Road, Pittsburg, PA 15235
146. Lawrence Woodworth, Brookhaven National Laboratory, Building 120, Upton, NY 11973
147. P. Zegers, Commission of the European Communities, 200 Rue de la Loi, Brussels 1049, Belgium
148. Alan Zimmerman, Special Products Group, The Coleman Company, Wichita, KS 67201
149. Congressional Information Service, Research Building 83, Kodak Park, Rochester, NY 14050
150. Edison Electric Institute, 8th Floor, 1111 19th Street N.W., Washington DC 20036
151. Office of the Assistant Manager for Energy R & D, U.S. Department of Energy, Oak Ridge Operations, Oak Ridge, TN 37830
152. National Energy Information Center, Library, Room 1404, 12th & Pennsylvania Ave. N.W., Washington DC 20461
153-391. Technical Information Center, Department of Energy, P.O. Box 62, Oak Ridge, TN 37830, for Dist. Category UC-95d
392-500. Energy Conservation Distribution, Oak Ridge National Laboratory, Bldg. 9102-2, Rm. 111, Oak Ridge, TN 37830

☆U.S. GOVERNMENT PRINTING OFFICE: 1982-546-067/70